LANDSCAPE ECOLOGY OF THE RANGIPO DESERT

A thesis presented in partial fulfilment of

the requirements for the degree of

Master of ~~Philosophy~~ Science in Soil Science

at Massey University

Andrew Mark Purves

1990

CHAPTER 1

GENERAL INTRODUCTION

1.1 Location Of The Study Area

In 1847, William Colenso, missionary, explorer, and botanist made his first crossing of the Rangipo Desert in foul weather: "At 3pm we crossed the sand desert called Te Onetapu (Rangipo)- a most desolate weird-looking spot, about 2 miles wide where we crossed it; a fit place for Macbeth's witches or Faust's Brocken scene!" Colenso (1884) was describing a landscape clothed by tussock, dunefields, barren gravelfields and deeply scoured watercourses.

The Rangipo Desert is situated on the exposed south-eastern portion of Mount Ruapehu's ring plain. Mount Ruapehu is New Zealand's largest andesitic massif and its summit is the highest peak in the North Island, reaching 2,797m. To the east of the Rangipo Desert uplifted ranges of indurated sandstone, argillite, and conglomerate make up the Kaimanawa Range (Grindley, 1960). The field study was, in the main, confined to the west and south of the Whangaehu River, to the north of the Waihianoa Aqueduct, and to the east of Makahikatoa Stream (Fig. 1.1). The field area, therefore, covers about 40km^2, most of which was gazetted to the New Zealand Army in 1943 (Birch, 1987). The altitude within the study area gradually increases from 910 metres above sea level at Waihianoa Aqueduct, to 1200 metres above sea level at the north-eastern margin of the study area.

The landscape of the Rangipo Desert is unique for its contrasts within a few kilometres. In one area eroding light yellow tephra, colonized by only scattered hardy plants, abuts against healthy enclaves of *N. solandri*; while, in another area only a kilometer away, dunes colonized by *Phyllocladus* and *Halocarpus bidwillii* are interpersed across a grey lag pavement covered by scattered boulders and even fewer plants. These contrasting features make the task of delineating the landscape into discrete regions simple.

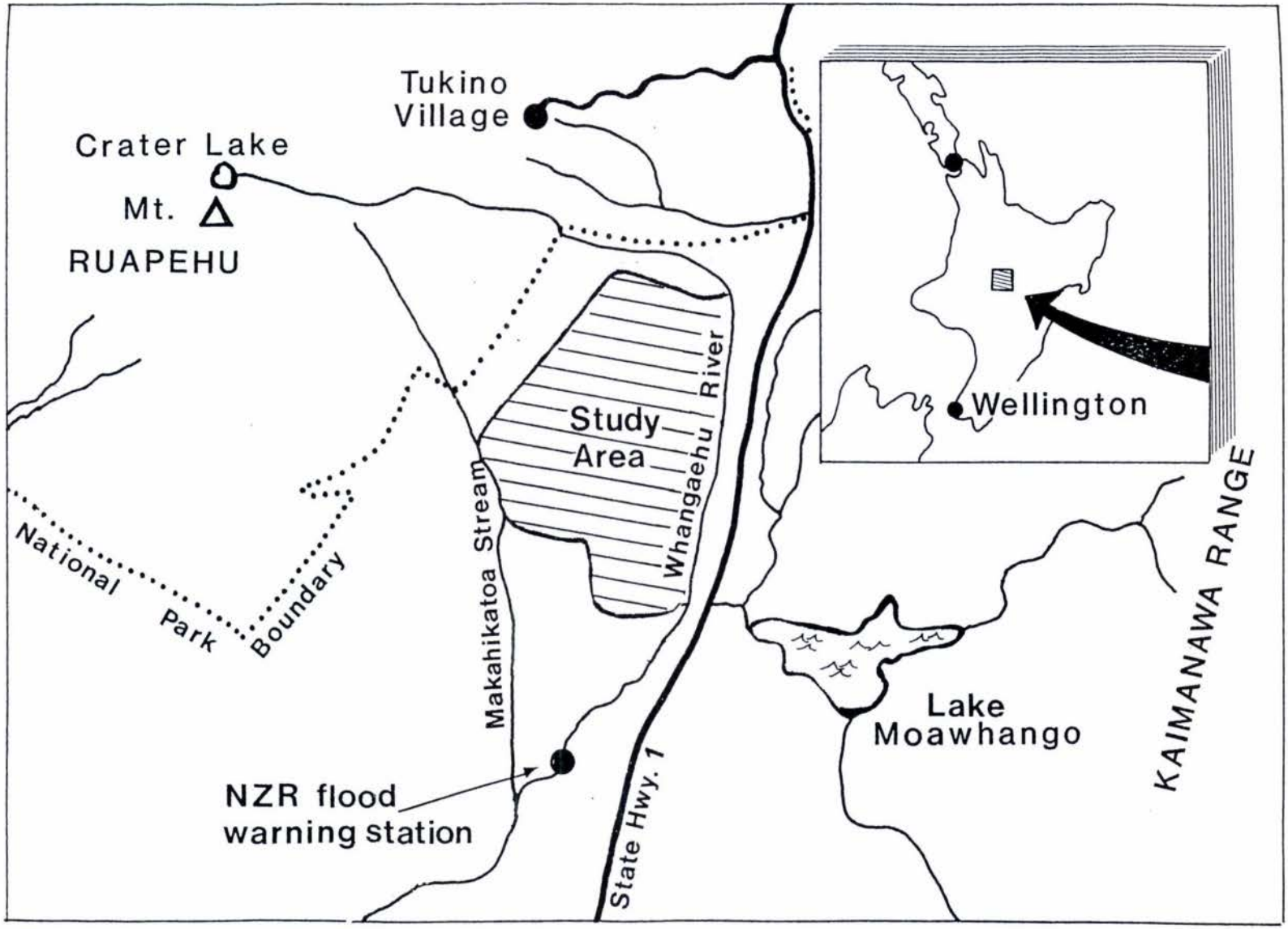

Figure 1.1 Locality Map of the Study Area

The study area is subdivided into two basic regions: a laharic and fluvial constructional surface to the east and an erosional surface to the west (Fig. 1.2, Plate 1.1). The fluvial and laharic constuctional surface is an extensive fan which has been further subdivided into 2 regions, called the active fan and the inactive fan. Many channels on the active fan are susceptible to inundation by lahars of all sizes, whilst the inactive fan is only engulfed when larger volume lahars over-top the channel confines of The Chute (a deeply incised lahar channel), or the upper reaches of the Whangaehu River (Fig. 1.2, Plate 1.1). The 1975 lahar is an example of a smaller lahar which inundated the major channels of the active fan, but did not over-top The Chute and flow across the inactive fan (Plate 1.2). Within the active and inactive fans are topographically higher areas which are less susceptible to inundation by lahars. These areas usually are covered in scrub, so the light green areas on the 1:50,000 topographical map (Fig. 1.2) in general represent these topographically higher areas.

1.2 The Rangipo Desert - An Enigma

It was not until Leonard Cockayne completed a detailed botanical and geological survey of Tongariro National Park in the summer of 1908 that suggestions as to the causes of the Rangipo Desert were made. He states: "To speak of deserts at all in a rain-forest climate seems a paradox, and the truth is that those of New Zealand are edaphic rather than climatic. Still, were the rainfall greater the desert areas would be less. As an example, true oases exist on the otherwise barren scoria slopes of Ruapehu in places where a spring gushes from the ground " (1908:25). Cockayne concluded that the effects of wind and insolation coupled with the coarse textured and easily removed soils, were the cause of the desert. He also believed that much of the desert could be replaced by plant-life with a change in the climatic conditions, even though he was aware that the landscape had changed little since Colenso's travels through the Desert.

Figure 1.2 Map of the Rangipo Desert from NZMS Series 260; Sheet T20. The black solid line is the boundary between the eroding surface to the west and the laharic and fluvial constructional surface to the east. The dotted line is the boundary between the active fan and the inactive fan on the laharic and fluvial constructional surface. The light green areas on the laharic and fluvial constructional surface represent dominantly *Phyllocladus* type scrub which occurs on topographically higher areas. The locality names are not approved New Zealand Geographic Names.

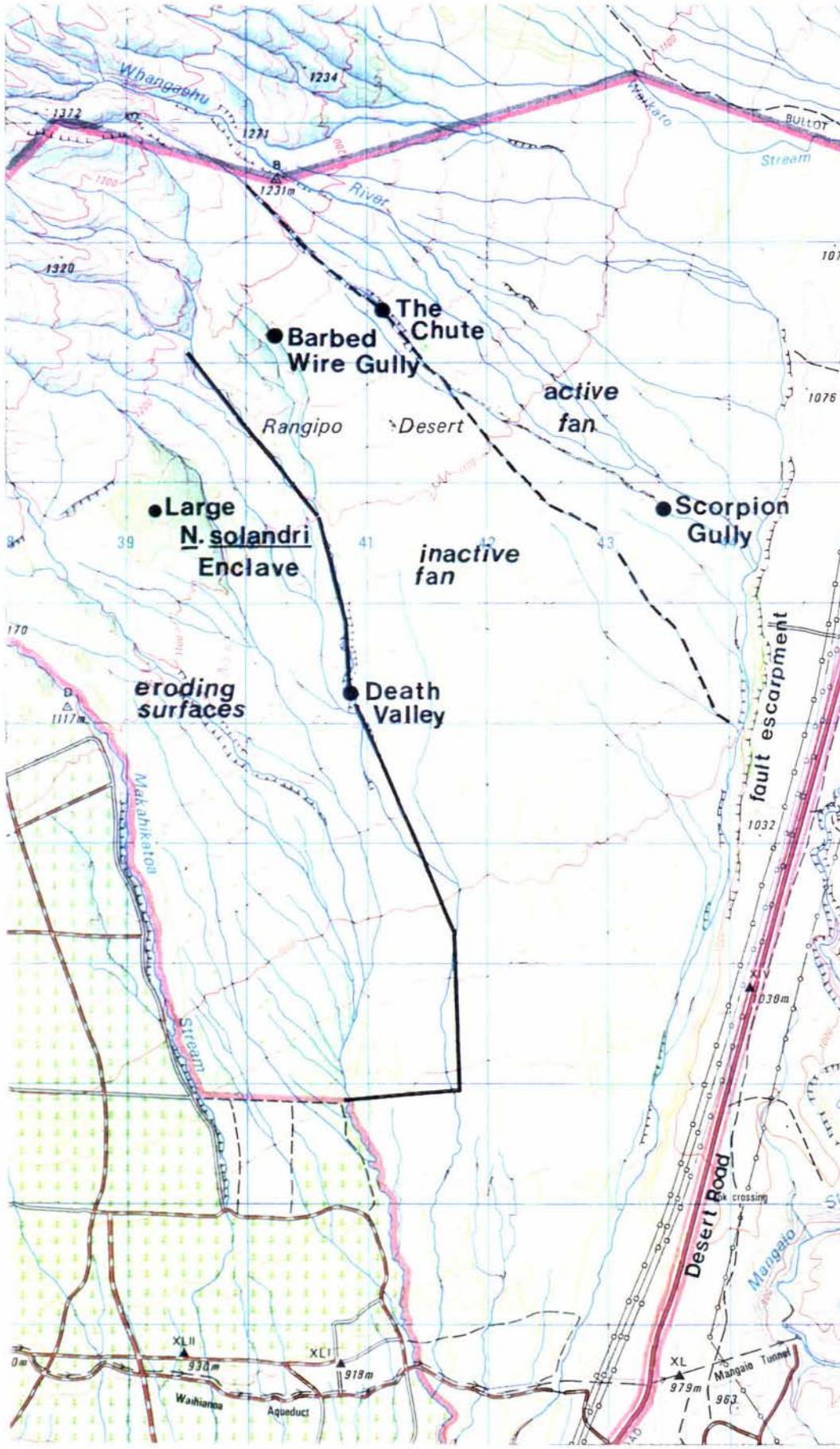
Whangaehu River
Waikato Stream
BULLOT
1234
1372
1271
1231m
1320
1072
1076
The Chute
Barbed Wire Gully
active fan
Rangipo Desert
Large N. solandri Enclave
Scorpion Gully
inactive fan
eroding surfaces
Death Valley
fault escarpment
1032
1117m
Makahikatoa Stream
1030m
Desert Road
Mangaio
Mangaio Tunnel
963
930m
918m
979m
Waihianoa Aqueduct
XLII
XLI
XL
39
41
42
43

ate 1.1 Photograph looking south-east across the study area from Te Heu Heu peak of Mt Ruapehu, taken in August 1989. The arrow in the foreground shows the locality where lahars flowing down the Whangaehu River often over-flow the channel confines and travel down The Chute. The Chute is seen in the photograph below this point whilst the Whangaehu River veers further north (left of the photograph) before re-appearing again at the foot of a fault escarpment (arrow in the background). State highway 1 crosses along the top of the escarpment. Lake Moawhango in the background is nestled between the foothills of the Kaimanawa Range. Exceptionally large volume lahars appear to over flow the Whangaehu River channel higher up on the mountain and cross the areas covered with snow in the right foreground of the photograph.

The right arrow points to the margin of a grey constructional surface made up from lahar and fluvial deposits which abuts against older surfaces that are light yellow in colour due to erosion of tephra coverbeds.

The grey lahar and fluvial lithologies interfinger *Phyllocladus* forest and scrub, and nearer the fault escarpment, interfinger tussockland. The dark green area surrounded by the eroding surfaces is Large *N. solandri* Enclave.

Plate 1.2 Residual water and silt lying on the active fan 12 hours after the 1975 lahar event. The white arrow points to The Chute which forms the natural boundary between the active and inactive fans. Source: Lloyd Homer, N.Z. Geological Survey.

The widespread presence of charcoalised logs in the Taupo Pumice ignimbrite led Cockayne (1908) to conclude that Mount Ruapehu was covered with heavy forest prior to the Taupo Pumice eruption. However, he did not speculate about the possibilities of reforestation after the eruption or subsequent deforestation from burning by the Polynesians. Since Cockayne's work, evidence suggests that much of the treeless Volcanic Plateau was indeed a result of Polynesian firing. (Fletcher 1914, Henry 1954, 1955, Nicholls in Vucetich and Wells 1978:23). Nevertheless, the question remains whether the actively eroding landscape of the Rangipo Desert reflects cumulative erosion of many hundreds of years or whether the intrusion of man, bringing fire, sheep, cattle, horses, rabbits, and hares to the Volcanic Plateau, accelerated the process (Gabites, 1986).

Of importance to understanding the genesis of the Desert is the geology. The Rangipo Desert is mapped as comprising of late post-glacial 'Lahars Of The Whangaehu River' (Grindley 1960). The lahar deposits, however, have not been differentiated and no investigations have been published on how these lahars have influenced the landscape in the Rangipo Desert.

Likewise, the vegetation of the study area (apart from the north-west sector; Atkinson, 1981) has not been described or mapped, nor have any studies been attempted to determine how natural or anthropogenic processes have affected the ecology or distribution of the plants.

1.3 Objectives Of The Study

The objectives for this study were firstly to elucidate the evolution of the physical landscape since the Taupo Pumice eruption of 186 A.D. by studying the stratigraphy in the study area; and secondly, examine the relationship between the present vegetation pattern and the evolution of the physical landscape. Once sufficient knowledge had been obtained about the landscape pattern from field studies, image analysis techniques were employed on black and white and coloured aerial photographs. An attempt was made to extract information about the landscape from this remotely sensed data and to then classify the landscape accordingly.

1.4 Approach To The Study

A study into geological, soil, and plant interrelationships requires an intergrated approach. After an initial reconnaissance of the landscape, the post-Taupo Pumice aeolian, lahar and fluvial stratigraphy was recorded and, where possible, deposits were correlated. The information gained from the stratigraphic sections was used in determining the periodicity and size of lahars which have inundated the study area, as well as interpreting the time when much of the present erosion was initiated. Field descriptions, augmented with laboratory information, were used to characterise the depositional and weathering history of the aeolian sands found in the Rangipo Desert.

The vegetation in the Rangipo Desert was described, and then studies were carried out on several plant communties in order to understand their distribution and ecology. The information gained from the earlier stratigraphic studies, augmented by soil fertility studies, was useful for this purpose. For the image analysis work, an identical region from the study area found on the black and white and colour photographs was delineated and digitized using a scanning microdensitometer. The resultant ditgitized images were then both enhanced and combined where necessary in an attempt to map and classify the vegetation and any surficial lithologies.

1.5 Geology

The Rangipo Desert is part of the extensive Mount Ruapehu ring plain that is mostly comprised of fragmental volcaniclastic detritus of laharic and fluvial origin. Mount Ruapehu is the southernmost massif of the Tongariro Volcanic Centre (Grindley, 1960) which forms part of the Taupo Volcanic Zone (Healy, 1962). The Taupo Volcanic Zone is a NNE-trending marginal basin of Pliocene to Recent volcanism and tectonic activity which extends across the central portion of the North Island (Healy, 1962; Cole, 1981). Mount Ruapehu is the largest edifice representing about 40% of the total volume of Taupo Volcanic Zone intermediate volcanics (Hackett, 1985).

A feature of Mount Ruapehu is Crater Lake, which is estimated by Dibble to contain 7 million cubic metres of water (referenced in Nairn, 1979). The Lake is thought to have been in existence for the last 2,000 yrs (Donoghue *et al.*, 1988). Its major outlet has probably always been at an ice cave at the head of a branch of the Whangaehu River (Gregg, 1960), which results in part of the Rangipo Desert being periodically inundated by lahars.

1.6 Stratigraphy

Studies of the regional late-Holocene stratigraphy have provided a useful framework for detailed stratigraphic study in the Rangipo Desert. The Taupo Pumice ignimbrite, the pyroclastic flow member of the Taupo Pumice Formation (Wilson and Walker, 1985) was used as the base marker bed because it is easily recognised[1] throughout the study area, and it is a well known and important late-Holocene (c.186 A.D.) stratigraphic marker found throughout many localities in the central and eastern North Island. The ignimbrite contains numerous carbonised logs and wood fragments which attest to the destruction of the forests (Atkinson, 1983) in this locality.

The Taupo Pumice ignimbrite is underlain by the Mangatawai Tephra, an andesitic tephra derived from Mounts Ngauruhoe and Ruapehu which accumulated on the landscape between c. 2,500 yrs B.P. and c. 1764 yrs B.P. (Topping, 1973,1974). The lower half of the Mangatawai Tephra is thought to have accumulated in a matter days or weeks while the upper half is thought to have accumulated during the remaining c. 700 years. This resulted in the development of a paleosol in the upper part of the Mangatawai Tephra (Topping, 1974). Beech leaves preserved within the Mangatawai Tephra confirmed Cockayne's (1908) belief that the landscape around eastern Tongariro was forested prior to the Taupo Pumice eruption (Gregg, 1960; Topping, 1974). No erosion is recognised during the deposition of the Mangatawai Tephra, implying a period of relative landscape stability (Topping, 1974) before the Taupo Pumice eruption.

[1] A general description of the Taupo Pumice ignimbrite's lithofacies, found in the study area, is given appendix 4.

After the destruction brought about from the Taupo Pumice eruption the regional stratigraphic record shows andesitic tephra deposition resumed. Topping (1973) has called this post-Taupo Pumice andestic tephra the Ngauruhoe Tephra, and from isopach data concludes the source is from Mounts Ngauruhoe and Ruapehu. The upper contact of the Ngauruhoe Tephra is the present day soil (Topping 1973).

A new formation status is being erected by S.L. Donoghue (pers. comm.) for post-Taupo Pumice eruptives that are derived exclusively from Mt. Ruapehu. This new formation will be called the Tufa Trig formation and consists of 18 informal ash or lapilli members. It is observed in Rangipo Desert and elsewhere on the south-eastern slopes of Mount Ruapehu.

The use of stratigraphy not only provides information on the depositional history of a landscape but also on the erosional history of a landscape. Several erosional unconformities are recognised within tephra sequences of the Tongariro Volcanic Centre over the last 20,000 years. However, the current erosion observed is more active than previous erosional periods recorded, and is more widespread than any previous erosional period seen for the last 14,000 years (Topping, 1974). The cause of erosion observed today was suggested by Topping (1974) to be a result of forest destruction by early Maori and European burning, and by noxious animals. He also suggested recent climatic change may be causing the increased frequency of heavy rain storms, and perhaps, was also inhibiting regeneration of forest.

1.7 Lahars

The word 'Lahar' is Indonesian for "volcanic breccia transported by water" (Van Bemmelen 1949, p.191). Because this term has often been misused and misunderstood, lahar has recently been re-defined as: "rapidly flowing mixture of rock debris and water (other than normal stream flow) from a volcano." (Smith and Fritz, 1989). This will be the definition followed here.

Although no attempt has been made previously to differentiate the lahar deposits on the Rangipo Desert, some of lahar deposits have been dated further downstream within the Whangaehu catchment. Estimated ages for three major post-Taupo Pumice lahar deposits, exposed on a low terrace of the Whangaehu River, near Mangamahu, were published by Campbell (1973). Using radiocarbon dates and lithologic evidence Campbell showed three periods of deposition were (1) some time after 1891 ± 78yrs B.P. and before 756 ± 56yrs B.P., (2) after 756 ± 56yrs B.P. and before 407 ± 70yrs B.P., and (3) after 407 ± 70yrs B.P. Donoghue *et al.*(1988) presented a maximum age of 450 ± 55yrs B.P. and a minimum age of 390 ± 55yrs B.P. for a major post-Taupo Pumice lahar deposit, down stream from the study area, near Tangiwai. A new formation, the Whangaehu Formation (undifferentiated), is being erected (S.L Donoghue pers. comm.) that will include all the post-Taupo Pumice lahar and fluvial deposits, derived from Mt Ruapehu.

Probably the first European account of a lahar crossing the Rangipo Desert was by James Crawford who observed in January 1862 (Crawford, 1880):

(a lahar) " had crossed the plain, or rather the inclined plain, for several miles, tearing up bushes and scarring the surface in its way".

Since 1861 at least 7 eruptions of Mount Ruapehu have produced lahars in the Whangaehu River (Patterson, 1976; for a historical review see Gregg, 1960). In addition, lahars generated in the Whangaehu Valley by the failure of ice or volcanic debris, which act to impound Crater Lake, have also been recorded (Healy, 1954a). Healy suggested the "Tangiwai Disaster" was due to a sudden collapse of an ash barrier impounding the lake because of crevassing movements in ice. After the collapse of the ash barrier a mass of water rushed down the Whangaehu River, damaging the railway bridge over the Whangaehu River at Tangiwai, which collasped as the Wellington-Auckland express crossed with 151 passengers being killed.

The largest lahar to engulf the Whangaehu River in recent times acccompanied the April 1975 eruption of Mount Ruapehu (Plate 1.2). From continuous water-level records, a volume of 1.8 million m^3 was calculated for the lahar. Therefore over half of the 3 million m^3 water estimated to have been ejected from the lake (Nairn, 1979) flowed down the Whangaehu catchment. The peak mean velocity recorded at the Wahianoa Aqueduct, which is 22.1km from Crater Lake, was 8 metres/second (Patterson 1976). Whether this is the largest lahar in European time is not known, but, the 1895 eruption was probably at least of similar magnitude. Of that event Allen in Gregg (1960) records, " the Whanganui River was discoloured down to the sea," and "the Whangaehu River was for several days a river of mud."

During the 1975 eruption at least 23% of the total volume of Crater Lake was erupted. Paterson (1980) predicted that it would be possible to eject more than double this estimate, and individual lahars could show an even greater increase in volume depending on wind conditions during the eruptions. Hewson and Latter (as referenced in Latter, 1981) suggest eruptions could eject up to 80% of Crater Lake's water.

1.8 Soils

The post-Taupo eruptives and intercalating Makahikatoa Sands found in the Rangipo Desert form the principle parent material of the Ngauruhoe soil series with the Ngauruhoe sand as the dominant soil type (Gibbs *et al.*, 1968). The Ngauruhoe series and associated Pihanga steepland soils, which occur on the steeper slopes of the Ruapehu-Tongariro massifs, belong to the sub-group 'central recent soils from volcanic ash'. East of State Highway 1, around Lake Moawhango, Campbell (1979) mapped 3330 hectares of the Ngauruhoe series. He cited erosion susceptibility, nutrient deficiency, and low soil temperatures as the major soil limitations for cropping, forestry, and pastoral use.

1.9 Climate

The climate of the central North Island has been described by Thomson (1984). The predominant airflow over the region is westerly though the Rangipo Desert winds are predominantly from the north-east and south-west quarters. This is due to funnelling of the windflow around Ruapehu and Tongariro massifs. Though the region as a whole is one of the least windiest in New Zealand, gale force conditions are common in mountainous areas. While many gales blow from the south-west or north-east, the strongest and most damaging winds blow from the east or south-east due to funnelling in the lee of the Kaimanawa Ranges.

The slopes and inner ring plain of Mount Ruapehu are often susceptible to increased rainfall because of orographic rise of the westerly airflows. However, by the time the air masses reach Waiouru further east, much of its moisture is spent (Table 1.1). No long term station exists in the Rangipo; however, 2 octapent[1] stations immediately adjacent to the study area, and other stations further afield, provide isohyets of 30 year rainfall normals across the Rangipo Desert (N.Z. Meteorological Service, 1973a).

The annual rainfall estimates for the Rangipo Desert ranges from 2,400mm at an altitude of 1100m to 1600mm at an altitude of 900m. An average of 2000mm has therefore been assumed for the Rangipo Desert (Table 1.1). The Rangipo Desert receives greater annual rainfall than Waiouru presumably because of the increased orographic influence.

[1] Octapent stations have their gauges read at irregular intervals so annual rainfall normals can be calculated. There is a ≈2% error for annual estimates (N.Z. Meteorological Service, 1973a).

Table 1.1 Rainfall normals for 5 stations around Mt. Ruapehu and calculated normal for the Rangipo Desert.

Station	Altitude (m)	Grid Reference NZMS 260	Rainfall Normals (mm)
Chateau Tongariro*	1119	S20/293196 North-west of Ruapehu	3965
Waikune#	744	S20/176190 North-west of Ruapehu	2476
Ohakune Junction*	629	S20/166956 South-west Ruapehu	1564
Karioi*	648	S20/262923 South of Ruapehu	1189
Rangipo Desert	1050	T20/415055 South-east of Ruapehu	2000
Waiouru*	823	T21/410890 South-est of Ruapehu	1048

*Source: N.Z. Meteorological Service Miscellaneous Publications 145 (1973a).
#Source: N.Z. Meteorological Service Miscellaneous Publications 177 (1980)

Waiouru is the closest meteorological station to the Rangipo Desert that has other climatic parameters recorded. Mean monthly temperatures (Fig. 1.2) range from 14°C in the summer to 4°C in the winter. Accompanying the cool winter temperatures is 16 days of snowfall and over 100 days of ground frosts (Fig. 1.3). Ground frosts occur all year around and over 10 weeks of ground frosts can be expected from the beginning of May to the end of September. Hail occurs most frequently in late winter and spring as do strong wind gusts, while fog occurs all year round (N.Z. Meteorological Service, 1980). The higher elevation of the Rangipo Desert would suggest more severe frosts, longer periods of snow covering the ground, and cooler temperatures than to Waiouru.

Summer temperatures, in contrast, nearly reach a mean daily maximum of 20° and are accompanied with a decline in rainfall. Thunder is associated with the warmer temperatures and is most common in December and January (N.Z. Meteorological Service 1980). From personal experience, the Rangipo Desert was also considerably windier than Waiouru in the summer periods of 1988 and 1989. These summer and winter extremes show some characteristics of a continental type of climate (Coulter, 1973).

Figure 1.3 Mean Monthly Temperatures for Waiouru

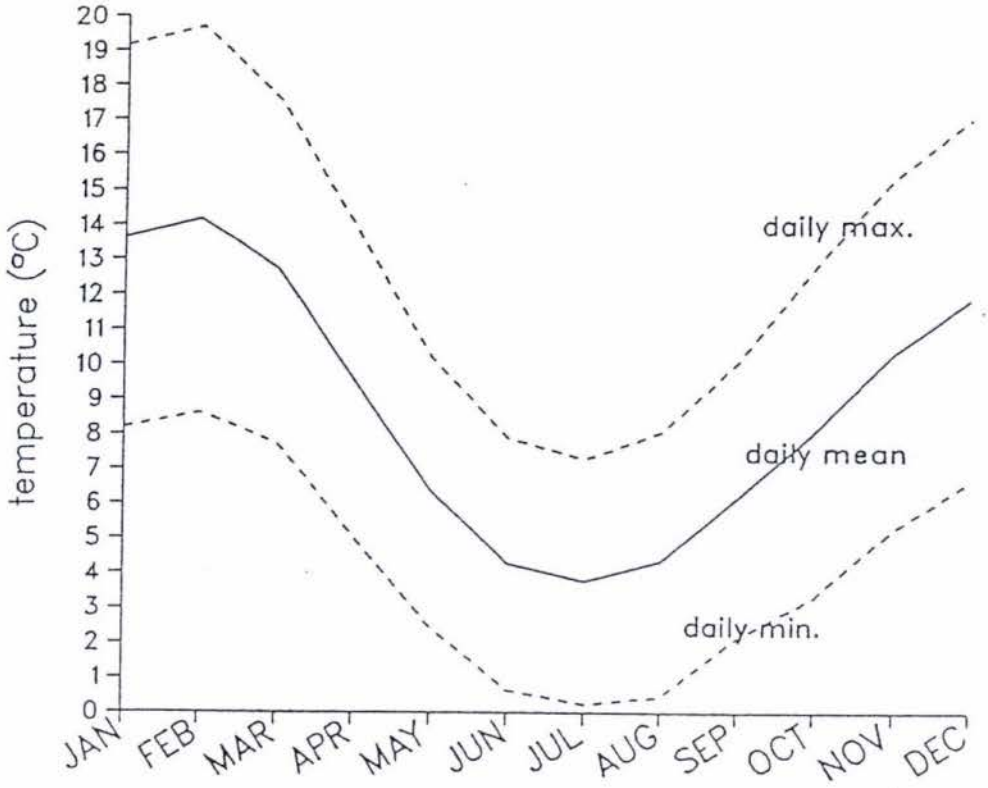

Source: Garnier, (1951)

Figure 1.4 Climatic Data For Waiouru Township (E95464)

Average Days Of Ground Frost	100.6	
Average Days Of Snow	15.8	
Average Days Of Hail	4.4	
Average Days Of Thunder	3.1	
Average Days Of Fog	8.6	
Average Days Of Wind Gusts of	63km or more	48.6*
	96km or more	2.6*

No sunshine hours were recorded
* From Waiouru Military Camp (E95465)
Source: New Zealand Meteorological Service Misc. Pub. 177.

1.10 Vegetation

1.10.1 Past Vegetation

The late Otiran-early Holocene climatic amelioration in the Tongariro region is thought to have occurred around 13,800 years ago (McGlone and Topping 1973). This interpretation is based on pollen spectra which show a transition from *Nothofagus* forest, *Phyllocladus* shrubland and grassland to podocarp forest. *Prumnopitys taxifolia* forest was dominant until about 10,000 yrs B.P., but then *Dacrydium cupressinum* forest became dominant in the region between 10,000 and 5,000 yrs B.P. as the climate became much wetter and milder, relative to today's climate. From 5000 yrs B.P. to the present the return of *Prumnopitys taxifolia* dominant forest, and the increase of *Nothofagus* forest suggest a general trend away from the mild climates to a drought and frost prone climate (McGlone and Topping, 1977). However, pollen spectra taken from Reporoa Bog in the Moawhango Ecological District, indicate *Prumnopitys taxifolia* and *Nothofagus* forest increases from 9,000-3500 years, then subsequently reduces (Rogers, 1987). A fire in the Reporoa Bog circa 3000 yrs B.P. suggests the *Nothofagas* and *Prumnopitys taxifolia* decline was due to natural fires in a more drought prone climate (Rogers, 1987).

Pollen spectra from north-west Ruapehu (Steel, 1989) show a sharp decline in *Nothofagus* immediately after the Taupo Pumice eruption. *Halocarpus* species followed by *Phyllocladus* and *Lagarostrobus colensoi* were the first woody colonizers after the eruption and *Nothofagus* had regained its dominance again by before 1000 yrs B.P. Steel notes, however, that beech did not recolonize the area north of its present limit at North-West Ruapehu. She suggests poor drainage and heavy frosts may have prevented the beech from recolonizing, and resulted in the local dominance of *Halocarpus* sp. and subdominance of *Phyllocladus*. In west Taupo Clarkson *et al.* (1986) estimated that tall podocarp forest had re-established within 450 years after the destruction caused by the Taupo Pumice pyroclastic flow. From pollen spectra, augmented with radiocarbon dates Steel (1989) concludes that Polynesian deforestation due to burning took place at 600 yrs B.P. Interestingly, she found that the beech was largely unaffected by the burning while the *Phyllocladus* scrubland was most affected. She assumed the *Phyllocladus* scrubland was the drier vegetation type and more susceptible to burning than the beech forest.

Rogers (1987) also found that the Taupo Pumice pyroclastic flow destroyed part of the *Nothofagus* forest in the Moawhango Head Waters, east of the Rangipo Desert. In this region *Nothofagus* pollen spectra indicates a permanent reduction in *Nothofagus* forest cover after the Taupo Pumice eruption, while Gramineae, *Halocarpus, Phyllocladus* and also podocarps spread into sites vacated by the *Nothofagus*.

Radiocarbon dates and maximum ages of *Libocederus* cohort trees indicate that the western sector of the Moawhango Ecological District (just east of the Rangipo Desert) was deforested c. 570 years ago (Rogers,1987).

Atkinson (1983) attributes the present beech gap and 'islands' of beech forest, in the northern and eastern thirds of Tongariro National Park, to the Taupo Pumice pyroclastic flow. He believes that the limited powers of dispersal, germination, and possible seed predation in the tussockland and open communities, and possibly the lack of mycorrhiza, have inhibited or drastically slowed the re-invasion of beech into these areas.

1.10.2 Present Vegetation

The first detailed inventory of plants living within the study area was made by Colenso (1869, 1894) when he collected plants during a crossing in 1847. Cockayne (1908) described the botany of Tongariro National Park in terms of plant formations. He described the formations in detail and discussed the ecological setting of each. It is of conjecture whether Cockayne actually crossed the study area. Atkinson (1981) mapped the north-east sector of the study area during his vegetation survey of Tongaririo National Park. Within this sector he compiled five vegetation mapping units: intact mountain beech forest, mountain toatoa scrub, monoao and red tussock shrubland to gravel and stonefields with sparse mountain inaka and bristle tussock.

CHAPTER 2

LAHAR AND FLUVIAL CONSTRUCTIONAL SURFACES

2.1 General Introduction

Laharic and fluvial constructional surfaces occupy two thirds of the study area (Plate 1.1) and dominate the landscape. The lahar and flood events which deposited the lithologies forming these surfaces have been an integral part of the evolution of the post-Taupo Pumice landscape. In this chapter the stratigraphy of the major lahar and fluvial deposits is examined to elucidate the periodicity of the post-Taupo Pumice lahars and the volume of their deposits. Some sedimentological aspects of the lahar deposits are also discussed.

2.2 Methods

2.2.1 Field Descriptions

(1) Lahar And Fluvial Deposits

The number and distribution of all the lahar and fluvial deposits were determined by measuring and describing selected sections. Detailed descriptions for all sections are found in appendix 1. Site localities for all sections are shown in Plate 2.2

Both the clasts and the matrix of each deposit were described. Clast descriptions include modal clast size, largest clast, percentage of clasts and clast type. Matrix is used here for any grain size finer than coarse pebble size (<16mm). The matrix description includes colour, grain size, and grain sorting, and any other distinctive features. For example, some deposits could be distinguished on their relative percentages of individual grain colours, degree of cementation, or amount of loam. The fabric describes the relationship between the clasts, and between the clasts and the matrix. Grain size and grain sorting measurements were carried out for the fluvial deposits. Grain size and sorting of all deposits, including the tephra and aeolian deposits, were assessed using the Geological Society of New Zealand field wallet.

(2) **Tufa Trig members**

The nomenclature used here for the Tufa Trig members follows that used by S.L. Donoghue. The members at present have informal status. Where an informal member cannot be correlated into the type section for the Tufa Trig Formation, a suffix is added on to the number. A common example is Tufa Trig member 7a. Tentative correlations between sections in this study are question-marked and uncorrelated members are designated as 'unnamed Ruapehu ash deposits.'

The Tufa Trig members were correlated on the basis of their morphology and on their stratigraphic position. Characteristics that aid in correlation are variations in grain size, grain sorting, and colour of the individual unit. The grain size classification for pyroclastic particles by Andrews (1982, pg 29) has been modified for these descriptions (Fig. 2.1). The modified nomenclature was used because there were recognisable grain size differences seen in the field within the ashes, and these differences were used for correlation of the tephra deposits.

Figure 2.1 Differences between Andrew's (1982) classification for pyroclastic particles and this study.

Andrew's Nomenclature		Nomenclature In This Study	
ϕ	Pyroclastic Particles	mm	Pyroclastic Particles
-1		2	
0		1	Coarse Ash
1	Coarse Ash	0.5	
2		0.25	Medium Ash
3		0.125	Fine Ash
4	Fine Ash	.0625	Very Fine Ash

(3) **Aeolian Deposits**

The parameters used to describe the aeolian deposits, formalised in chapter 3 as the Makahikatoa Sands, are:

1) Munsell colour
2) grain sorting
3) grain size
4) soil texture
5) soil structure
6) soil penetration resistance
7) worm casts
8) roots
9) rhizomorphs and
10) boundaries.

Pedogenesis was of interest in this study partly to assess the weathering and soil forming history of Makahikatoa Sands, and partly to investigate the physical and chemical fertility of the Makahikatoa Sands for plant growth. Therefore, much of the description follows the criteria of Taylor and Pohlen (1962).

The Makahikatoa Sands often displayed similar morphological characteristics despite being separated by interbedded Tufa Trig members. Therefore, each section is described in terms of a typical Makahikatoa Sand deposit, and any distinctive differences to the typical deposit are additionally described. The same applies for the paleosol developed in Makahikatoa Sands.

2.2.2 Correlation Of Debris-flow And Fluvial Deposits.

The presence of interbedded Tufa Trig Members was useful to separate and correlate the post-Taupo Pumice lahar and fluvial deposits, particularly in stratigraphic sections that are located on the inactive area of the fan where they are better preserved (Plate 2.1). Where tephric and aeolian stratigraphy was absent, deposits were correlated using the lithological criteria discussed earlier. This was especially the case for deposits found on the active fan, which have limited tephra control.

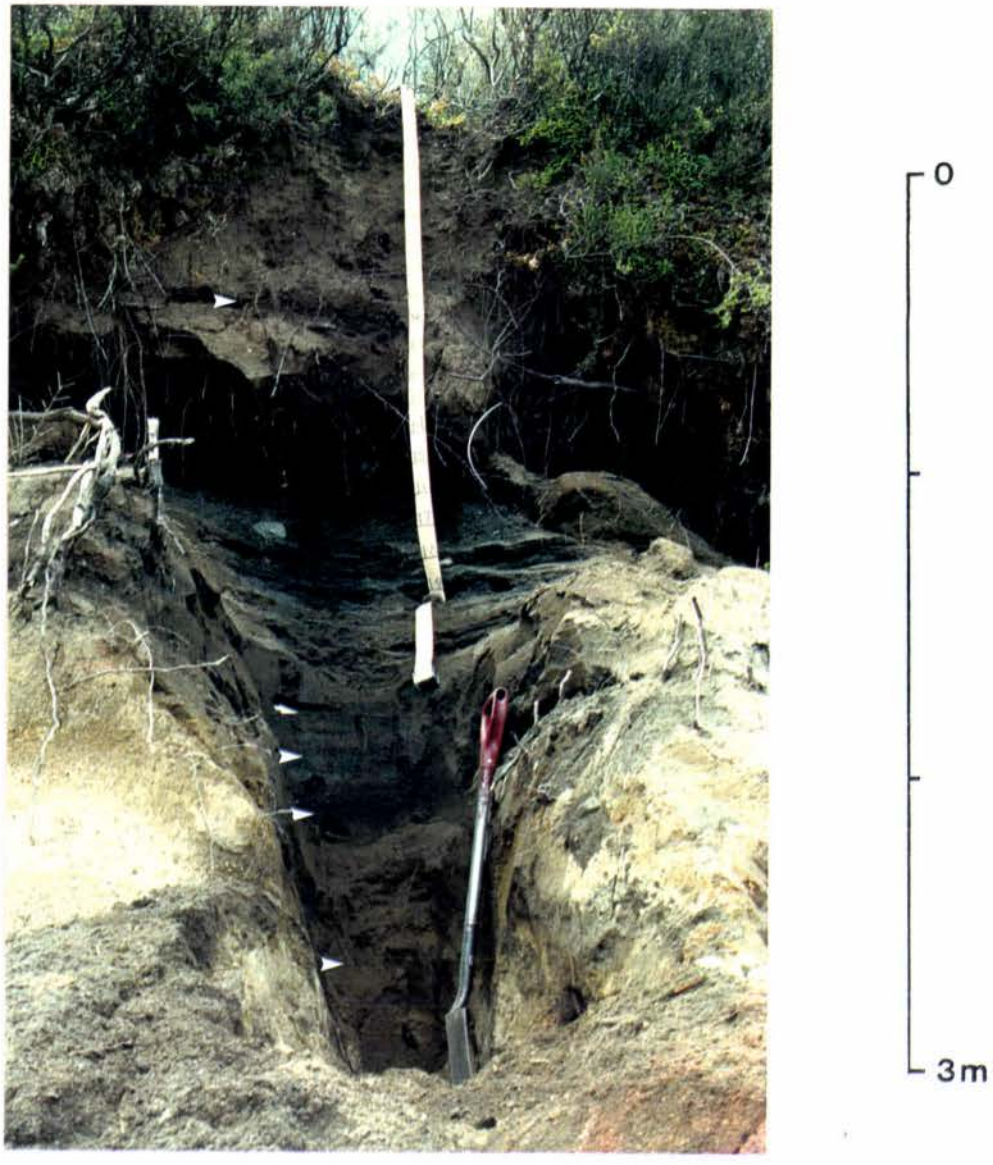

Plate 2.1 Section 8 - Death Gully

Tufa Trig members (arrows) provide stratigraphic control on the fluvial deposit found between 1.4 and 1.9m. The third arrow below the deposit points to Tufa Trig member 4 which is dated at 850 yrs B.P. Although not visible in the photograph, the Kaharoa Ash, dated at 665 yrs B.P., immediately overlies the fluvial deposit. Thus a bracketing date of 665 B.P. to 850 yrs B.P. is obtained for this fluvial deposit.

2.2.3 Distribution Of Debris-flow And Fluvial Deposits

The distribution of the lahar and fluvial deposits was determined by traverses, and checking of numerous stratigraphic sections. Boundaries were drawn on 1:25,000 aerial photographs (photographs enlarged from 1:28,000 and 1:30,000 aerial photographs) and later tranferred on to a 1:25,000 cadastral maps (Fig. 2.4).

2.2.4 Chronology For Lahars And Flood Events

A chronology for the lahar and fluvial deposits was developed by: 1) describing sections which contained lahar deposits intercalated with Tufa Trig members that are dated elsewhere and correlated into these sections, 2) radiocarbon dating of charcoal preserved in the Makahikatoa Sands that underlie and overlie the lahar deposits, and 3) tree-ring dating.

2.3 Results And Discussion

2.3.1 Correlation and Spatial Distribution

The correlation of lahar and fluvial deposits between stratigraphic sections located both on the active and the inactive fan (Plate 2.2) has enabled the distribution of these deposits to be mapped. Therefore the discussion draws on stratigraphic correlation columns (Figs. 2.2 and 2.3), and on distribution maps of the lahar and fluvial deposits (Fig. 2.4).

Plate 2.2

Site localities of stratigraphic sections 1-12 are described in the stratigraphic correlation columns for lahar and fluvial deposits (Figs. 2.2 and 2.3). Sections 2 and 15 occur south of this photograph at T20/421993 and T20/433984.

Sections 1, 7, and 13-20, are descibed in the stratigraphic correlation columns for the Makahikatoa Sands (Figs. 3.2 and 3.3). Detailed descriptions of all sections are found in Appendix 1.

The white arrow by sections 10 and 11 points to reference locality Scorpion Gully (see Fig. 1.2). The white arrows higher in the photograph from left to right point to reference localities Death Valley, Barbed Wire Gully and The Chute respectively. The dark region by sections 21 and 16 is part of Large N. solandri Enclave.

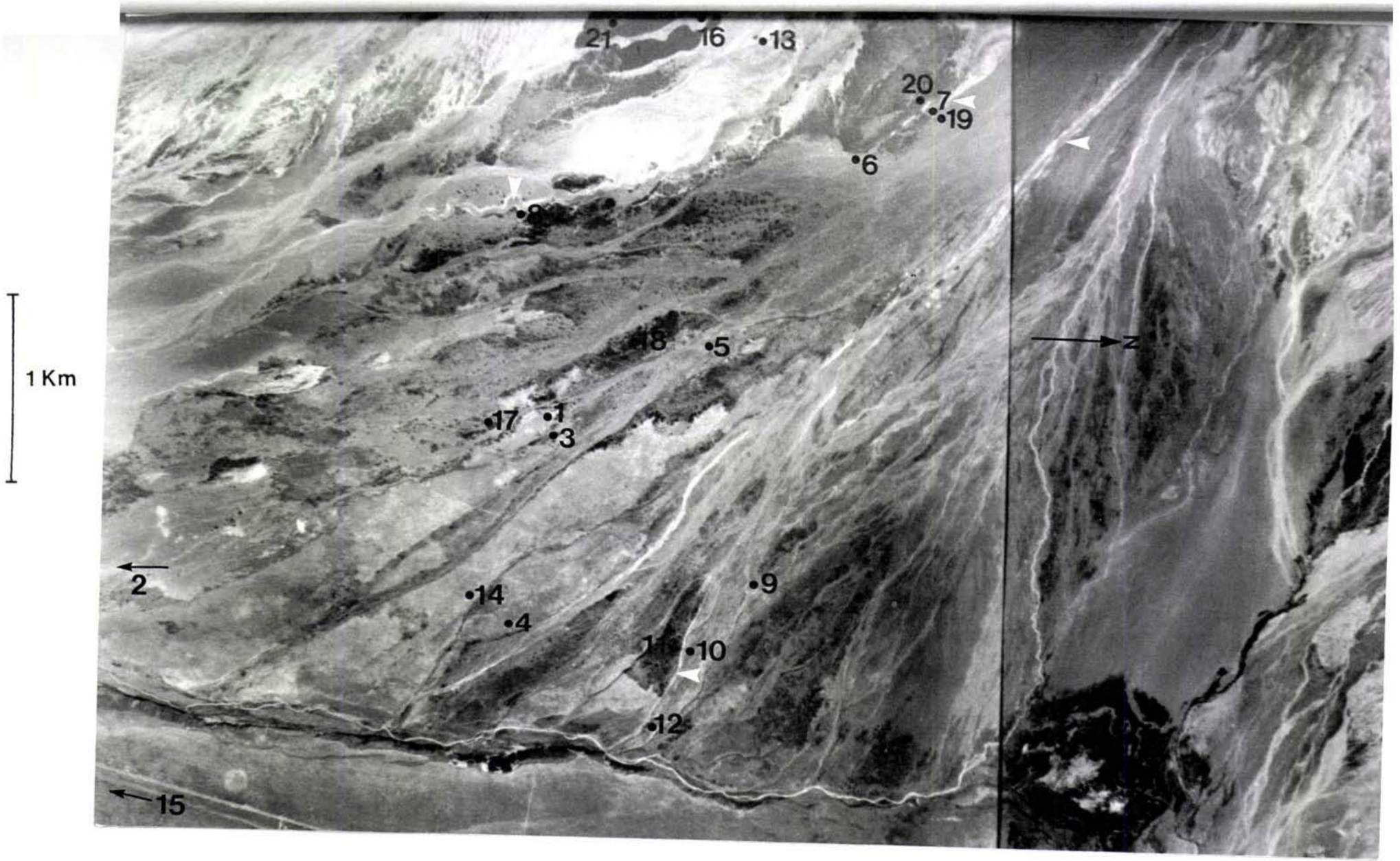
21
16
13
20
7
19
6
8
18
5
17
1
3
2
14
4
9
10
12
15
z
1 Km

Figure 2.2 Stratigraphic correlation columns for sections located on the inactive fan.

The diamictons are numbered chronologically from 1 (oldest) to 11 (youngest). Informal tephra members belonging to the Tufa Trig formation are ordered chronologically and prefixed by the letter T. The datum line is drawn at the base of Tufa Trig member 4. The Kaharoa Ash is prefixed by the letter K., and the fluvial deposits are prefixed by the letter F. Localities of all sections are shown in plate 2.2. For detailed descriptions of the sections see appendix 1.

Deposit Symbols

Matrix supported diamicton: ungraded

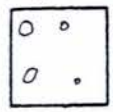

Clast supported diamicton:
* (matrix supported at base) Grading

ungraded reverse*

Fluvial Deposits

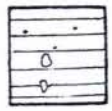

Makahikatoa Sands

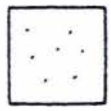

Paleosol developed in Makahikatoa Sands

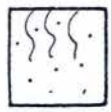

Taupo Pumice ignimbrite

Dashed lines represent a tentative correlation of a deposit to other sections, using the criteria of stratigraphic position and/or lithologic similarity.

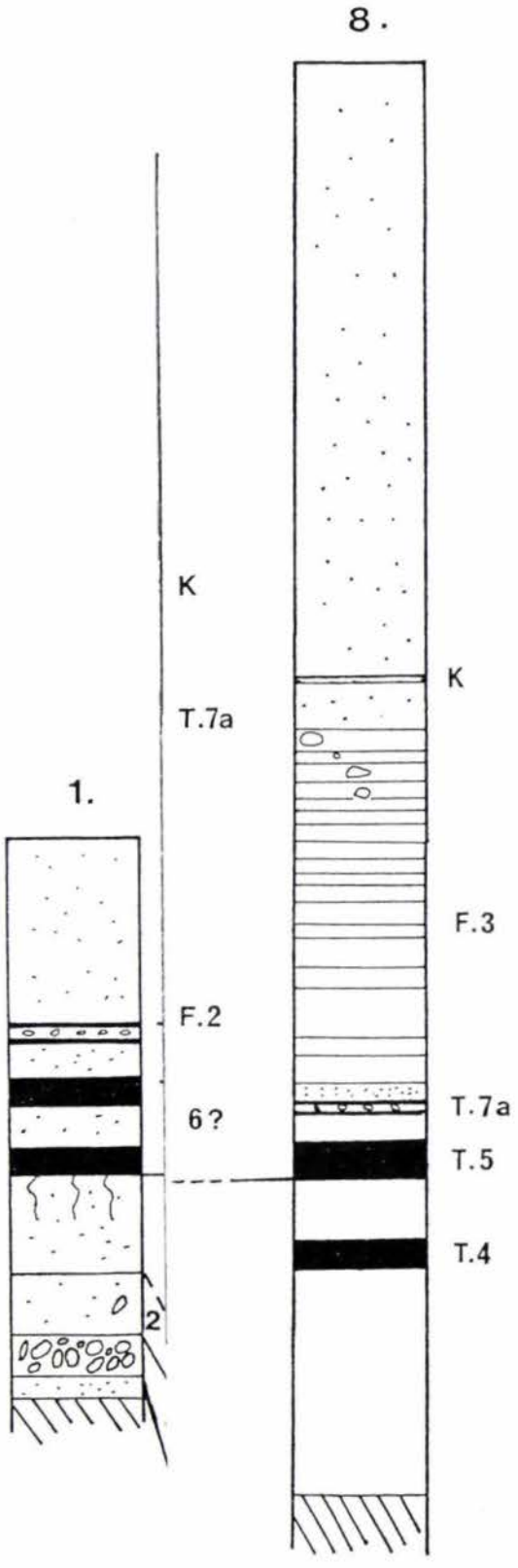
8.
K
T.7a
1.
F.3
F.2
T.7a
6?
T.5
T.4
2

Figure 2.3 Stratigraphic correlation columns for sections located on the active fan.

The diamictons are numbered chronologically from 1 (oldest) to 11 (youngest). Informal tephra members belonging to the Tufa Trig formation are ordered chronologically and prefixed by the letter T. The datum line is drawn at the base of Tufa Trig member 4. The Kaharoa Ash is prefixed by the letter K., and the fluvial deposits are prefixed by the letter F. The Mangaio Formation located in secton 10 is a pre-Taupo Pumice lahar deposit (S.L. Donoghue pers. comm.). Localities of all sections are shown in Plate 2.2. For detailed descriptions of the sections see appendix 1.

Deposit Symbols

Matrix supported diamicton: Grading

ungraded reverse

Clast supported diamicton:
* (matrix supported at base)
# (matrix supported at top) Grading

ungraded normal # reverse *

Fluvial Deposits

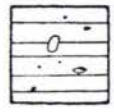

Makahikatoa Sands

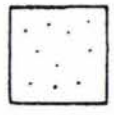

Paleosol developed in Makahikatoa Sands

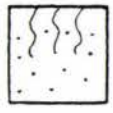

Taupo Pumice ignimbrite

Dashed lines represent a tentative correlation of a deposit to other sections, using the criteria of stratigraphic position and/or lithologic similarity.

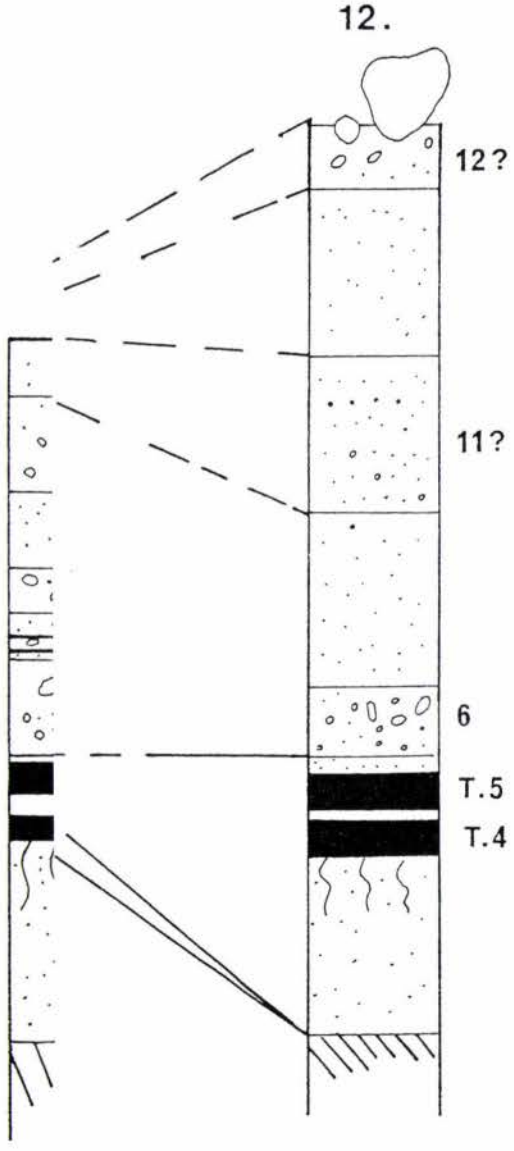
12.
12?
11?
6
T.5
T.4

Figure 2.4 Distribution maps of informal members of the Whangaehu Formation.

Two types of distribution maps are presented. The first is a generalised distribution map where mapping units represent the youngest lahar deposit of a sequence found in a given area, irrespective of the tephra cover beds or overlying Makahikatoa Sands (Map 1 - located in back pocket). The legend for Map 1 (facing page) also names the older lahar and fluvial deposits found within each mapping unit.

The second type of distribution map (Maps A to D - see following pages) is more specific. Here the mapping units (shown below) represent the areas inundated by individual lahars inferred from the distribution of their deposits. The area covered by lahars 3 and 4 could not be mapped individually because their deposits were preserved in only 1 locality (Fig. 2.2).

MAP LEGEND FOR MAPS A TO D

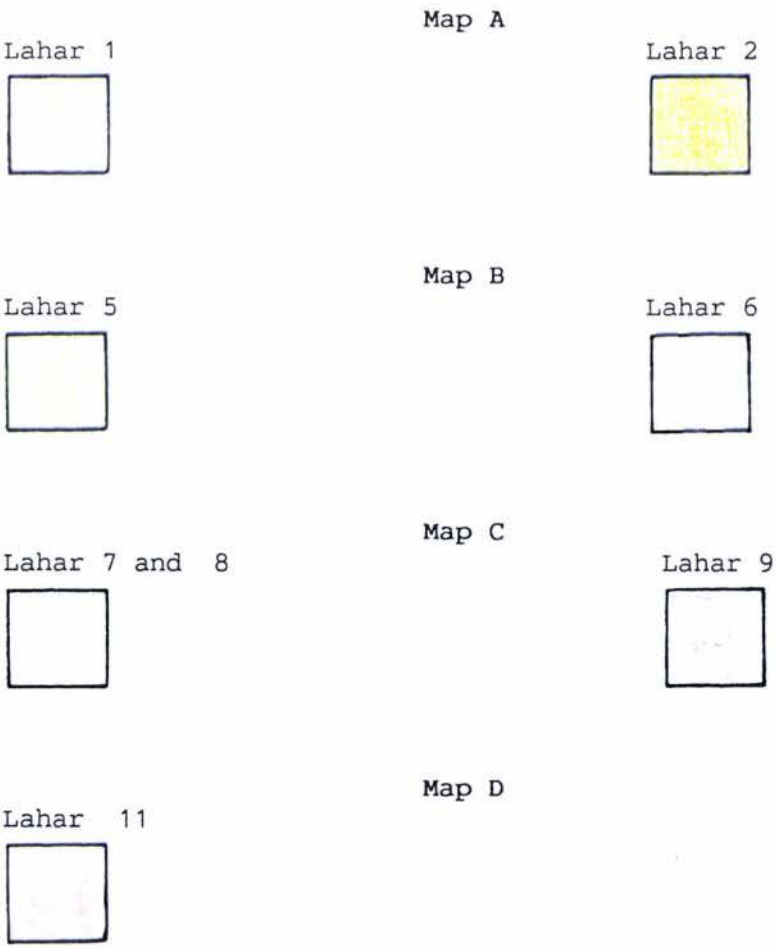

Note: the grids in maps 1 and maps A-D represent 1 km² on the ground (1:25,000); vertical lines equal grid north.

MAP LEGEND FOR MAP 1

- accompanying map is located in the back pocket

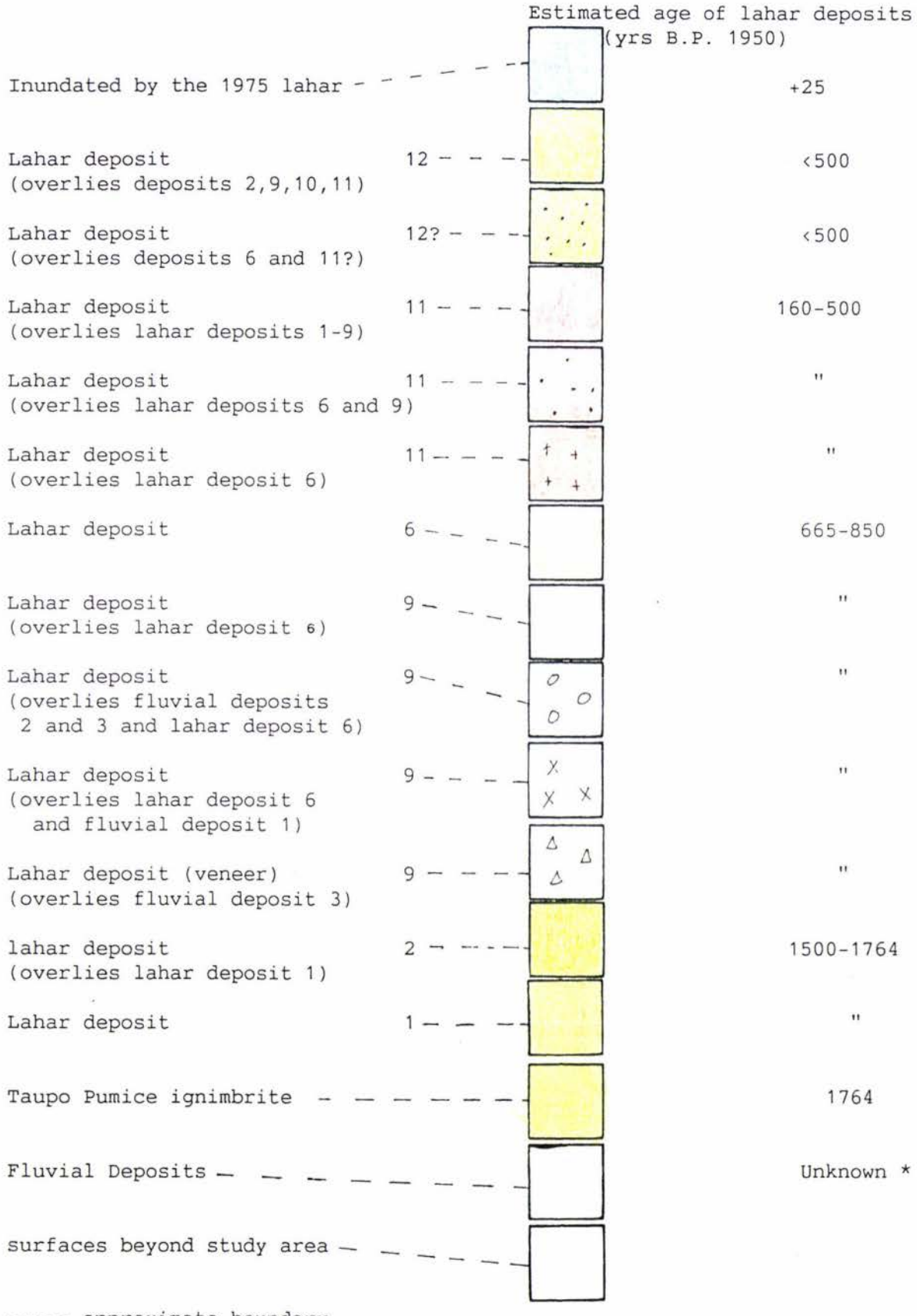

----- approximate boundary

*Fluvial deposits range in age from the present day in age to 1764 yrs B.P.

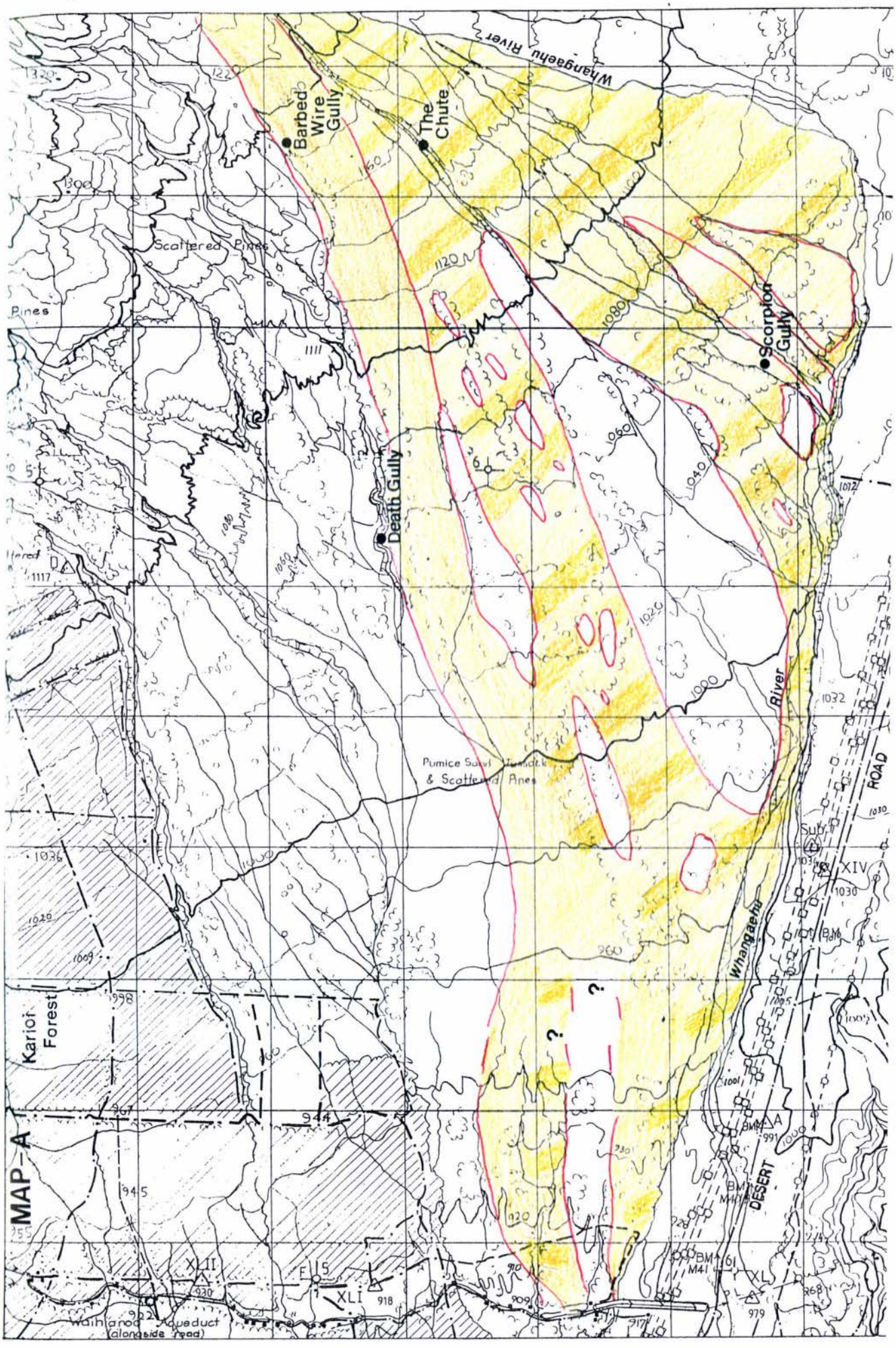
Whangaehu River
Barbed Wire Gully
The Chute
Scattered Pines
Scorpion Gully
Death Gully
Pumice Sand Tussock & Scattered Pines
Whangaehu River
ROAD
Karioi Forest
MAP-A
DESERT
Waihanoa Aqueduct (alongside road)
Pines

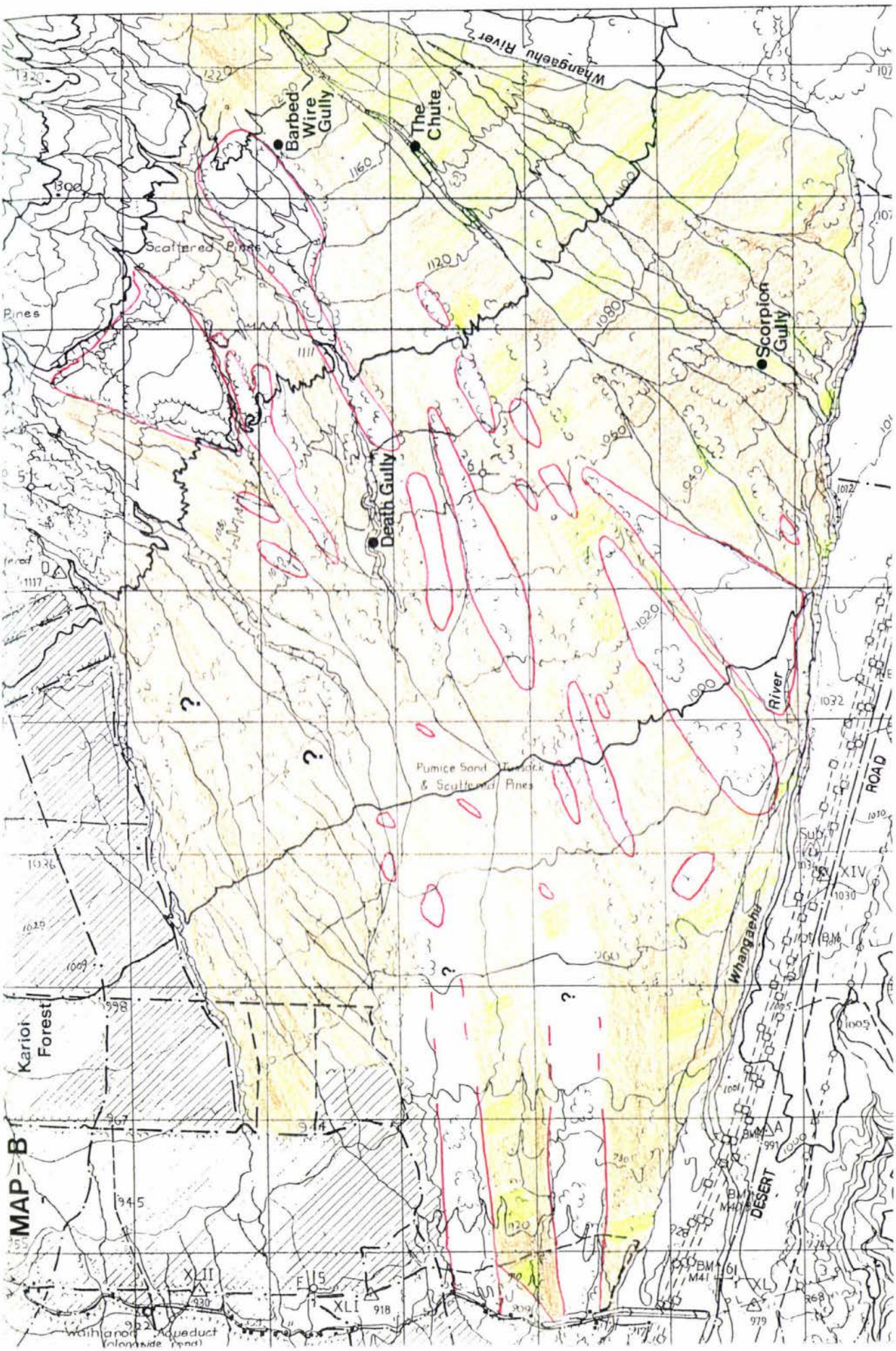
Whangaehu River
Barbed Wire Gully
The Chute
Scattered Pines
Pines
Scorpion Gully
Death Gully
Pumice Sand Flowdack & Scattered Pines
River
ROAD
Whangaehu
DESERT
Karioi Forest
MAP=B
Waihanoa Aqueduct

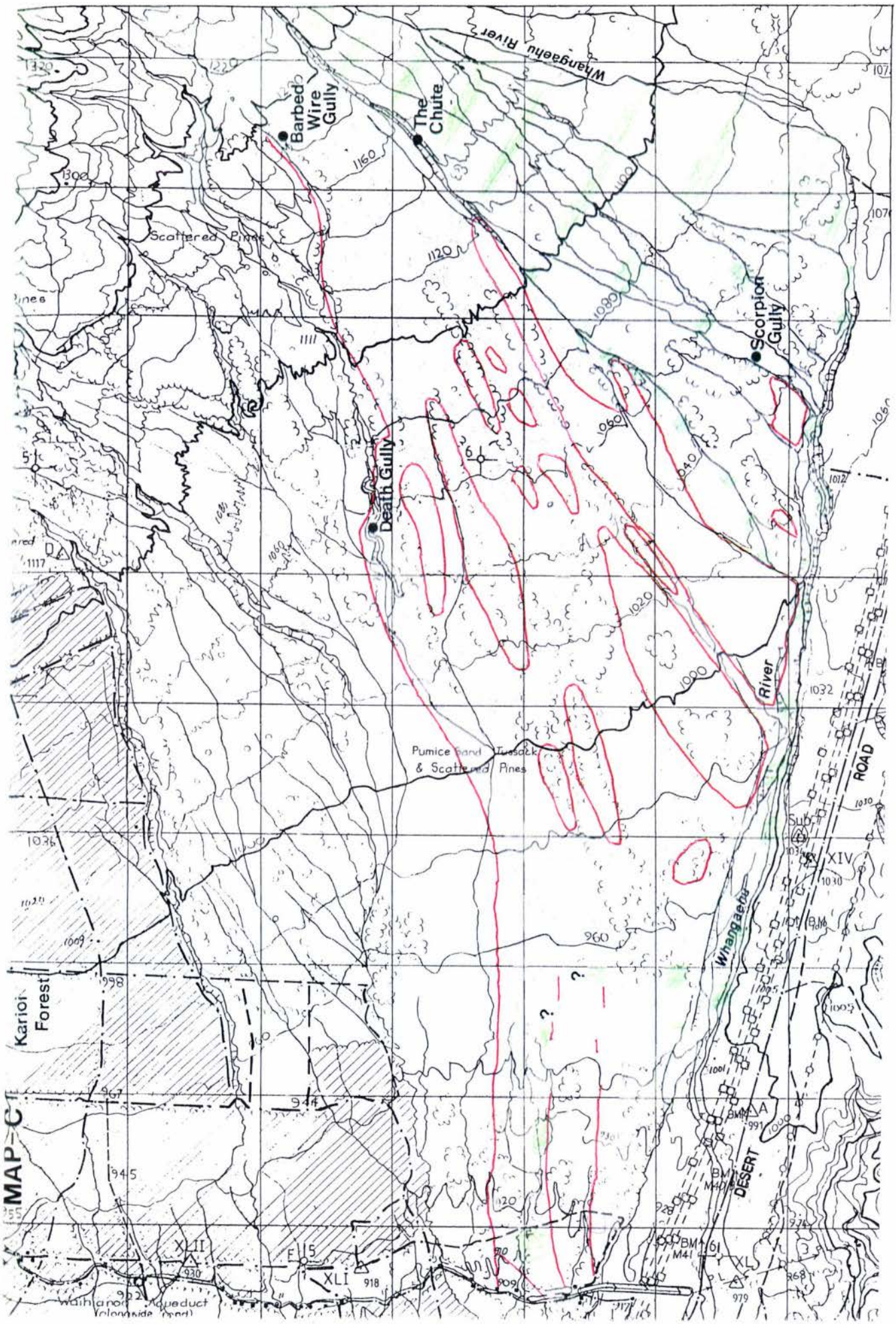
Whangaehu River
Barbed Wire Gully
The Chute
Scattered Pines
Scorpion Gully
Death Gully
Pumice Sand Tussock & Scattered Pines
River
ROAD
Whangaehu
DESERT
Karioi Forest
MAP=C
Waihanoa Aqueduct

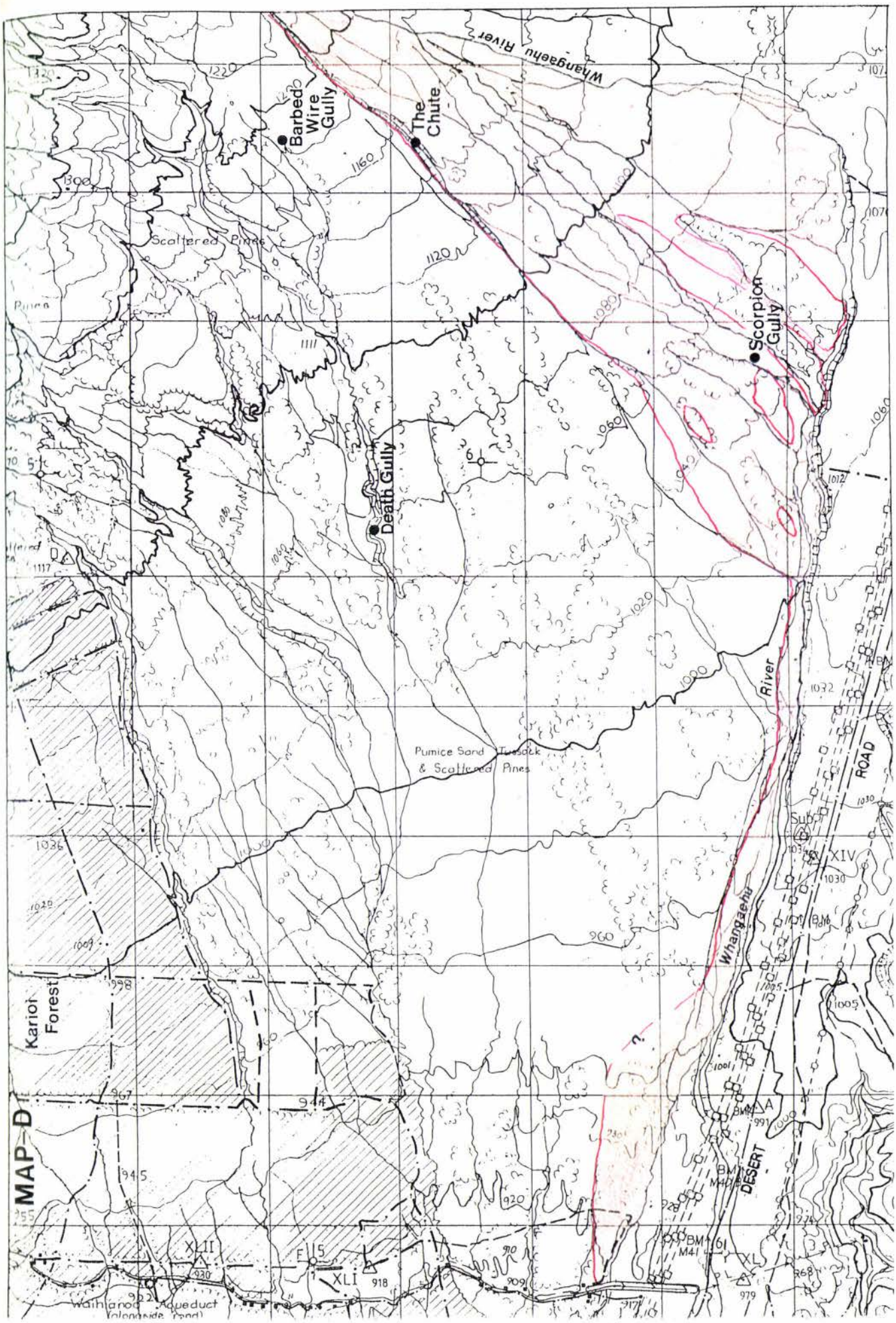
Whangaehu River
Barbed Wire Gully
The Chute
Scattered Pines
Scorpion Gully
Death Gully
Pumice Sand Tussock & Scattered Pines
Whangaehu River
ROAD
DESERT
Karioi Forest
MAP D
Waihanoa Aqueduct

Stratigraphic correlation columns show that at least ten major lahar events have inundated the Rangipo Desert since the Taupo Pumice eruption. Of these ten lahars, six (numbered 1,2,5,6,9 and 11) over-topped The Chute and deposited their respective lithologies on the inactive fan (Fig. 2.2, Fig. 2.4). Two of the remaining four major lahars, numbered 7 and 8, deposited their lithologies over the active fan but are only tentatively identified in a distal locality on the inactive fan (Fig. 2.2, Plate 2.2). It is possible that lahars 7 and 8 did in fact flow across the rest of the inactive fan but their respective lithologies have since been re-worked or buried. As a result, the area awashed from lahars 7 and 8 (Fig. 2.4, Map C) is considered a minimum estimate. Similarly, the deposits of lahars 3 and 4, which are preserved at the same distal locality on the inactive fan as lahar deposits 7 and 8, have probably also been re-worked or buried on the active fan and on other parts of the inactive fan.

Lahar deposits 1 and 2 are found mainly on the remnant 'islands' located on the inactive of the fan. An example of a remnant 'island' can be seen in Plate 2.2, where stratigraphic section 18 is located. These 'islands' are composed of preserved Taupo Pumice ignimbrite deposits underlain by older tephra formations. Lahar deposits 1 and 2 occur within the post-Taupo Pumice paleosol immediately above the Taupo Pumice ignimbrite. They are either covered by a sequence of Makahikatoa Sands and interbedded with Tufa Trig members (section 1, Fig. 2.2), or exposed at the surface.

Surrounding these 'islands,' on the inactive fan are wide, semi-confined channels that have been infilled by fluvial and lahar deposits. Lahar deposits 6 and 9 (section 5, Fig. 2.2) are commonly found overlying a sequence of fluvial deposits within these channels (Plate 2.3). In these areas lahars 6 and 9 are separated by a thin deposit of aeolian sands; however, further northwards (up slope) the two deposits are separated by a thick fluvial deposit (section 6, Fig 2.2). As a result the correlation lines between these two deposits at sections 5 and 6 are tentative. If this correlation were proved wrong at a later date then this would imply that a further lahar deposit occurs in the sequence which over-topped The Chute between lahar deposits 5 and 6. The boundary marking the change between the sequence of deposits found in sections 5 and 6 could not be located, therefore, a dashed line is drawn on Map 1 (Fig. 2.4).

Plate 2.3 Boulders supported by thin matrix comprising lahar deposits 6 and 9, located on the wide, semi-confined channels of the inactive fan. Underlying fluvial deposits are exposed by the spade.

The influx of debris associated with the deposition of lahar deposits 6 and 9 provided an extensive source of material available for re-working. Fluvial deposits located in sections 6, 7, and 8 (Fig. 2.2) were deposited as a result of the re-working of this debris. The deposition of these fluvial deposits was, however, not a synchronous event as illustrated between sections 7 and 8. Tufa Trig member 7a overlies fluvial deposit F.2 at section 7 but underlies fluvial deposit F.3 at section 8. This implies that the fluvial deposition migrated down slope (south) over time, depositing first at section 7 and subsequently at section 8. Section 6, located between stratigraphic sections 7 and 8, appears to have received a continual influx of reworked debris which spans the periods of fluvial deposition recorded in the other 2 sections.

Lahar deposit 11 is located extensively over the active fan as a surface deposit (Fig 2.3.; Fig. 2.4, Map D) but is located only in a limited area on the inactive fan, just south-west of the Chute (section 4, Fig. 2.3). This deposit represents the last major lahar to inundate the Rangipo Desert, although, it did not quite have the sufficient volume required to over-top The Chute up slope of Barbed Wire Gully.

Lahar deposits found in sections 9 and 10 (Fig. 2.3) are typical sequences found on topographically lower areas of the active fan. On the other hand sections 11 and 12 are found on topographically higher areas on the active fan, and therefore, contain thinner or fewer lahar deposits. The reason for the height variations between these areas was due to the suseptibility of surfaces being cut during the degradational period between c.1500 yrs B.P. and yrs 850 yrs B.P. Although the cut surfaces were infilled by lahar and fluvial deposits, as shown in sections 9 and 10, they still remain topogaphically lower and more susceptible to lahar inundation. Scorpion Gully (Plate 2.4) represents the boundary between two such surfaces.

Lahar deposits 10 and 12 (Fig. 2.3) were not deposited by large lahar events, instead they represent smaller lahars which locally over-topped locally at Scorpion Gully.

Plate 2.4 Location: Scorpion Gully

Section 9 (Fig. 2.3) is located to the right (north) of Scorpion Gully whilst section 11 is located to the left (south) of Scorpion Gully where the *Phyllocladus* scrub is observed.

During a degradational period between c. 1,500 yrs B.P. and c. 850 yrs B.P. the surface to the right of Scorpion Gully was cut, resulting in the erosion break now observed in section 10 between the pre-Taupo Pumice and post-Taupo Pumice lahars. On the other hand, the surface to the left side of Scorpion Gully was not cut, as evidenced by a conformable sequence between the pre-Taupo Pumice and post-Taupo Pumice lahars.

The surface on the right side of Scorpion Gully has since been infilled by both lahar and fluvial deposits, as shown in section 10; whilst the surface on the left side has been surmounted by a limited number of lahars as they over-topped from the surfaces to the right.

The distribution of the 1975 lahar (Plate 2.5) shows that today the topographically lower right hand side of Scorpion Gully is still more susceptible to inundation from lahars.

Scorpion Gully

Plate 2.5 Aerial photograph taken 12 hours after the 1975 lahar. Areas that were inundated by the flow are recognised from the residual water and silt lying on the surface. The 1975 lahar shows that the topographically lower north side of Scorpion Gully continues to be more susceptible to lahar inundation. Source: Lloyd Homer, N.Z. Geological Survey.

Section 22 (appendix 1), located between Makahikatoa Stream and Large *N. solandri* Enclave, records the deposition of a post-Taupo Pumice Pumice lahar deposit. Since lahar 6 is the largest post-Taupo Pumice lahar deposit found in the study area (Table 2.3), and its matrix is similar to the deposit found in stratigraphic section 22, it suggests that these deposits correlate. However, as there is no tephra control, the correlation is tentative and the corresponding area is question-marked as belonging to lahar deposit 6 on map 1.

2.3.2 Periodicity Of Major Lahars

Calculation of lahar periodicity was achieved by providing bracketing dates on the lahar deposits where possible. Table 2.1 details the radiocarbon dates used in the chronology and Fig. 2.5 illustrates the relationship between the stratigraphy and the chronology.

Table 2.1 Radiocarbon Dates Used In This Study

	d13C (permil)	Converted Age (yrs B.P.)	New Age (yrs B.P.)
NZA 601	-26.97	< 200	< 200
WK 1487	-26.8	490 ± 65	500 ± 70
Wk 1488	-27.4	650 ± 50	660 ± 50
Wk 1489	-27.9	830 ± 60	850 ± 60

see Figure 2.5 for stratigraphic position of dates

Wk1488 and Wk1489 were kindly supplied by S.L. Donoghue from Ngamatea Swamp.

The white rhyolitic marker bed found in the study area is the Kaharoa Ash (S.L. Donoghue, pers comm.) and is dated at 665 ± 58 yrs B.P (Lawlor, 1980). It has been identified in sections 16 (Fig. 2.5), sections 7 and 8 (Fig. 2.2), and recognised in other localities. The presence of Tufa Trig member 7a, the datum line in Fig. 2.5, is the first informal Tufa Trig member found below the Kaharoa Ash. The age of Tufa Trig member 7a is therefore greater than 665 ± 58 yrs B.P. An age of 730 yrs B.P. is suggested for Tufa Trig member 7a based on accumulation rates of the Makahikatoa Sands (section 3.6). The presence of three lahar deposits between Tufa Trig members 7a and 4, suggests that the true age of Tufa Trig member 4 is closest to its underlying radiocarbon date of 850 ± 60 yrs B.P. (WK 1489) which measured from peat sampled at Ngamatea Swamp.

Figure 2.5 Correlation columns showing the position of radiocarbon samples which are the basis for the chronology of the post-Taupo Pumice deposits. Further chrononlogies are provided by the Kaharoa Ash and the Taupo Pumice ignimbrite and one tree-ring date.

Numbers 6,9 and 11 represent lahar deposits belonging to the Whangaehu formation. T.4, T.5, and T.15 represent informal members of the Tufa Trig formation. Details for stratigraphic sections 4, 16 and 21 are located on Plate 2.2 and described in appendix 1.

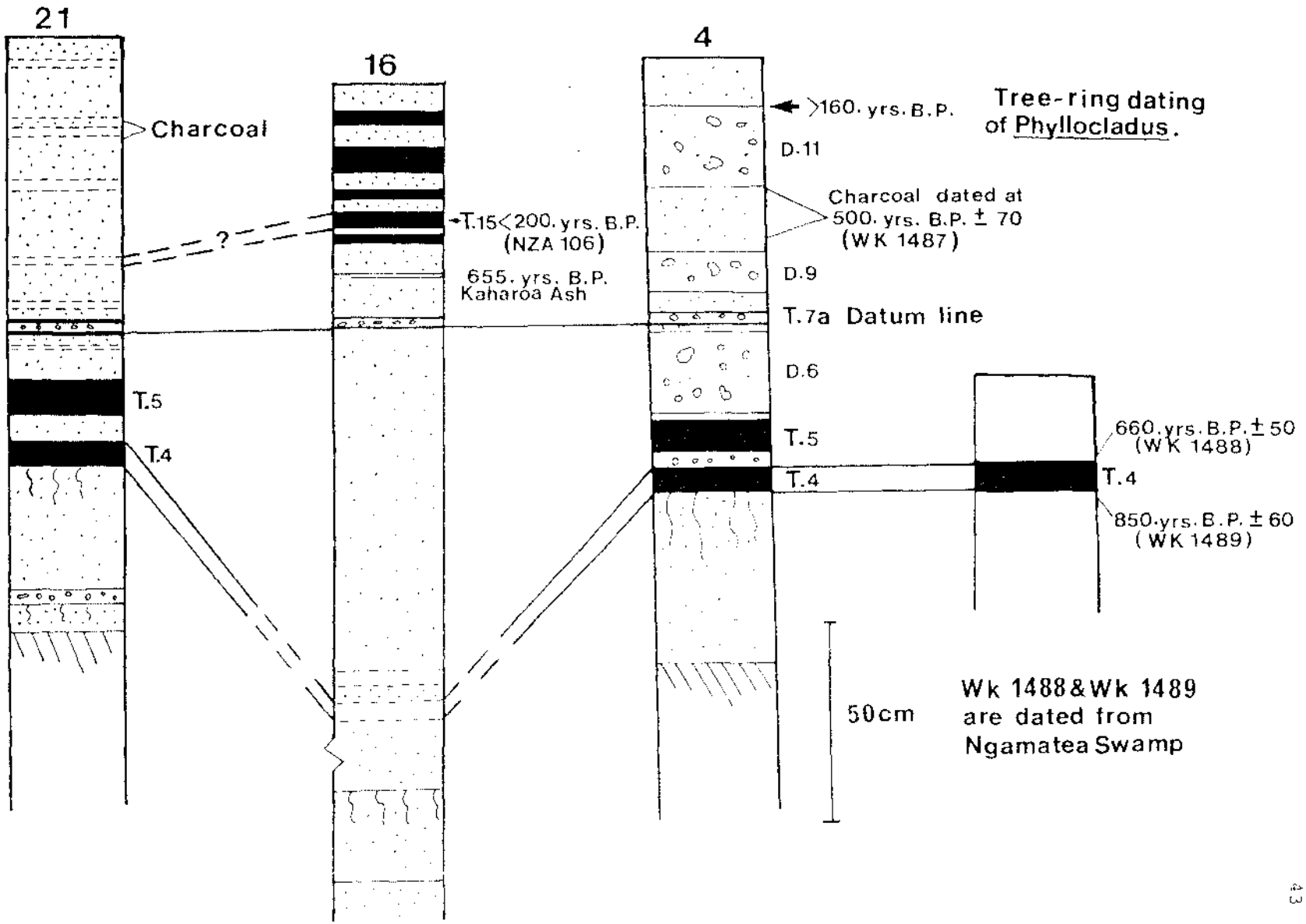
21
16
4
Charcoal
?
T.15<200. yrs. B.P.
(NZA 106)
655. yrs. B.P.
Kaharoa Ash
>160. yrs. B.P.
Tree-ring dating
of Phyllocladus.
D.11
Charcoal dated at
500. yrs. B.P. ± 70
(WK 1487)
D.9
T.7a Datum line
D.6
T.5
T.4
T.5
T.4
660. yrs. B.P. ± 50
(WK 1488)
850. yrs. B.P. ± 60
(WK 1489)
50cm
Wk 1488 & Wk 1489
are dated from
Ngamatea Swamp

From this chronology the periodicity of major lahar events could be calculated (Table 2.2).

Table 2.2 Periodicity Of Major Lahar Events In The Rangipo Desert.

Age (B.P. 1950)	Lahar Events (inferred from lahar deposits)
c. 160-500	Lahar 11
c. 500-800	Lahar 6,7,8 and 9
c. 800-850	Lahar 5
c. 850-1500	Lahars 3 and 4
c. 1500-1764	Lahars 1 and 2
c. 1764	(Taupo Pumice ignimbrite)

Lahar deposit 1 (Fig. 2.2), which is separated by about 5cm of Makahikatoa Sands from the Taupo Pumice ignimbrite, is aged between 1500-1800 yrs B.P. Lahar deposit 2 immediately overlies it, and therefore, is in the same age range. Lahar deposits 3 and 4 are only found at one location (Fig. 2.2) and, at present, there is no evidence to establish when these events occurred within the 850-1500 yrs B.P. time frame. The estimated age of lahar 5 is based on the thickness of aeolian sands that separate Tufa Trig members 4 and 5 in sections where the lahar deposit is not found. Lahar deposits 6,7,8, and 9 were deposited between 800-665 yrs B.P. This is calculated using the Kaharoa Ash found in section 8 (Fig. 2.2). Lahar deposit 6, which immediately overlies Tufa Trig member 5, is estimated to be about 800 yrs B.P. The widespread distribution of the

lahar 6 deposit (Fig. 2.4), and the large volume of its deposit (section 2.3.3), suggests this deposit correlates with the lahar deposit found further downstream in the Whangaehu catchment dated at 756 ± 56 yrs B.P. (Campbell, 1973). Lahar deposit 11 represents the last major event that inundated the study area sometime post-500 yrs B.P. but before 160 yrs B.P.

The average periodicity of major lahars to inundate the study area since the Taupo Pumice ignimbrite is, therefore, 1 every 160 years. However, between 850 yrs B.P and 665 yrs B.P., the periodicity increased to 1 every 37 years. Since 500 yrs B.P., to the present, only 1 major lahar has inundated the Rangipo Desert. Between the Taupo Pumice eruption and 850 yrs B.P. the periodicity is one major lahar every 229 years.

2.3.3 Volumes

The surface stratigraphy indicates that a series of large lahars have swept down the Whangaehu River since the Taupo Pumice eruption c. 186 A.D. An attempt has been made to calculate both the volume of lahar deposits that have accumulated within the study area, and the total volumes of the lahars themselves. It must be stressed that the calculations for the volumes of these deposits are minimal estimates, calculated on present deposit thicknesses; and do not allow for post-depositional erosion, deposits downstream of the study area, or the water content of the original lahars. The lahar of 1975 (Plate 2.6) left a 2-3cm veneer deposit in the study area (Plate 2.6) which has an estimated volume of 0.09×10^6 m^3. However, the total volume of the 1975 lahar, which was calculated from discharge rates based on a downstream hydrograph, was 1.8×10^7 m^3 (Page and Patterson, 1976). Thus only about one twentieth of the total volume of the lahar was deposited in the study area. This 1:20 ratio of the total volume to amount deposited in the study area has been applied to other deposits in Table 2.3. This compares to 1:33 ratio used by Scott (1988) to estimate the total volume of a lahar to the amount deposited in the late Holocene stratigraphy at Mount St. Helens.

Plate 2.6 Distinctive light yellow-brown coloured veneer deposit from the 1975 lahar contrasts with the older grey surface in the foreground. The channel the 1975 lahar over-topped can be seen in the right background.

Table 2.3 Volume estimates for informal members of the Whangaehu Formation.

Lahar deposit number	Estimated Volume of deposit ($\times 10^6$ m^3)	Projected total volume ($\times 10^6$ m^3)
1975	0.09	1.8*
	ratio = 1:20	
1	2.8	56
2	1.8	36
3	0.8	16
6	12.0#	242#
7	1.3	26
8	2.1	42
9	4.4	88
11	3.4	68
	total 28.7	574

* Measured total volume Source: Page and Patterson, 1976

\# volumes for lahar deposit 6 based on inferred distribution (see Fig 2.4, Map B).

The possible hazards a future major lahar could have down stream of the study area, and also in other catchments of the mountain receiving discharge, has been documented by numerous authors (Neall 1976a and 1976b; Patterson, 1976, 1980; Latter, 1981, 1985). The potential hazard of lahars down the Whangaehu Catchment has been estimated using cumulative total volumes since the Taupo Pumice eruption (c. 1764 yrs), based on the dated lahars deposits at Mangamahu (Campbell, 1973) and recorded lahar events since 1861 (see Latter, 1985). The cumulative total volumes of the 8 major lahars shown in Table 2.3 far exceed these earlier predictions. Furthermore, these 8 lahars do not include the period of 160 yrs B.P to the present. Therefore, the potential risk of lahars in the lower catchment may be higher than earlier believed by Latter (1985).

All of these major events also exceed the total volumes of the two lahars (c.14 x 10^6 m^3) which swept down Pine and Muddy Creeks, after the 1980 eruption of Mount St. Helens (Pierson, 1985). However, from the late-Holocene stratigraphic record at Mount St. Helens, the total volume of the largest lahar was estimated to be in order of 1km^3 (Scott, 1988) which is about 4 times the size of the inferred total volume of the lahar 6 (24.2 x 10^7 m^3). Therefore, whilst lahar 6 is extremely large compared to modern day analogs, its estimated total volume is smaller than the largest late Holocene lahars at Mount St. Helens.

2.3.4 Aggradational and Degradational Periods

Since the Taupo Pumice eruption two periods of degradation and one period of aggradation have been elucidated from the geomorphology and post-Taupo Pumice stratigraphic record. After the deposition of lahar deposits 1 and 2, between c. 1,800 and 1,500 yrs ago, a period of degradation ensued until c. 850 yrs B.P. During this time wide channels were cut on the active fan by normal stream processes (Plate 2.4).

Fifty to seventy percent of the post-Taupo Pumice debris transported by the major lahars was deposited in the study area between 850 yrs B.P. and 665 yrs B.P. This was a period of major aggradation both on the active and inactive fans. Extensive re-working of this debris followed and is seen throughout the study area as thick aggradational fluvial deposits (see stratigraphic sections 6,8 and 9, Figs. 2.2 and 2.3).

Since 665 yrs B.P. degradation has resumed. The present channel at Scorpion Gully (Plate 2.4), as well as other channels on the active fan, have been cut since 665 yrs B.P. The same situation is also found on the inactive fan. Death Gully (Fig. 1.1) was cut when the aggradation of fluvial deposit 3 ceased (stratigraphic section 8) just prior to the deposition of the Kaharoa Ash dated at 665 yrs B.P. Death Gully has now incised over 10m in places.

2.3.5 Sedimentology

In the Rangipo Desert two categories of lahar deposits are recognised: these are the debris-flow deposit (Nemic and Steel, 1984; Shultz, 1984; Pierson and Costa, 1987; Costa, 1988) and the hyperconcentrated-flow deposit (Pierson and Scott, 1985; Smith, 1986; Pierson and Costa, 1987; Costa, 1988)). However, the hyperconcentrated-flow deposits were scarce and will not be discussed further in this study.

The debris-flow deposits found on the Rangipo Desert generally display four of the five characteristic features of debris-flow deposits defined by Nemic and Steel (1984). These are: (1) sheetlike or lenticular beds without erosive contacts; (2) non-graded to markedly graded beds; (3) distinct boundaries between beds but no obvious internal stratification; (4) maximum particle size showing correlation to bed thickness. Beds appear poorly sorted, but no quantitative data is given on the fifth feature that Nemic and Steel describe, bimodal to polymodal grain size distribution, often with outsized clasts.

The lithofacies of these debris-flow deposits varied over time and in space. In this study the lithofacies were divided based on changes in fabric, bed thickness and clast size (Fig. 2.6). After using this criteria for dividing up each lithofacies it became apparent that various regions of the study area possessed distinctive lithofacies assemblages. As a result four lithofacies assemblages were created which encompassed six different regions (Fig. 2.7). The distinctive nature of each lithofacies assemblage is illustrated using representative stratigraphic sections which contain each assemblage type (Fig. 2.8)

Lithofacies assemblage 1 (Plate 2.7) is found on the topographically lower areas on the active fan and the Whangaehu River. This assemblage suggests that these areas have been inundated over time by both large high-competence, and small dilute, debris-flows.

Figure 2.6 Diamicton lithofacies

Code
D = diamiction
m = matrix supported
c = clast supported
u = ungraded n = normal graded r = reverse graded
t = thin beds
b = large boulders sitting in a thin bed and protuding the surface
p = few outsized clasts in a finer matrix

Lithofacies	Fabric	Thickness (m)	Clast Size (m)
Dmu	matrix supported, ungraded	0.5-1.3	up to 4
Dmut	matrix supported, ungraded	0.1-0.2	up to 0.05
Dmub	matrix supported, ungraded with boulders protuding the surface	0.05-0.2	up to 2.5
Dmup	matrix supported, ungraded clast poor	0.1-1	up to 0.5
Dcu	clast supported, ungraded	0.3-0.0.6	up to 0.5
Dcut	clast supported, ungraded	0.1-0.25	up to 0.15
Dcn	clast supported, normal graded	0.1-0.3	up to 0.15
Dcr	clast supported, reverse graded	0.2-0.4	up to 0.25
Dcrt	clast supported, reverse graded	0.2	up to 0.05

Figure 2.7 Lithofacies Assemblages

Assemblage	Lithofacies		Location
	Common	Minor	
1	Dmu	Dcu,Dcn Dcr,Dmut, Dmub.	topographically low area on the active fan and the Whangaehu River
2	Dmub		wide, semi-confined channels on the inactive fan and topographic highs on the active fan
3	Dcut	Dmut	topographic highs on the inactive fan
4	Dmup	Dcrt	channel, southern boundary of study area, 0.75km west of Whangaehu river

Figure 2.8 Representitive facies assemblages observed in the Rangipo Desert

Assemblage 1 (section 9)
Located in wide, infilled, channels of the fan - channel deposits (over-bank deposits)

Assemblage 2 (section 9)
Located on topographic highs on the fan and wide semi-confined channels off the fan (sheet-flood deposits)

Assemblage 3 (section 1)
Located in topographic highs off the channel (over-bank deposits)

Assemblage 4 (section 2)
Located in channel at southern boundary of study area, 0.75km west of Whangaehu River (dilute deposits)

Facies Assemblage :

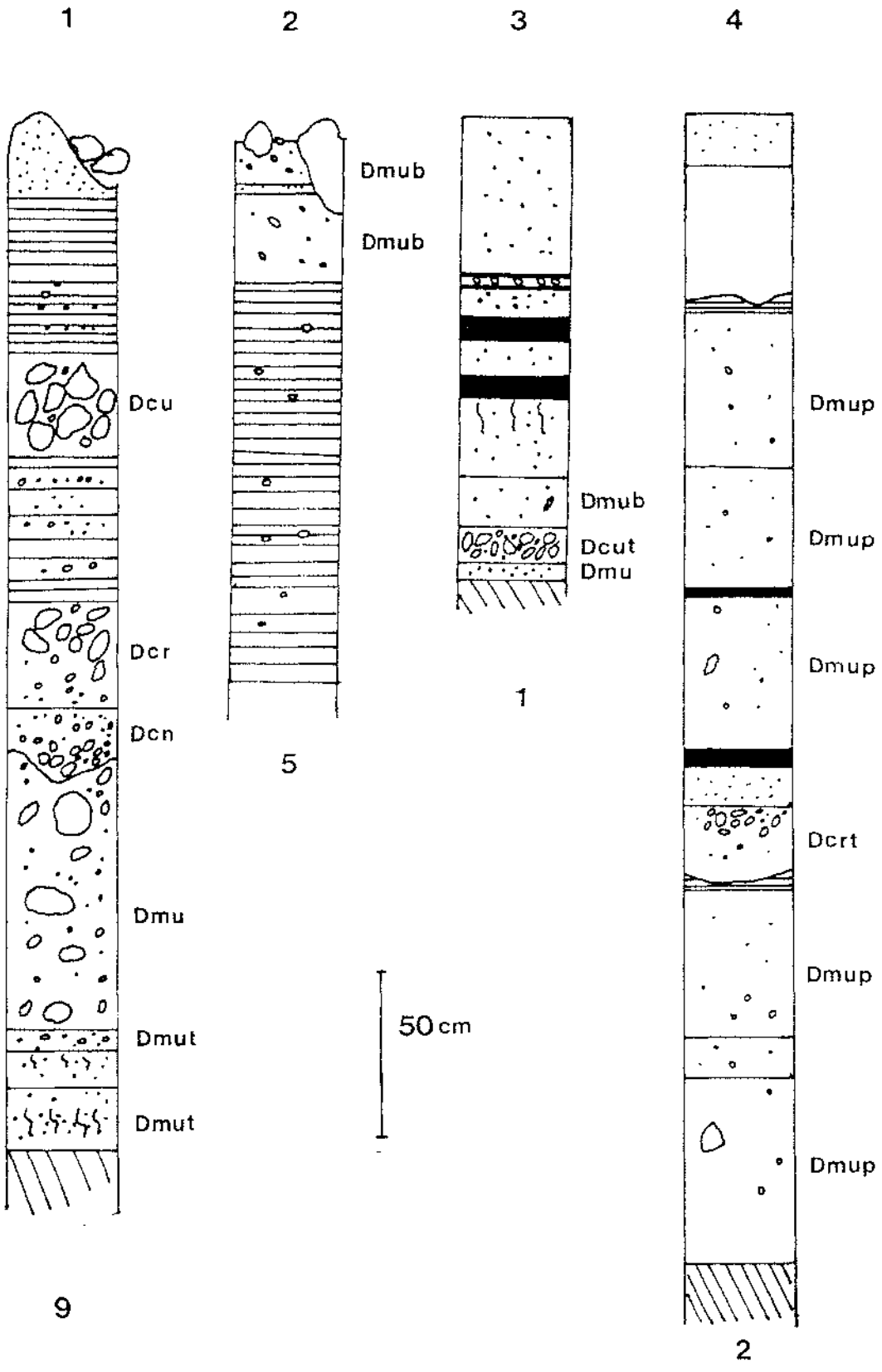

Plate 2.7 Recent stream channel cut exposes 4 deposits typical of lithofacies assemblage 1. Lithofacies Dmu (base of the spade) is the common lithofacies found in the topographically lower, wide channels on the active fan. Fluvial re-working has occurred in much of the upper part of the sequence.

Dmu = matrix supported, ungraded diamicton.
Dcn = clast supported, normal graded diamicton.
Dcr = clast supported, reverse graded diamicton.
Dcu = clast supported, ungraded diamicton.

Lithofacies assemblage 2 (Plate 2.3) is found on the topographical highs of the active fan and also on the inactive fan within wide channels. This assemblage suggests that large high-competence debri-flows have over-topped these topograhical highs, or over-topped The Chute, and became unconfined. The result is a loss of velocity behind the flow head, and the stranding of boulders in a thin matrix. Rodolfo et al. (1989) found a similar type of facies at Mount Mayon where boulders up to 5m in intermediate diameter projected from surface deposits that were less than 2m thick in over-bank areas.

Lithofacies assemblage 3 (Plate 2.8) is found on topographic highs adjacent to the wide channels described above. The presence of these deposits show that the large high-competence debri-flows that over-topped The Chute, and became unconfined, were also large enough to deposit debris on some of these adjacent higher areas. However, the lithofacies suggest that these over-flows were small and dilute, thus indicating it was only the margins of the large lahars that reached these areas. Boulders associated with these flows are assumed either eroded or buried under fluvial and more recent debris-flows in the wide semi-confined channels.

Lithofacies assemblage 4 (Plate 2.9) is found in a relict channel on the southern margin of the inactive fan. The assemblege suggests that debris-flows in this area were dilute. The boundary between diluted debris-flow deposits and hyperconcentrated flow deposits is poorly understood (Pierson and Scott, 1985; Smith,1986; Costa, 1988), however, the absence of internal stratification and the presence of outsized clasts with discernible orientation, indicates that lithofacies Dmup is formed from debris-flows, albeit diluted. Dilution has occurred because debris from these flows was stranded as the flows became very thin up stream in the semi-confined channels before reaching this area. This lithofacies was not observed at a similar distance from source along the Whangaehu River, indicating that the river channel was the major artery for large and competent lahar flows down the catchment.

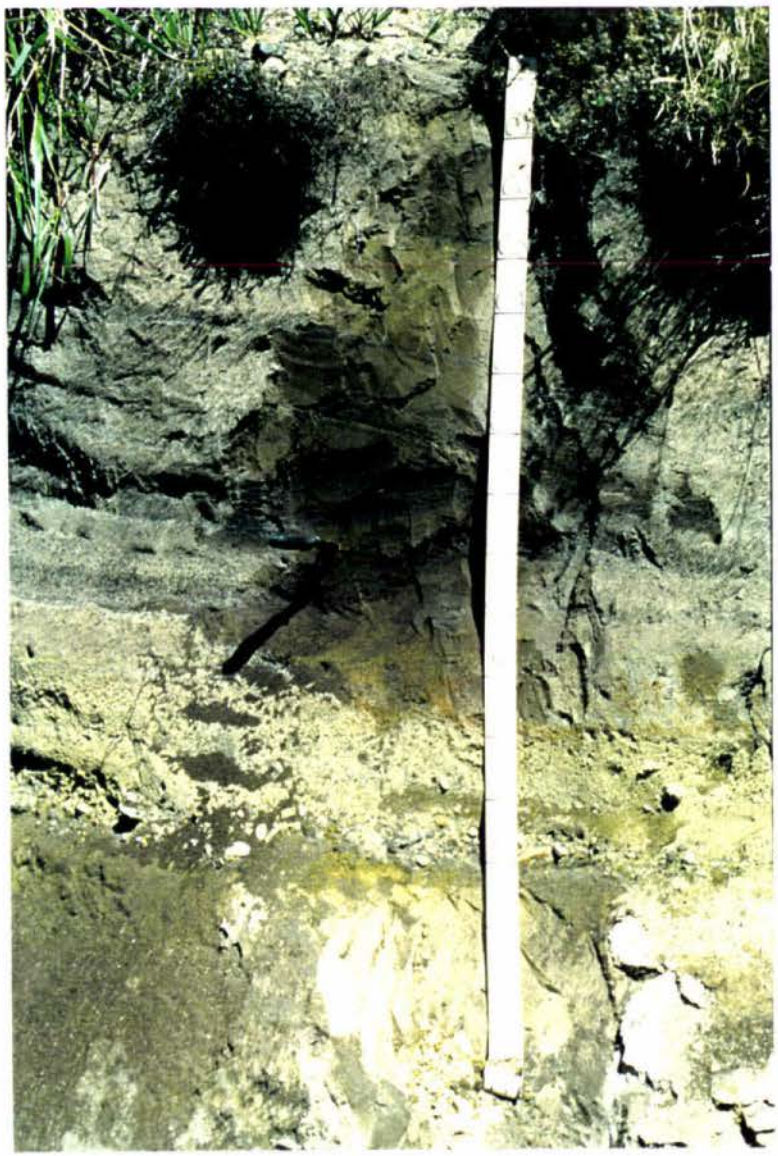

Plate 2.8 Photograph of section 1 which represents lithofacies assemblage 3 located on topographic highs on the inactive fan. The Taupo Pumice ignimbrite is also preserved in these areas and can seen in the photograph between 1.3m and the bottom of the photograph. The two over-bank deposits, typical of lithofacies assemblage 3, are located between 1.1m amd 1.3m. The lower deposit is a clast-supported diamicton whilst the upper deposit is a matrix supported diamicton.

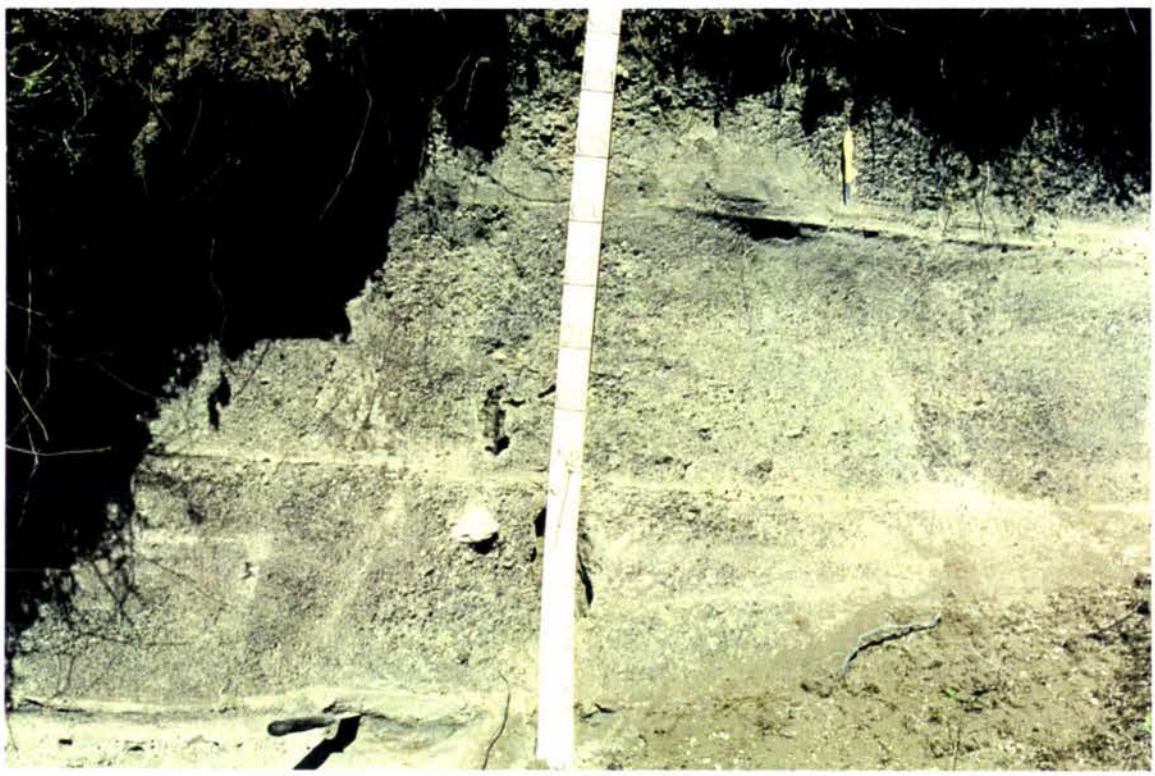

Plate 2.9 Photograph showing the three top debris-flow deposits belonging to lithofacies assemblage 4. Dilution of the debris-flow deposits is evidenced by the small number of outsized clasts in a poorly sorted matrix. Fine fluvial deposits found by the pen, just below 1.0m, and at the pocket knife separate each deposit. Note the erosive base of the top debris-flow deposit by the pen. Overlying the top deposit are Makahikatoa Sands which extend to the surface of the profile.

2.4 Conclusions

The constructional landscape of the Rangipo Desert has been inundated by ten major lahars since the Taupo Pumice eruption of c. 1764 yrs B.P. Six of these events are shown to have over-topped The Chute, and evidence strongly suggests another 4 events also over-topped The Chute. Minimum volume estimates of the deposits show that debris-flow deposit 6 was the largest and deposited at least 8.9×10^6 m^3 of debris, but quite possibly 12.0×10^6 m^3. This is between two and three times the volume of any other deposit. The 1975 lahar's total volume, calculated from a discharge hydrograph of the Whangaehu River, was 1.86×10^6 m^3 (Page and Patterson, 19), yet the volume of the resultant deposit is estimated at only 0.09×10^6 m^3. This gives a 1:20 ratio of the total volume to amount deposited in the study area for the 1975 lahar. This ratio has been applied to the other deposits, and the results indicate that the cumulative total volumes of major lahars which crossed the study area from c. 1764 yrs B.P. to 160 yrs B.P. far exceeds earlier predictions for the Whangaehu catchment. The potential hazard of a future lahar causing damage in the Whangaehu catchment area is, therefore, higher than earlier predicted.

Periodicity of major lahars to inudate the study area since the Taupo Pumice ignimbrite is 1 every 160 years. However, between 850 yrs B.P and 665 yrs B.P., the periodicity increased to 1 every 37 years. Since 500 yrs B.P., only one major lahar has inundated the Rangipo Desert. Debris-flow deposit 6, the largest deposit recorded in the study area, is estimated to have been deposited by a lahar c. 800 yrs B.P. It is therefore believed to correlate to the lahar deposit found further downstream dated at 756 ± 56 yrs B.P. (Campbell, 1973). Approximately 50-70% of the total post-Taupo Pumice debris transported by the major lahars was deposited during the period between 850 yrs B.P. and 665 yrs B.P. This was a major period of aggradation on the constructional surface, both as lahar deposits and subsequent fluvial deposits. Before and after this period fluvial degradation was the dominant process. Today, floods and smaller lahars are cutting channels into the debris-flow deposits and the older aggradational fluvial deposits.

Most of the lahar deposits in the Rangipo Desert are debris-flow deposits. The lithofacies associated with these deposits have been grouped into 4 assemblages that were found in six regions of the study area. Lithofacies assemblage 1 shows that both large high-competence and small dilute flows were common on the topographical lows on the active fan. Lithofacies assemblage 2 suggests large high-competence flows inundated the topographical highs on the active fan and wide channels on the inactive fan. Where flow volumes were exceptionally large, small dilute over flows washed from the wide channels onto adjacent topographical highs to deposit lithofacies assemblage 3. As these flows continued down the wide channels, boulders became stranded in a thin matrix resulting in a dilution of the flow. These diluted flows then re-channeled down slope to bulk (evidenced by lithofacies assemblage 4) and continue flowage throughout the entire Whangaehu catchment to the sea.

CHAPTER 3

AEOLIAN DEPOSITS

3.1 General Introduction

The aeolian sands in the Rangipo Desert have added diversity to both the physical landscape, in the form of dunes, and to the biotic landscape by providing additional unique vegetation associations. A relationship between the aeolian sands and the vegetation was discussed by Cockayne (1908) who recognised that the trapping of aeolian sand by plants such as *Muehlenbeckia axillaris* and *Podocarpus nivalis* were crucial for dune fixing to begin. Cockayne states:

"A shrub whose seeds can germinate, producing a seedling that can tolerate the station, may arrest such a drift, and, provided it can increase by rooting near its growing-point, will build up smaller or larger mounds where other plants can settle"..... " A slightly less unstable substratum or a more sheltered position and true desert dunes are formed.".

Cockayne also recognised that curious vegetated mounds, which were still accumulating aeolian sand, represented the remnants of a once stable landscape. The presence of these mounds, referred to here as "pedestals", in the Rangipo Desert and on the slopes of eastern Tongariro led Topping (1974) to suggest that current erosion was largely due to Polynesian deforestation (chapter 1).

In this chapter the post-Taupo Pumice aeolian deposits are formally designated as the Makahikatoa Sands. The depositional and weathering history of the Makahikatoa Sands have been characterised using stratigraphy and laboratory procedures. Laboratory procedures are also used to compare the physical and chemical fertility of the Makahikatoa Sands with that of an incipient soil found on the fluvial/laharic surfaces. The results in this chapter, together with the findings of chapter 2, provide new information for the initiation of the present day erosion found in the Rangipo Desert.

SECTION A: Depositional And Weathering History Of The Makahikatoa Sands

3.2 Methods

3.2.1 Introduction

One of the major factors controlling the weathering of tephra or aeolian sand is the time weathering processes are able to operate effectively (i.e., time at land surface). Thus, if deposition rates of the tephra or aeolian sand increase, the opportunity for weathering and pedogenesis decreases (Gibbs,1971). The depositional and weathering rates of the Makahikatoa Sands were studied by measuring and describing stratigraphic sections, and then analysing for carbon, allophane and phosphate retention from selected samples in the laboratory. Carbon provides a measure of the time period that has permitted accumulation of organic matter, whilst allophane provides a measure of the time period that has permitted formation of short-range order clays from the primary minerals (Lowe, 1986). An indirect measure of the allophanic content of the soil is also provided by analysing the soil's phosphate retention (Saunders, 1965).

Particle size analyses of sand, silt and clay fractions were performed to elucidate the provenance of the Makahikatoa Sands, to provide information on the environment of deposition, and to quantify rates of weathering.

3.2.2 Laboratory Procedures

Sections were described in the field[1] and then selected samples were taken back for laboratory analysis. A representative sample was taken from each sample bag and the procedures described below were followed for each analysis. Ratings given to any analyses in this study follow the criteria of Blakemore *et al.*(1987).

[1] Methods used to describe stratigraphic sections are given in section 2.2.1.

Tamms Oxalate-Extractable Iron, Silica, And Aluminium

The acid oxalate shaking extraction method as described by Blakemore *et al.* (1987) was used. A 1+5 diluent was used for the Al and Si extracts, while a 1+5 and a 1+9 diluent was required for the Fe extracts. The extracts were analysed using an aa spectrophotometer.

Pyrophosphate-Extractable Iron And Aluminium

The method described by Blakemore *et al.* (1987) was used. Extracts were cleaned by centrifuging at 14000 rpm. for 50 minutes and the addition of `superfloc'. The extracts were analysed using an aa/ae spectrophotometer.

Allophane was estimated using the formula of Parfitt (1986).

Carbon

Gravimetric determination of the % organic carbon was measured using a Leco high induction furnace (after Nelson and Sommers, 1982.) Carbon (multiplied by 1.7) provides an approximate measure of organic matter content (Blakemore and Millar, 1968).

Phosphate Retention

This method followed that of Blakemore *et al.* (1987).

Particle Size Analyses

In this study chemical dissolution, using acid-oxalate extraction of short range order clays and organic complexes (SROCO), was employed as a pre-treatment procedure for particle size analysis (after Alloway, 1989). Literature suggests that acid-oxalate selectively dissolves SROCO materials that are composed of allophane or ferrihydrite, and if conducted in the dark, dissolution of crystalline oxides and layer silicates is very limited (see Alloway p. 243, 1989). Organic matter was removed initially using hydrogen peroxide, but later this pre-treatment was abandoned because differences were found to be negligible between treated and untreated samples.

The samples were air dried and gently disaggregated so as to pass through a 1mm sieve. Two representative 3 gram sub-samples were respectively placed into two 250ml centrifuge bottles, and each bottle was filled with 0.2M acid oxalate (pH 3.0-3.5). These were shaken end over end in the dark at 20°C overnight. The samples were then poured through a 63µm sieve, thus separating the dissolved SROCO material, and the lattice clays and silt, from the sand fraction. The captured SROCO material, plus lattice clays and silt were left to settle for 12 hours. The dissolved SROCO material was then decanted from the residual clay and silt. The residual clay and silt fraction is then transferred with water to centrifuge tubes, and is separated at 850 rpm for a length of time, depending on the temperature (hence the viscosity) of the liquid. The suspended clay is decanted off and the procedure repeated until the supernatent is relatively clear. The silt and clay fractions are dried and weighed. The sand fraction, and any silt that was not originally filtered, was wet sieved. SROCO content was calculated as the difference between the other fractions combined weight and the original weight.

Therefore,

Weight (or %) of sand + unfiltered silt + filtered silt + lattice clays + residual SROCO material = weight (or 100%) of sub-sample. Samples were duplicated or triplicated, where necessary.

This method was reasonably fast, particularly since there was only a small percentage of lattice clays present. However, a major limitation is that in most of these samples the <63µm residue is too small for accurate pipette analysis.

3.3 Results And Discussion

3.3.1 Makahikatoa Sheet Sands And Dune Sands

The Makahikatoa Sands found in the Rangipo Desert are described here as either sheet sands or dune sands. The distinction is based both on their extent and their geometry. The sheet sands typically occur over wider areas than the dune sands, although, they are found on small, eroding, pedestals in some localities. The physiography of the sheet-sand deposits is relatively flat (Plate 3.1), whereas the dune sands occur as discrete convex deposits (Plate 3.2). A few of the larger dunes have developed basins as sands have built up at faster rates around the periphery. Neither the dune sands nor the sheet sands found in the study area exhibit any diagnostic bedding features.

The dunes sands cannot be grouped and classified into specific dune types because of the absence of cross-bedding and no preferred alignment directions. The presence of intact Tufa Trig members in most dunes confirms Cockayne's (1908) observation that the dunes were stationary features that could increase in size, providing plants were present to ensure stability. There are a number of large dunes, upwards of 5 meters in height, but medium sized dunes (>1m in height) are more numerous, and a multitude of small dunes are present.

Sheet-sand deposits overlie the Mangatawai Tephra and the Taupo Pumice ignimbrite preserved in non-eroded areas. The dune sands usually overlie the laharic or fluvial deposits but also have formed occasionally on areas where the Mangatawai Tephra and the Taupo Pumice ignimbrite are preserved. The dune sands have also formed on areas where tephric coverbeds have been eroded in recent times.

Both the sheet-sand deposits and large dunes are covered by *N. solandri* and *Phyllocladus* forest. *Phyllocladus* scrub occurs almost exclusively on medium sized dunes whilst shrubs are found on small dunes. Seral shrublands and tussocklands have colonised both the sheet sands and dune sands as a response to historical fire.

Plate 3.1 Characteristic uniform terrain formed by sheet sand deposits which overlie the post-Taupo Pumice paleosol.

Plate 3.2 In contrast to the sheet sands, the dune sands form a distinctive dune like geometry. In this photograph dunes colonised with *Phyllocladus* or tussock provide relief to the otherwise barren laharic surface. Mount Ngauruhoe is in the background.

3.3.2 Description Of Sheet Sands

Type Section For The Makahikatoa Sands

The type section (section 13) for the Makahikatoa Sands is located on a large sheet sand pedestal (Plate 3.3), immediately adjacent to a widespread erosional surface at T20/398064. The formation name, Makahikatoa Sands, is named after the nearby Makahikatoa Stream (Fig. 1.1) which runs into the Whangaehu River (T20/390030).

A feature of the Makahikatoa Sands observed in the type section (Fig. 3.1, Plate 3.4). is a 70cm thick post-Taupo Pumice paleosol developed in Makahikatoa Sands which overlies the Taupo Pumice ignimbrite, and is in turn overlain by a further 3m of Makahikatoa Sands. The boundary between the post-Taupo Pumice paleosol and the overlying Makahikatoa Sands is defined at an unnamed ash, found immediately below Tufa Trig member 4 at a depth of 3.52m. The bottom 10cm of the paleosol has developed in the Taupo Pumice ignimbrite, while the rest of the paleosol has developed in the Makahikatoa Sands; for simplicity the paleosol is referred to as being developed from Makahikatoa Sands.

Morphological differences between the paleosol and the overlying sands were distinctive. The paleosol was distinguished by its: 1) yellower hue, 2) greasier texture, 3) firmer consistence, 4) moderate block structure, and 5) presence of rhizomorphs. Cracking, due to differential shrinking, which occurs in some paleosols (Topping 1974), is not present in the post-Taupo Pumice paleosol (hereafter referred to as pTPp). In addition, allophane (Fig. 3.2) and carbon (Fig. 3.3) percentages, measured from samples taken from the type section, were higher in the pTPp than the overlying sands. However, the decline in allophane and carbon percentages was not inversely proportional to the corresponding 5 fold increase (0.66mm/yr to 3.8mm/yr) in the accumulation rate of the overlying sands (Fig. 3.4). Allophane percentages declined from a high of over 8 percent in the pTPp to about 5 to 6 percent in the overlying sands. Phosphate

Plate 3.3 The remnant pedestal of *N. solandri* seen on the left of the photograph is the locality for the type section (section 13) of the Makahikatoa Sands. Part of the eroding surface seen in this photograph provides a stark contrast to the *N. solandri* forest enclaves.

Section 15 is located near the outer margin of the stand of *N. solandri* to the right edge of the photograph.

Figure 3.1 Type section for the Makahikatoa Sands (T20/398064)

Informal members of the Tufa Trig formation, numbered T.1, 1a, 2, 4, 5, 14, 15, 15a, 16, and 17, have been correlated throughout the Rangipo Desert. Tufa Trig members 4, 5 and 14-17 are black lapilli or ash deposits, while members T. 1 and 2 are light brown and orange pumiceous lapilli deposits, and T.1a is a cream and orange fine ash deposit. The dashed lines represent Tufa Trig members which were not correlated to other stratigraphic sections. A single dashed line represents a very thin unnamed ash. The arrow represents a lahar or fluvial deposit that appears to have admixed with Makahikatoa Sands. For a detailed description of the type section (section 13) see appendix 1.

Symbols

Makahikatoa Sands 

Paleosol developed in Makahikatoa Sands 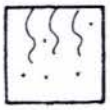

Black lapilli and ash 

Light brown or orange pumiceous lapilli and ash 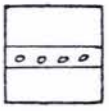

Taupo Pumice ignimbrite 

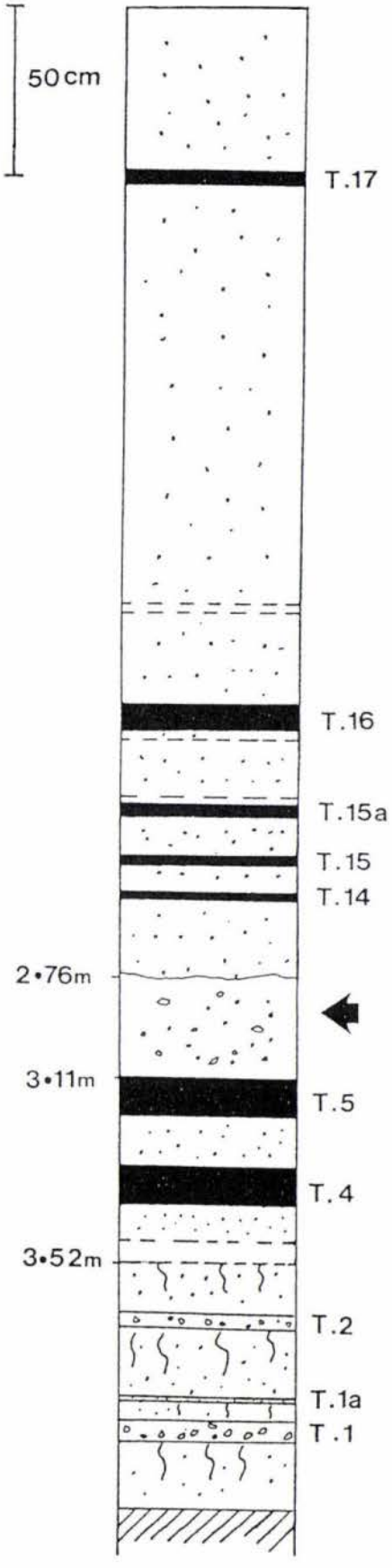
50 cm
T.17
T.16
T.15a
T.15
T.14
2•76m
3•11m
T.5
T.4
3•52m
T.2
T.1a
T.1

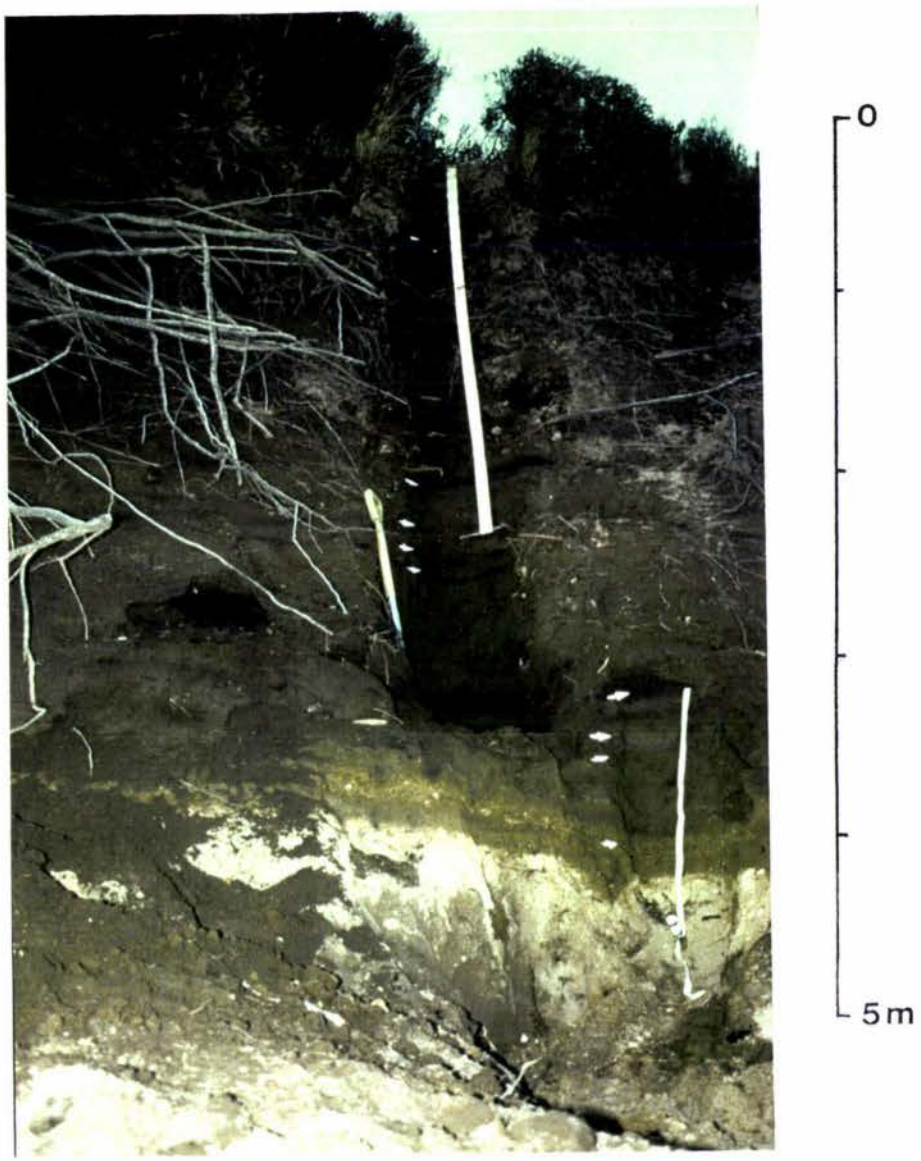

Plate 3.4 Type Section For The Makahikatoa Sands

The Taupo Pumice ignimbrite is found at the base of the section. The bottom arrow points to Tufa Trig member 1 which is one of the pumiceous tephra interbedded in the post-Taupo Pumice paleosol. The second and third arrows from the bottom point to bands of oxidised (red) iron which sandwich a band of reduced (grey) iron. These redox changes in iron indicate lateral movement of water through the upper part of the paleosol. The fourth arrow from the bottom points to Tufa Trig member 4, a coarse tephra deposited c. 850 yrs B.P. The boundary between the paleosol and the overlying Makahikatoa Sands is found 10cm below Tufa Trig member 4. The upper arrows point to Tufa Trig members that are interbedded with the Makahikatoa Sands.

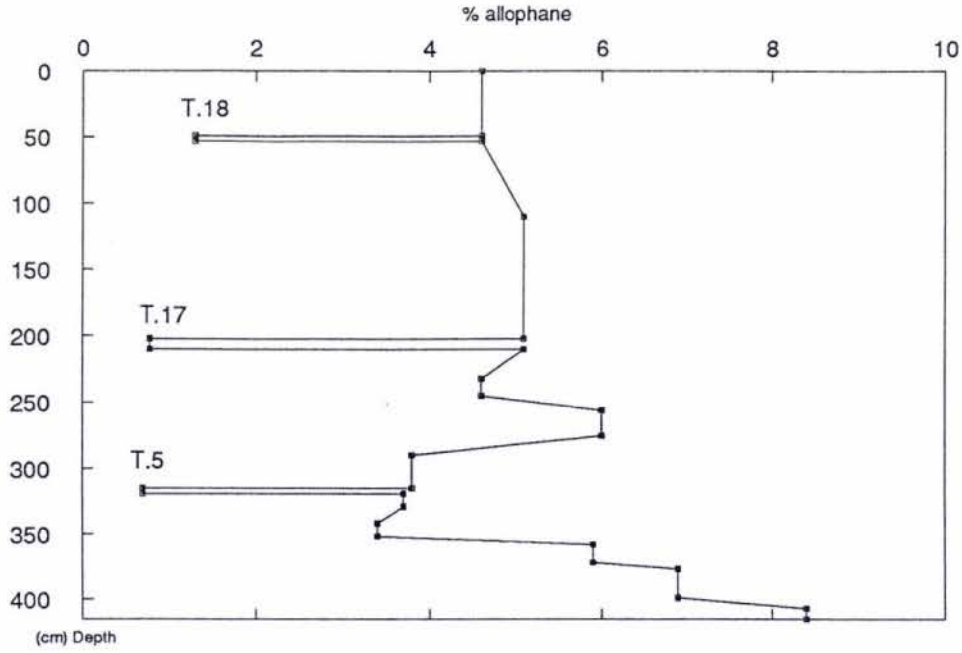

Figure 3.2 Percent allophane[1] for section 13 (type section)

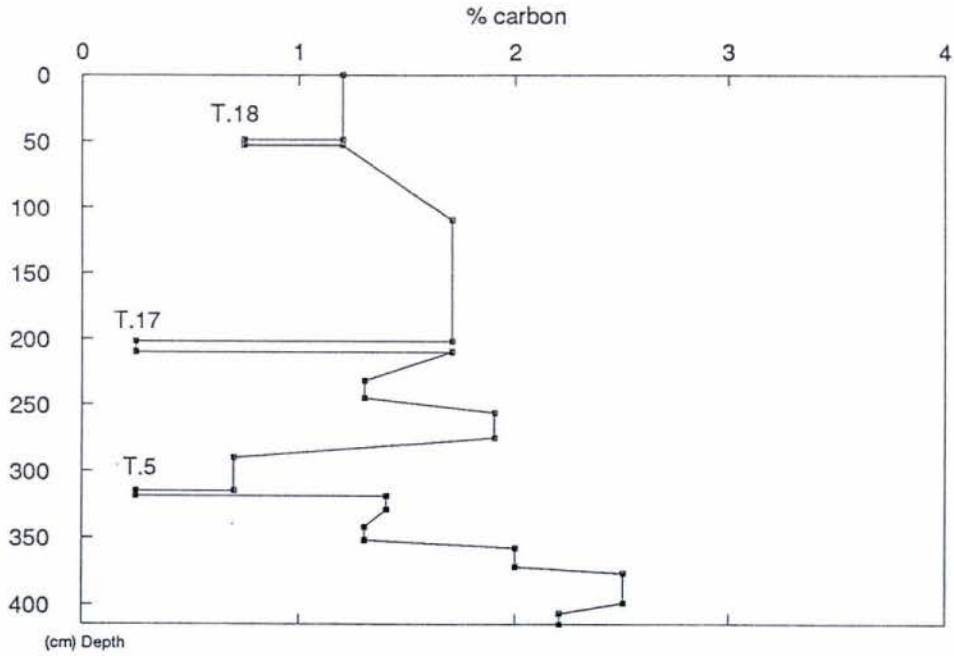

Figure 3.3 Percent carbon for section 13 (type section)

[1]General explanation of the graphs
Vertical lines between the dots on the graphs represent the thickness and depth of each sample taken for analyses. The sloped lines represent the interval between samples. On some graphs no lines are shown due to only a few sampling intervals. To help compare the graphs with the described stratigraphic sections in the text or appendix 1, some Tufa Trig members are indicated. On some graphs a question mark after a Tufa Trig member indicates that member is tentatively identified, based on stratigraphic position. The raw data for the graphs is presented in appendix 2.

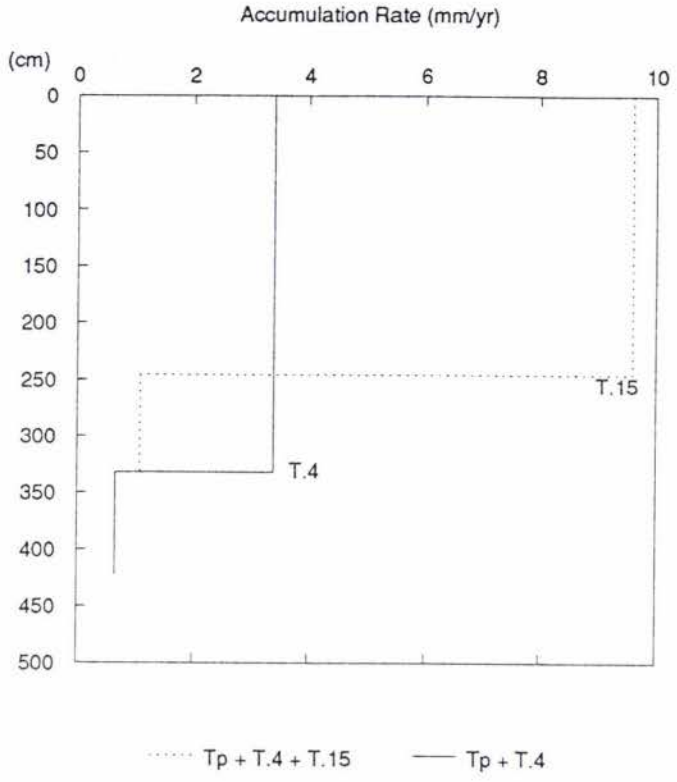

Fig. 3.4 Accumulation rates[1] for section 13 (type section)

[1]Explanation of the above graph
The solid line Tp + T.4 means that two accumulation rates have been calculated. The first rate is based on thickness of the Makahikatoa Sands between the Taupo Pumice ignimbrite (Tp) dated at 1764 yrs B.P. and Tufa Trig member 4 (T.4) with an estimated date of 850 yrs B.P.
ie. 63mm ÷ (1764-850) = 0.66 mm/yr. The accumulation rate between T.4 and the surface is calculated from a profile thickness of 2890mm divided by 850 yrs. (ie 850 yrs B.P. to the present). The same procedure is done with the dotted line except Tufa Trig member 15 (estimated dated of 200 yrs B.P.) is included in the calculation. Therefore the profile thickness between T.4 and T.15 is measured and divided by the age: 850 yrs B.P. - 200 yrs B.P.). The same procedure is done between T.15 and the surface.

Some graphs shown later may have another time plane present (ie,. another dated Tufa Trig member) so a further rate can be included in the profile calculation. Other time planes are described in the post-Taupo Pumice chronology (Fig 2.5; section 2.3.2).

retention trends (appendix 1b) paralleled allophane as expected (Saunders, 1965); they declined from over 80 percent in the pTPp to 60 percent in the overlying sands. Similarly carbon levels declined from over 2 percent to between 1 and 2 percent in the overlying sands. Carbon levels are nonetheless low in the pTPp which suggests that organic cycling was limited despite the slower accumulation rates measured for the pTPp (Fig. 3.4).

In the overlying Makahikatoa Sands at a depth between 3.11m and 2.56m the deposit becomes less sorted and coarsens with granules and one 2.5cm pebble present. These granules and the pebble was unexpected given the relatively large amount of pre-weathered sand also found within the deposit. An explanation could be that this deposit represents the distal edge of a lahar deposit. This is possible given that the deposit immediately overlies Tufa Trig member 5, which is known to have been deposited at the same time as when the largest post-Taupo Pumice lahar crossed the study area (chapter 2). This locality is found within the inferred distribution of this lahar (Fig. 2.4, Map B). The high content of weathered silt and sands is assumed to be the result of pre-weathered Makahikatoa Sands being incorporated into the deposit as the margin of the flow crossed the landscape. Alternatively, the deposit may be of fluvial origin. It is possible that coarse material located up slope from the type section was re-worked, and deposited at the type section, during a period of surface runoff.

The coarse deposit is also noted for the increased presence of re-worked pumice derived from the underlying Taupo Pumice ignimbrite (hereafter referred to as re-worked Taupo Pumice). From the coarse deposit to the surface, the Makahikatoa Sands grade into a soft, friable, and well sorted medium to coarse sand. Re-worked Taupo Pumice remains conspicuous to the surface.

A decline in carbon and allophane[1] percentages (Figs. 3.2, 3.3) indicate the lahar or fluvial deposit is comparatively less weathered than the aeolian deposits, but is still decisively more weathered than the primary tephra deposits. Regardless of whether the primary tephra deposits were laid down just after the Taupo Pumice eruption or in the last few hundred years, amorphous clay contents are almost non-existent. Moreover, very low residual carbon percentages, indicative of limited organic matter buildup, suggest the raw nature of the primary deposits are inimical to plants roots.

Particle size analyses show (Fig. 3.5) a decrease in the silt fraction from 35% in the pTPp to 15-20% in the overlying Makahikatoa Sands. The amount of silt being deposited has probably not decreased in real terms, and in fact, may have increased; however, the proportionately greater increase in the deposition of fine to very fine sand from the surrounding eroding surfaces results in drop in silt percentage. The medium to coarse sand fractions increased dramatically as expected in the lahar or fluvial deposit but have also declined in the upper 2 metres of the profile to levels below that of the pTPp. In contrast, the fine sand and particularly the very fine sands fractions have increased in the upper two metres of the profile. This indicates that the modal grain size of the source material is predominantly a fine or very fine sand. The decline in the medium to coarse fraction being deposited may be due to the pedestal surfaces becoming increasingly isolated from the surrounding deflating surfaces, thus making it increasingly difficult for the larger grains to saltate (Pye, 1987) up onto the surface of the pedestal.

[1] Percentage allophane was calculated using the method of Parfitt (1986) involving acid-oxalate Al and acid-oxalate Si ratios (appendix 2). The ratios are consistently between 1.6 and 2 in most deposits in this profile, although some ratios reach up to 3 in other sections. These Al:Si ratios suggest that the short range order clays formed in the study area are dominantly proto-imogolite allophane, with some silicate tetrahedra absent in the proto-imogolite allophane when ratios of >2 are present (Parfitt, 1986).

Figure 3.5 Particle size distribution for section 13

(type section)

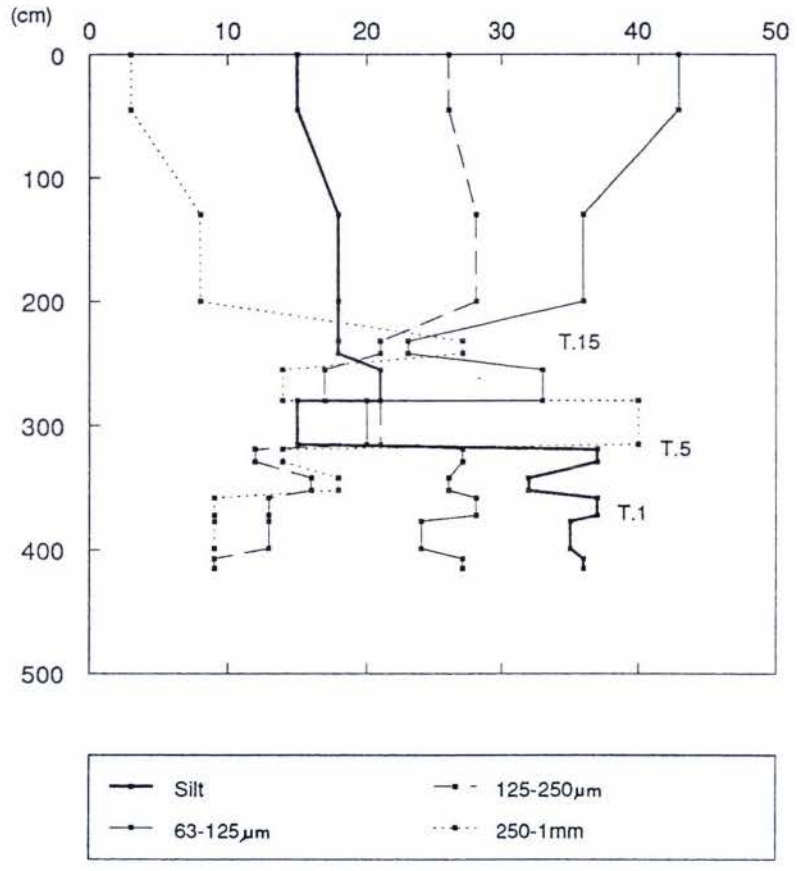

Reference Sections For The Makahikatoa Sands

Reference stratigraphic sections for the sheet-sand deposits are located adjacent to the laharic/fluvial surfaces, south-east of the type section, both near and on the fault escarpment (Plate 2.2). These sections, unlike the type section, are characterised by fine grained aeolian deposits that are less than a meter thick (Fig. 3.6). Profile thicknesses vary little between these sections which is reflected in a uniform physiography found in the areas where these deposits occur (Plate 3.1). In addition, the Tufa Trig members decrease in thickness and number as the section sites occur further from Mount Ruapehu.

Accumulation rates for the Makahikatoa Sands were generally consistent between the reference sections (Fig. 3.7), and were five to seven times slower than in the type section. However, despite the decline in the accumulation rates there was no field indication that the sands had weathered to any greater degree due to increased pedogenesis. This was subsequently verified when allophane (Fig. 3.8) percentages were found to be lower in the reference sections compared to the type section. An allophane percentage measured in the pTPp for section 14 was almost identical to the allophane percentages in the pTPp of the type section but measurements in the overlying sands varied between 2 and nearly 4 % in section 14 compared to 6-7% in the type section. Carbon percentages also declined above the pTPp in section 14 (Fig. 3.9) but unlike the type section percentages near the surface increased, reflecting an increase in organic cycling.

The similarity between the particle size distribution and profile thicknesses between section 1 and a sample from section 15, which occurs on the fault escarpment (appendix 3b), indicates the very fine sand and silt fractions are being transported across the landscape and deposited on the fault escarpment at comparable rates. However, local site conditions appear critical for deposition of the coarser grain size. For example coarser textures occur in section 14, compared to section 1 (Fig. 3.10), despite the latter's closer proximity to the extensive laharic/fluvial surfaces (Plate 2.2). This has been attributed to a number of large dunes near section 1 that are acting as a local trap for the larger, saltating sand grains.

Figure 3.6 Correlation columns showing the change in thickness of the Makahikatoa sheet-sand deposits between section 13 (the type section) and reference sections 1, 14 and 15. Informal members of the Tufa Trig formation, numbered T.1, 2, 4, 5, and 7a, were correlated between these sections, while T. 16 and 17 were only found in section 13. A Tufa Trig member which is question marked is a tentative identification. Tufa Trig member 4 is the datum line for the columns. Deposits D1 and D2 represent clast supported and matrix supported diamictons respectively. For detailed descriptions of the sections see appendix 1.

Symbols

Makahikatoa Sands 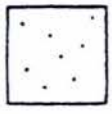

Paleosol developed in Makahikatoa Sands 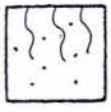

Black lapilli and ash 

Light brown or orange pumiceous lapilli and ash 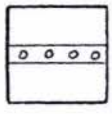

Taupo Pumice ignimbrite 

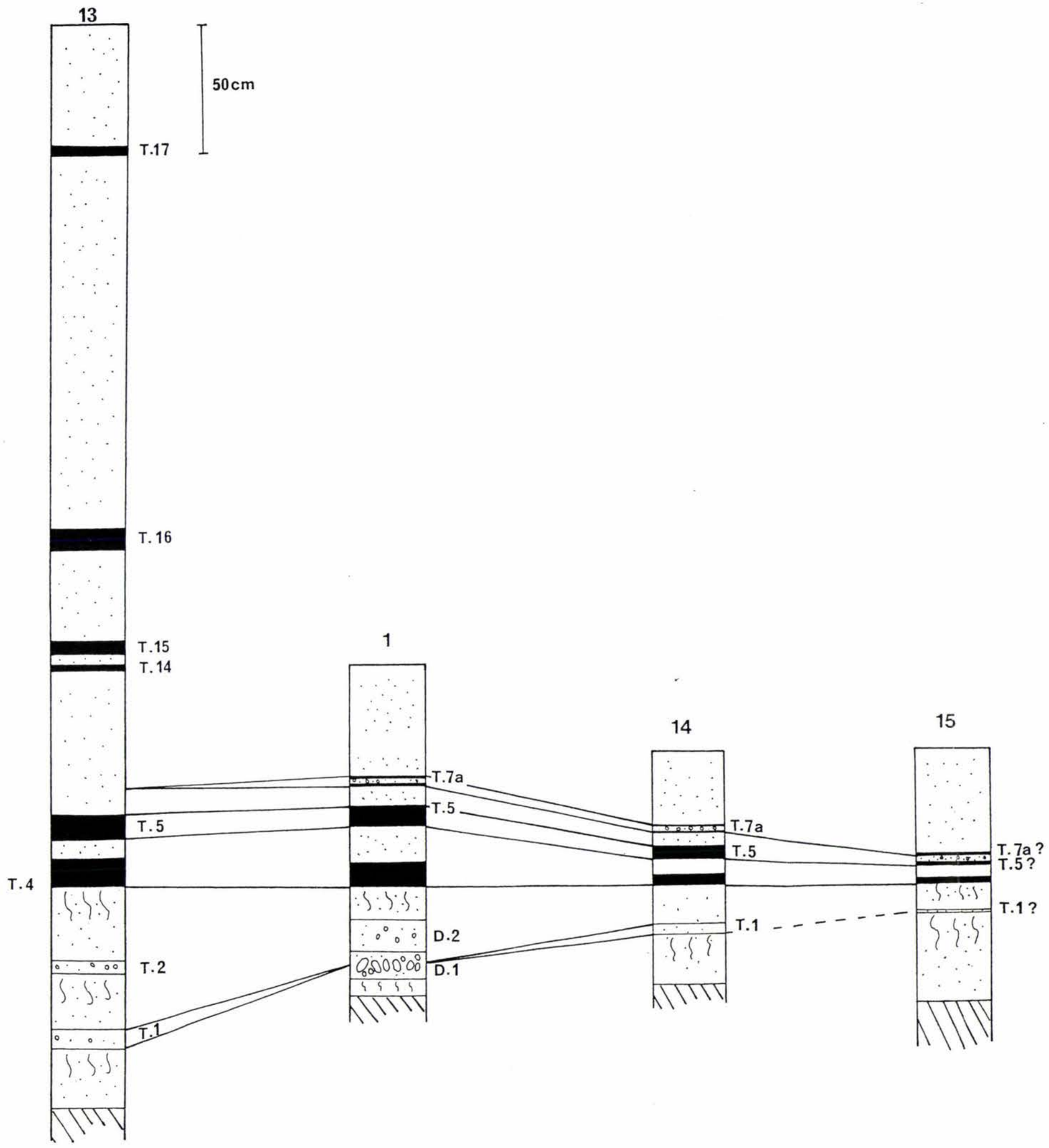
13
50cm
T.17
T. 16
T.15
T.14
T.4
T. 5
T. 2
T. 1
1
T.7a
T.5
D.2
D.1
14
T.7a
T.5
T.1
15
T. 7a ?
T.5 ?
T.1 ?

Fig.3.7 Accumulation rates for reference sheet sand sections

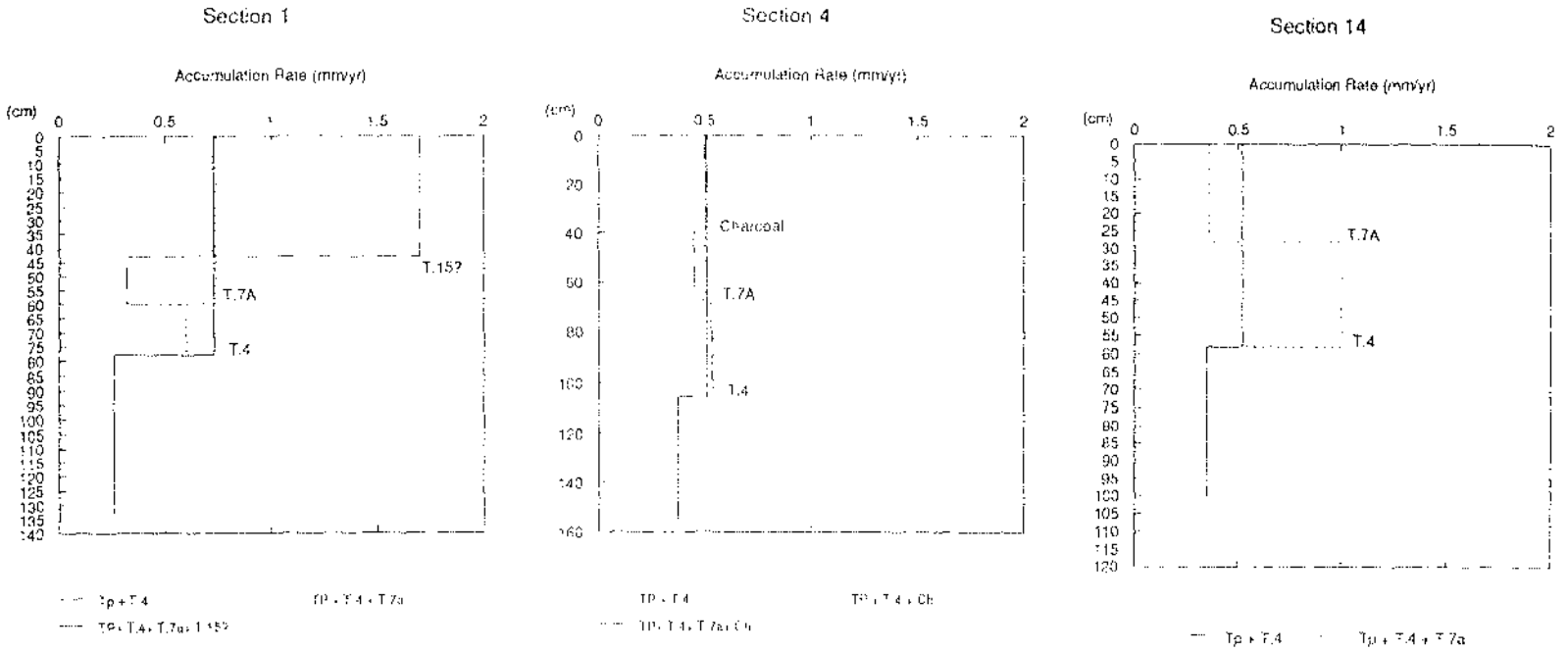

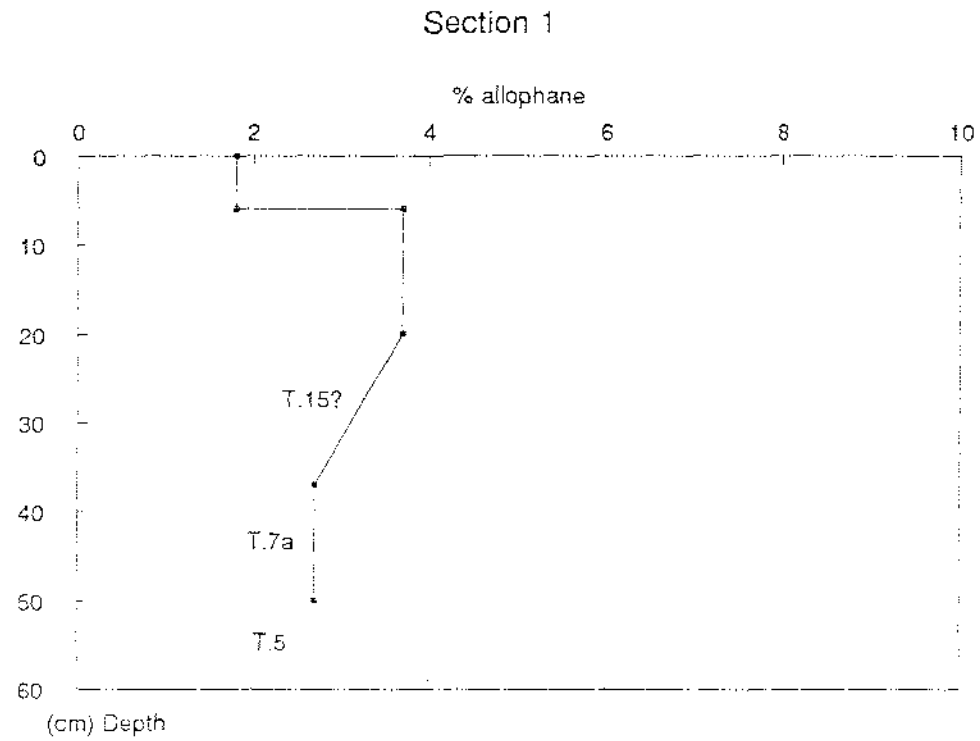

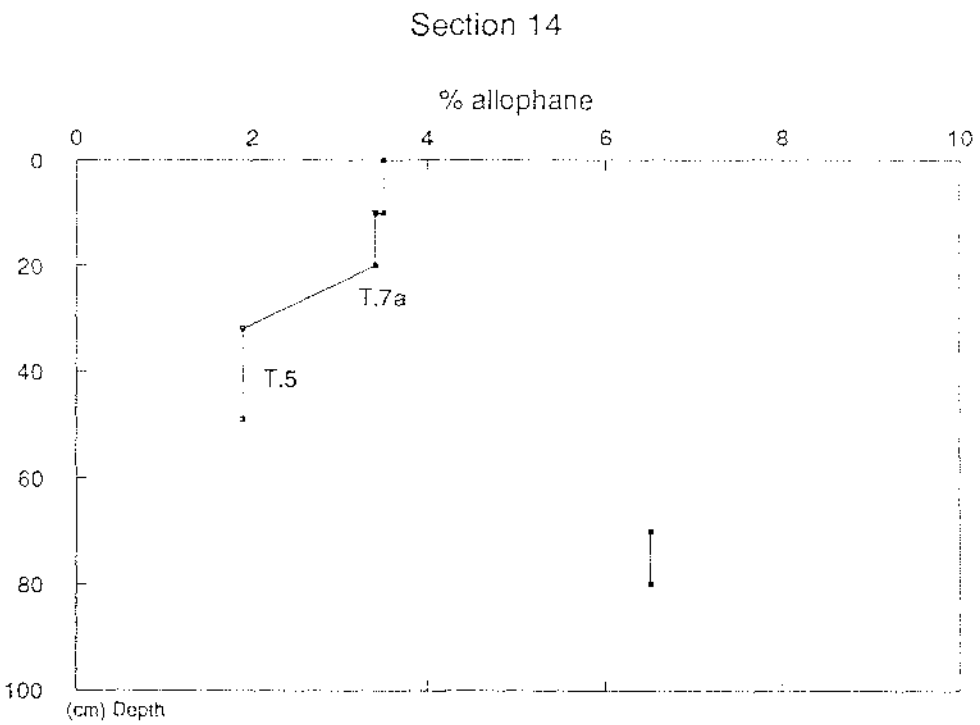

Fig. 3.8 Percent allophane for reference sheet sand sections

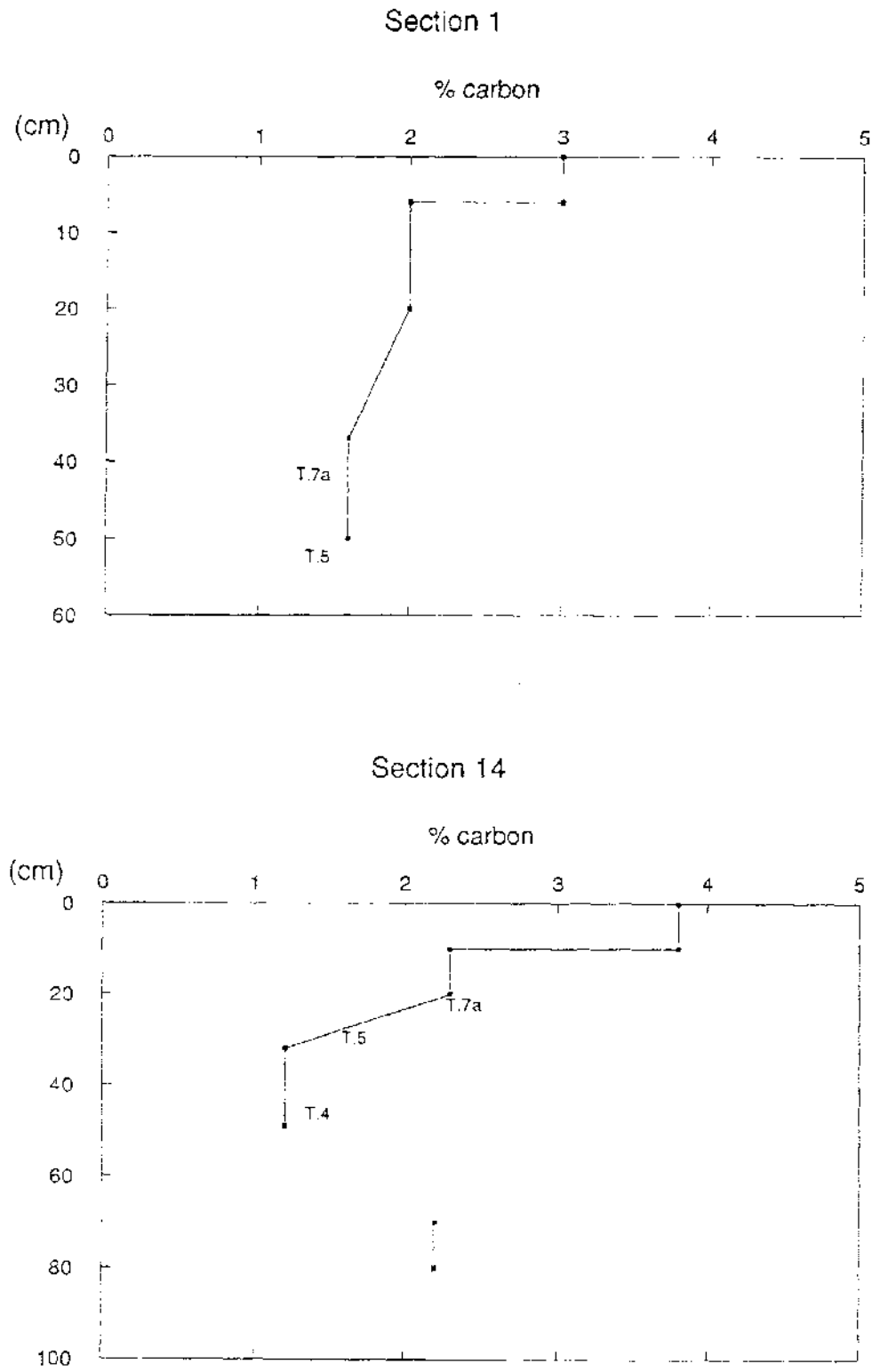

Fig. 3.9 Percent carbon for reference sheet sand sections

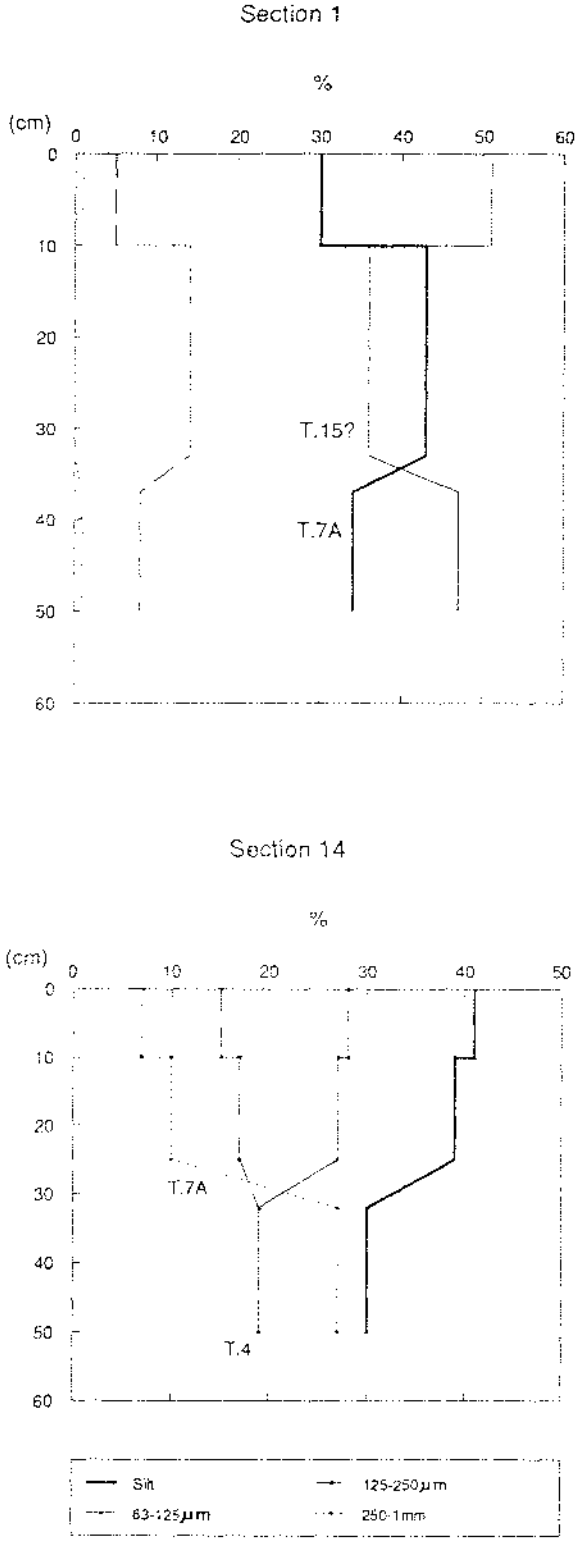

Fig. 3.10 Particle size distribution for reference sheet sand sections

Temporal changes also occur in particle size distributions. In section 14 (Fig. 3.10) the medium and coarse grain size fractions are greater between Tufa Trig member 4 and 7a than those higher in the profile. As well as the coarsening of modal grain size, an increased accumulation rate (resulting in over-thickening), and comparative decrease of allophane and carbon percentages also occurred. These changes are attributed to increased local influxes of sand. It is not known whether this increase was due to different site factors during this time, or due to an increased amount of source material available for re-working. The latter is a possibility as a large volume material was deposited from lahars throughout the study area, between the times when Tufa Trig members 4 and 7a were deposited (chapter 2).

3.3.3 Discussion of Sheet Sands

The ubiquitous presence of re-worked Taupo Pumice throughout the Makahikatoa Sands above the lahar or fluvial deposit (in the type section) suggests that the major source of the sands is from adjacent eroding surfaces. The re-worked Taupo Pumice indicates that its source became established when the Taupo Pumice ignimbrite, deposited on the adjacent surfaces became exposed and began to deflate.

Despite accumulating at a rate some 16 times faster than the reference sections, the Makahikatoa Sands in the type section are comparatively more weathered. This is a further indication that most of the aeolian sand deposited at the type section was derived from pre-weathered tephra found on adjacent eroding surfaces. Today hoar frosts are observed to fragment the exposed, partially cemented, pre-weathered tephra. Wind then either suspends or saltates the tephra particles for a short time (Pye, 1987) off the eroding surface (Plate 3.5), and onto the adjacent areas covered in vegetation. Re-working by water after tephra fragmentation is also often an intermediary process.

Plate 3.5 This photograph was taken on an erosional surface during a dust storm created by strong north-west winds on 28th January, 1988. Dusts storms carrying dust to a height of 300 metres were witnessed.

It is therefore concluded from the depositional history of the section that the present eroding surfaces began to deflate during or just after the time when a coarse lahar or fluvial deposit disturbed the pre-existing vegetation pattern. Where the coarse deposit is absent, the stratigraphy suggests adjacent surfaces began to erode c. 800 yrs B.P.

Field and laboratory results indicate that the initial rise in the accumulation rates from c. 850 yrs B.P (at a depth of 3.52m) was probably due to an increase in source material caused by a newly formed lahar or fluvial deposit, or perhaps a period of extreme climatic conditions (ie. increased winds). This is because low allophane (Fig. 3.2) and carbon (Fig. 3.3) percentages, and the lack of re-worked Taupo Pumice, indicate that the aeolian sediment deposited at this depth was not derived from adjacent deflating surfaces.

The friable nature of Makahikatoa Sands in the upper 2 metres of most profiles, together with nearly 1.5 metres thickness sandwiched between Tufa Trig members 16 and 17, indicate accumulation rates escalated in the upper part of the profile. This suggests either the source area has increased or erosion rates have increased (or both). This is probably due to gullies continuing to expand and undermine the remnant interfluves on the eroding surfaces; acceleration of this process due to increased climatic instability may be possible.

In contrast to the type section, the provenance for the Makahikatoa Sands found in the reference sheet sand sections is the surrounding laharic/fluvial surfaces. These sections, unlike the type section, are found in locations which are either comparatively distal from their source areas or are surrounded by dunes that trap much of the sediment that is being re-worked from the source areas, which thus restricts the amount of sediment available for deposition. Accumulation rates and grain size of the Makahikatoa Sands have, therefore, decreased in these localities (Figs. 3.7, 3.10). Although the presence of recognisable A horizons developed within the sheet sands indicate increased organic cycling, the unweathered nature of the source material, derived from the fluvial/laharic surfaces, has limited the formation of short-range order clays (Fig. 3.8). The over-riding factor which has therefore determined the short-range order clay content for the Makahikatoa Sands has been the nature of the source material, not subsequent soil forming factors.

3.3.4 Description Of Dune Sands

Although localized over-thickening occurs in some of the sheet sands, they are comparatively uniform in thickness compared to the dune sands. The huge variation in sizes of the dunes in the Rangipo Desert reflects the differences in the ability of a dune to accumulate sand and silt, conditions which are dependent on the site locality and proximity to source. Sections 17 and 18 (Fig. 3.11) represent large dunes found on, or adjacent to, the laharic and fluvial surfaces. Accumulation rates in section 17 reflect the large size and height of the dune (Fig. 3.12, Plate 3.6). Since the deposition of Tufa Trig member 4 the accumulation rates have increased 45 fold (from 0.18mm/yr to 8.1mm/yr), reflecting the influx of sediment available from the adjacent lahar deposits. Section 18 is located within the basin of a large dune, and despite preferential accumulation on basin margins, the increase in accumulation rates is nevertheless 5 fold since the deposition of Tufa Trig member 4 (Fig. 3.12). Particle size analyses (Fig. 3.13) reflect the comparative shelter of the basin as very fine sand is the modal fraction present in the profile.

Section 19 (Plate 3.7) is found on a young dune which has formed on an extensive lahar and fluvial lag surface. It is one of the outer dunes in a number that are encroaching on to this adjacent lag surface. Two samples from this profile reveal (Fig. 3.13) that the silt and very fine sand content form only between 20-30 % of the < 1mm fraction, with the remainder comprising medium to coarse sand. The raw nature of the deposits in this young dune are reflected in low allophane percentages (Fig. 3.14), and low carbon percentages (Fig. 3.15).

Figure 3.11 Correlation columns showing the change in thicknesses of the Makahikatoa Sand dune-sand deposits. Informal members of the Tufa Trig formation, numbered T.1, 4, 5, 7a, 14, 15, 15a, 16, and 17, were located in these sections. A Tufa Trig member only tentatively identified is question-marked. Dashed lines represent Tufa Trig members not correlated elsewhere. Tufa Trig member 7a is the datum line for the columns. Deposit D6 represents a matrix supported diamicton, while F. represents sequences of fluvial deposits. The dune sands reach a height of 6 metres in section 17. For detailed descriptions of the sections see appendix 1.

Symbols

Makahikatoa Sands 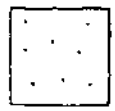

Paleosol developed in Makahikatoa Sands 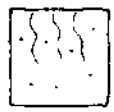

Black lapilli and ash 

Light brown or orange pumiceous lapilli and ash 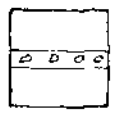

Taupo Pumice ignimbrite 

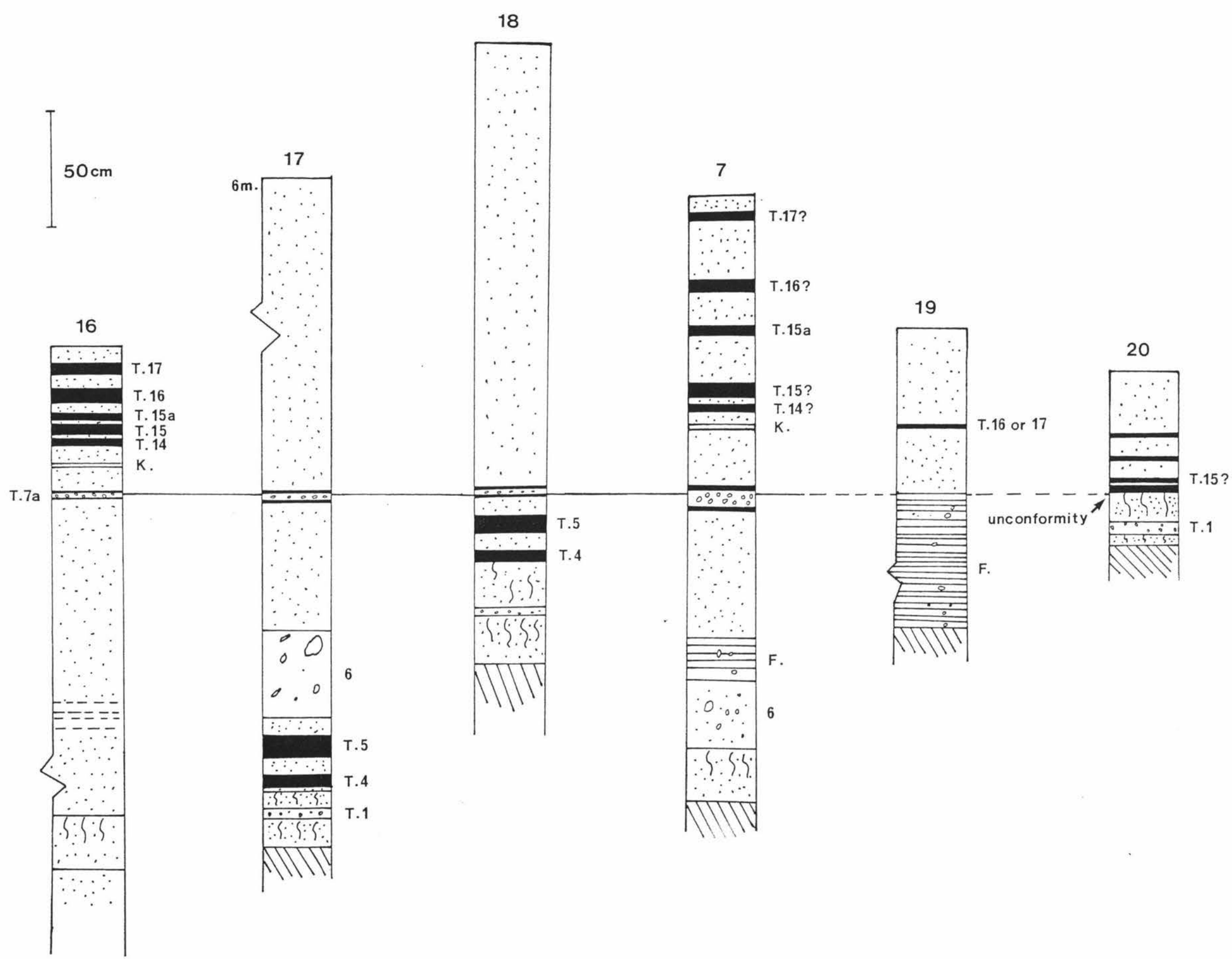
50cm
16
T.17
T. 16
T. 15a
T. 15
T. 14
K.
T.7a
17
6m.
6
T.5
T.4
T.1
18
T.5
T.4
7
T.17?
T.16?
T.15a
T.15?
T.14?
K.
F.
6
19
T.16 or 17
F.
unconformity
20
T.15?
T.1

Figure 3.12 Acccumulation rates for reference dune sand sections

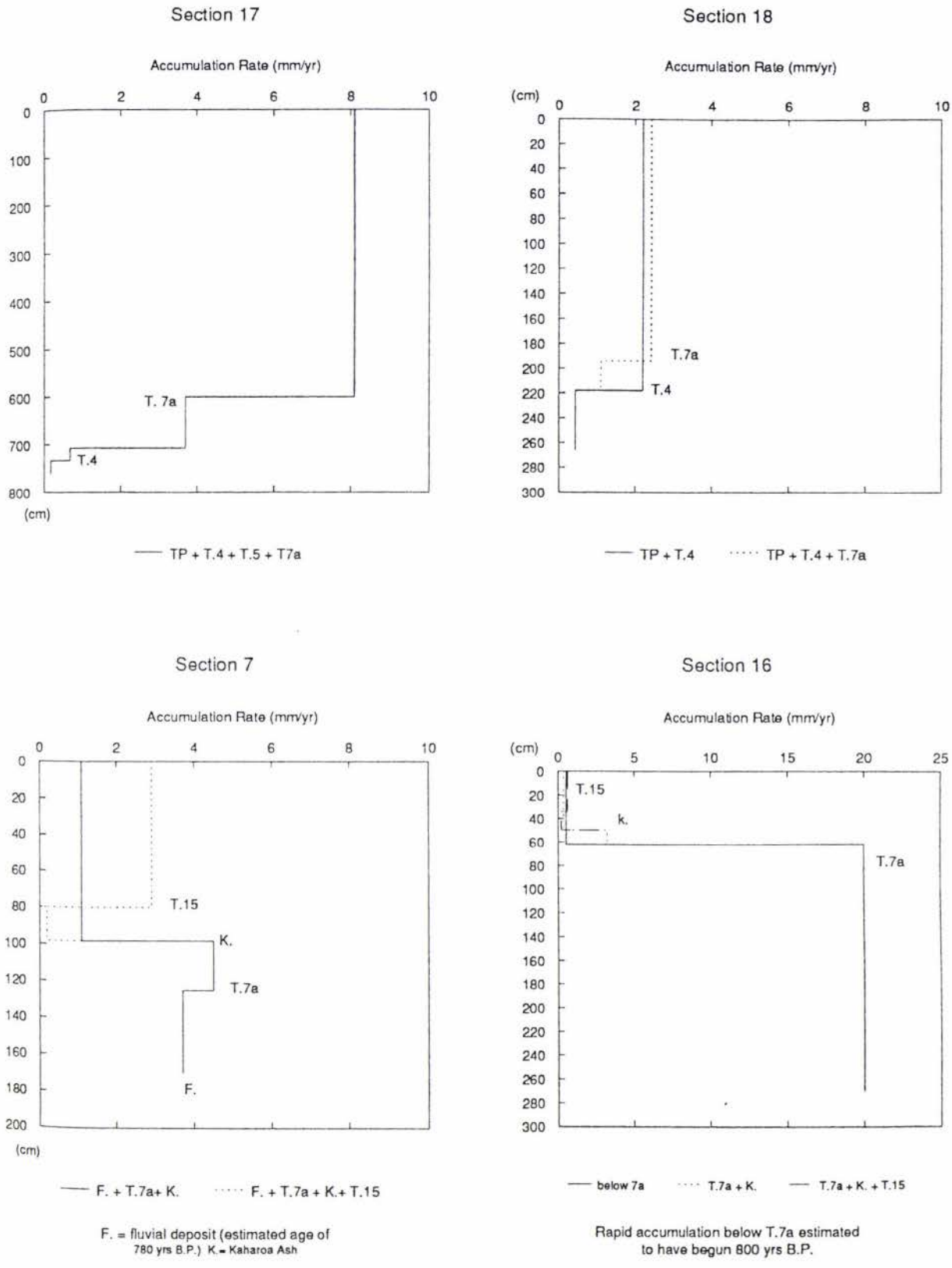

Plate 3.6. Section 17 is located on this large dune. The vegetation traps aeolian sediment which is blown up from the surrounding laharic and fluvial surfaces. The *Halocarpus bidwilli* leaning on a precarious looking angle was tree-ring dated at 280 years.

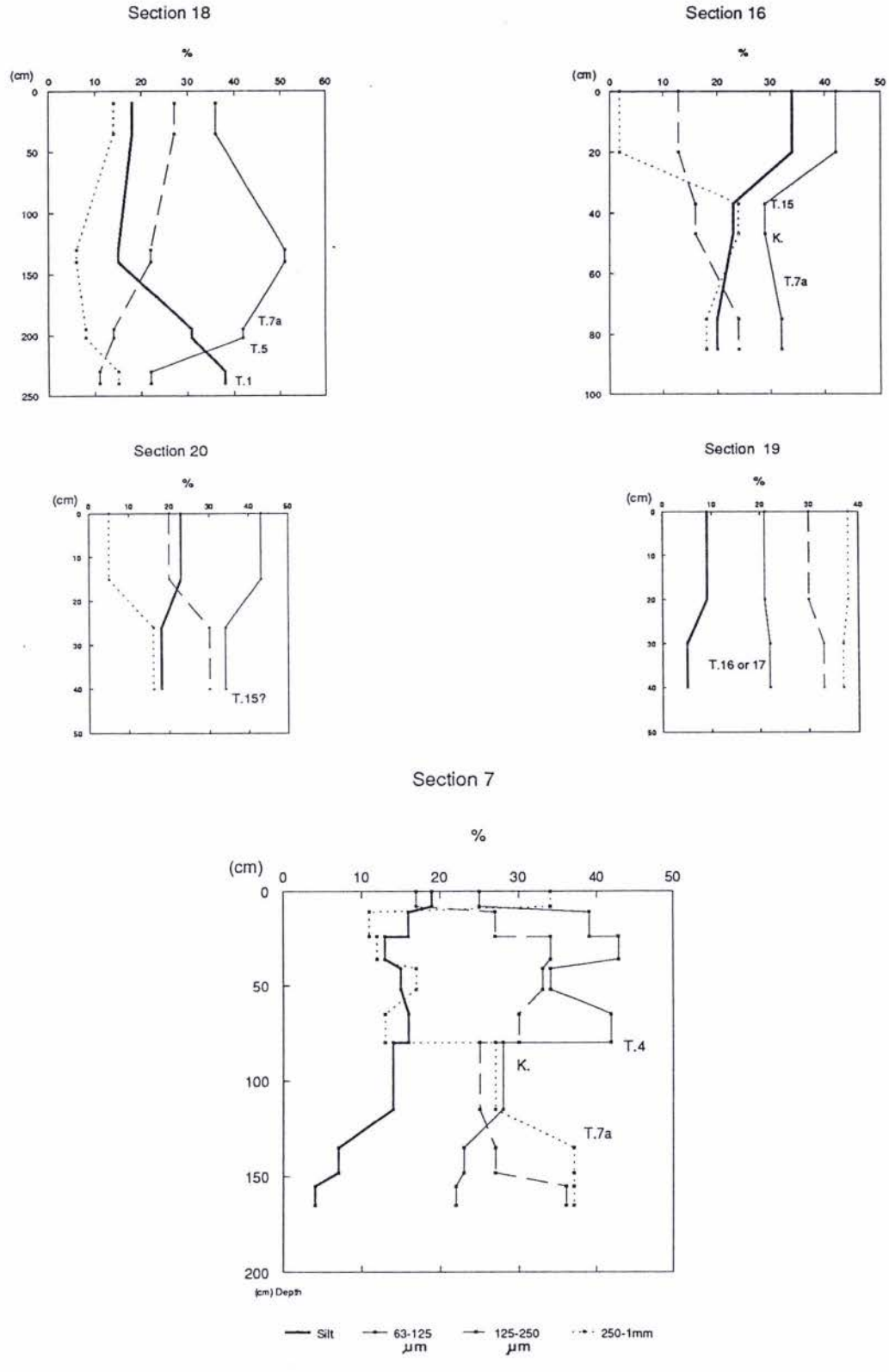

Fig. 3.13 Particle size distribution for dune sand sections

Plate 3.7 Photograph looking to the south-west showing dunes which have encroached onto the laharic and fluvial surfaces at Barbed Wire Gully. Section 19 is found on a young dune (right arrow). Stratigraphy suggests it established between 100 and 150 years ago. *Dracophyllum subulatum* and *Hebe venustula* are the largest shrubs which have formed on this dune, although a young *Phyllocladus* seedling was also sighted.

Stratigraphic section 7 is found on a larger dune (left arrow). This dune formed about 750 years ago. *Phyllocladus* on this dune was tree-ring dated at 154 years, so is therefore, much younger than the dune itself.

Only a few prostrate shrubs, *Leucopogon fraseri*, being the most common, and the tussock *Rytidosperma setifolia* can survive directly on the lag pavement of the laharic and fluvial surface in the foreground.

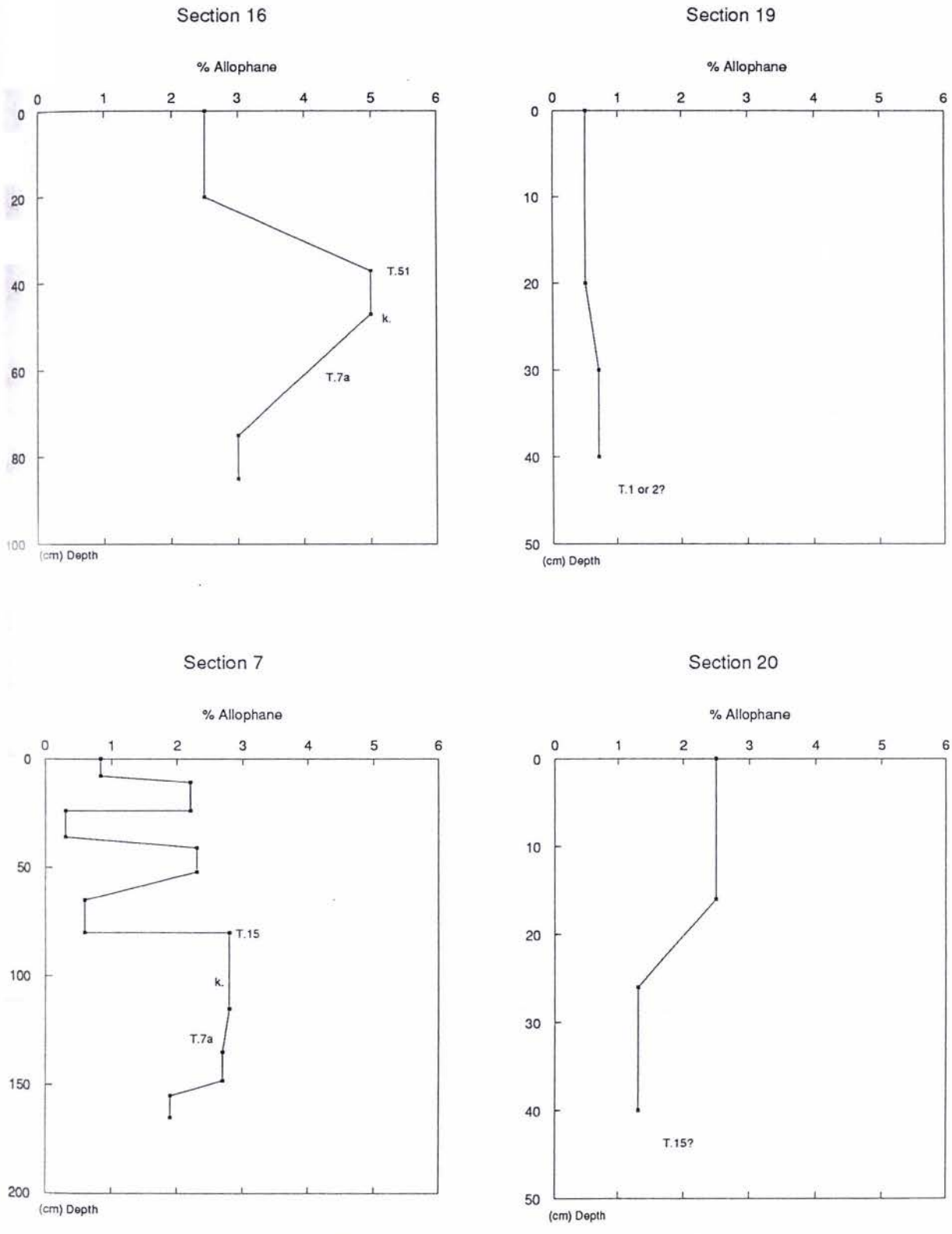

Fig. 3.14 Percent allophane for reference dune sand sections

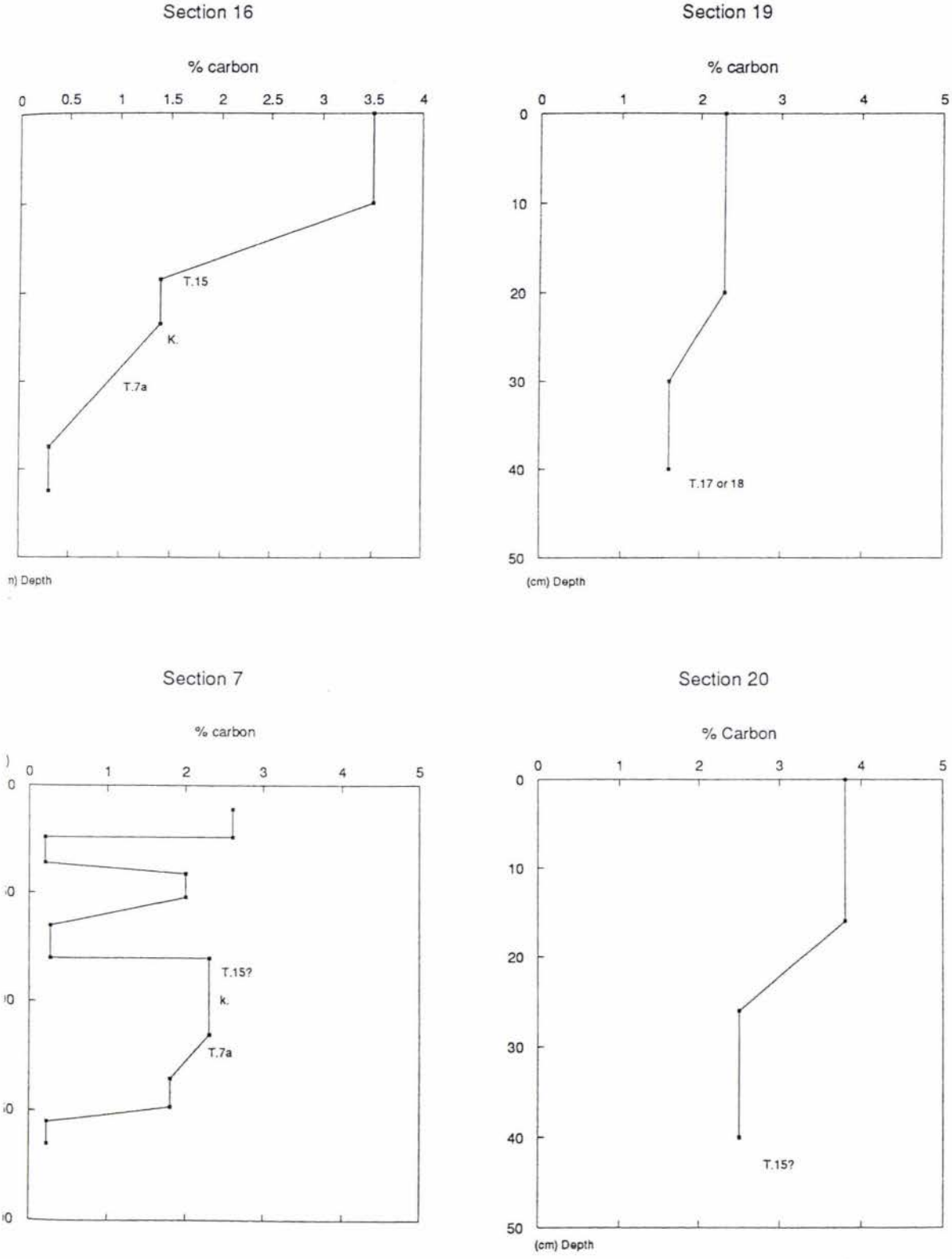

Figure 3.15 Percent carbon for reference dune sand sections

Section 7 is found on a larger dune which is about 10 meters away from section 19. This dune lies close to the boundary between the laharic and fluvial lag surface and an older Taupo Pumice ignimbrite veneer surface (Plate 3.8). The presence of Tufa Trig member 7a indicates that this dune began to develop about 750 years ago. The accumulation rates increase nearly two fold between Tufa Trig member 7a and the Kaharoa Ash, and then subsequently decline above the Kaharoa Ash (Fig. 3.14). The silt and very fine sand fractions (fig 3.15) gradually increase upwards from the bottom of the profile to a depth of 80cm. From 80cm to the top of the profile the percentages (particularly for the very fine sand fraction) vary considerably . Allophane and carbon percentages mirror the very fine sand fraction trend up to 80cm depth, but then trend inversely to the surface.

Section 20 (Fig. 3.11), is located on a dune that is about 50m from the the dunes which contain sections 19 and 7. This dune overlies the pTPp which is located on an older Taupo Pumice ignimbrite veneered surface (Plate 3.8). The increased distance from source is reflected in the grain size distribution although there is still 30% medium sand found in the lower part of the profile. Allophane (Fig. 3.14) and carbon percentages (Fig. 3.15) have increased as the finer grain sizes became dominant higher in the profile.

The stratigraphy of section 20 (Fig. 3.11) shows that Tufa Trig members 4,5 and 7a are missing between the base of the Makahikatoa Sands and the pTPp. This is a feature observed for the majority of these dunes that overlie the pTPp suggesting that these dunes did not encroach onto this area until some time after 850 yrs B.P. Using stratigraphic superposition it appears that Tufa Trig member 15, present near the base of the dune, overlies the pTPp. From evidence presented in section 3.6. Tufa Trig member 15 maybe about 300-400 years old. Therefore, it is concluded that these dunes encroached over the pTPp located on a Taupo Pumice ignimbrite veneered surface about 300-400 years ago.

Plate 3.8 Photograph of Barbed Wire Gully showing the boundary between a post-Taupo Pumice laharic and fluvial surface on the left, and an older Taupo Pumice ignimbrite veneered surface on the right. In the left hand side of the gully the younger deposits overlie the Taupo Pumice ignimbrite. Dunes colonised with *Phyllocladus* scrub are seen encroaching on to the younger surface. Sections 7 and 19 are found on these dunes. Section 20 is found on a dune located on the older surface to the right of this photograph.

Section 16 is located on a sequence of dunes (Plate 3.3) that rapidly coalesced against sheet sands between 800 and 700 yrs B.P. Because these dunes have coalesced, they look similar to the sheet sands (Plate 3.9) although the terrain is generally more undulating. Unlike other dunes, the accumulation rates of these dunes decline rapidly after the deposition of Tufa Trig member 7a. With this decline a greater opportunity existed for soil forming processes to occur which is reflected in increased allophane (Fig. 3.14) and carbon percentages (Fig. 3.15).

3.3.5 Discussion Of Dune Sands

The modification of laharic/fluvial surfaces by aeolian processes has resulted in extensive lag pavements, and has provided a large source of aeolian sands for dune formation in the Rangipo Desert. As Cockayne (1908) suggested, for dune formation to occur, a degree of shelter is required to enable the initial stabilisation of sand.

Barbed Wire Gully (Plate 3.7) is an example of how the local shelter from one dune facilitates the development of other dunes further onto the lag surface. Section 7 was one of the first dunes to develop here on the lahar and fluvial surface. As the dune provided increased shelter to the *Raoulia albosericea*,*Rytidosperma setifolia*, and other plants on the lahar and fluvial surface, the balance seems to have been tipped, and these plants begin to coalesce and trap sand, initiating the beginning of a new dune. It appears that when the dune, on which section 7 is located, was about a meter high the dunes in front of it began to trap increasing amounts of Makahikatoa Sands. As a result accumulation rates began to slow (Fig. 3.12), and silt and very fine sand was deposited preferentially over the coarser grain sizes (Fig. 3.13). The particle size distribution, carbon and allophane (Figs. 3.14, 3.15) contents also began to fluctuate indicating that the dune changed from one receiving sand at a reasonably rapid rate to one receiving only periodic influxes. However, there is an anomaly during this period of influxes. Intervals when deposition decreased and soil formation increased also strangely coincide with increases in grain size. A possible explanation is that these periods were overall more climatically stable, but were punctuated by the occasional storms with strong winds which caused an influx of saltated grains.

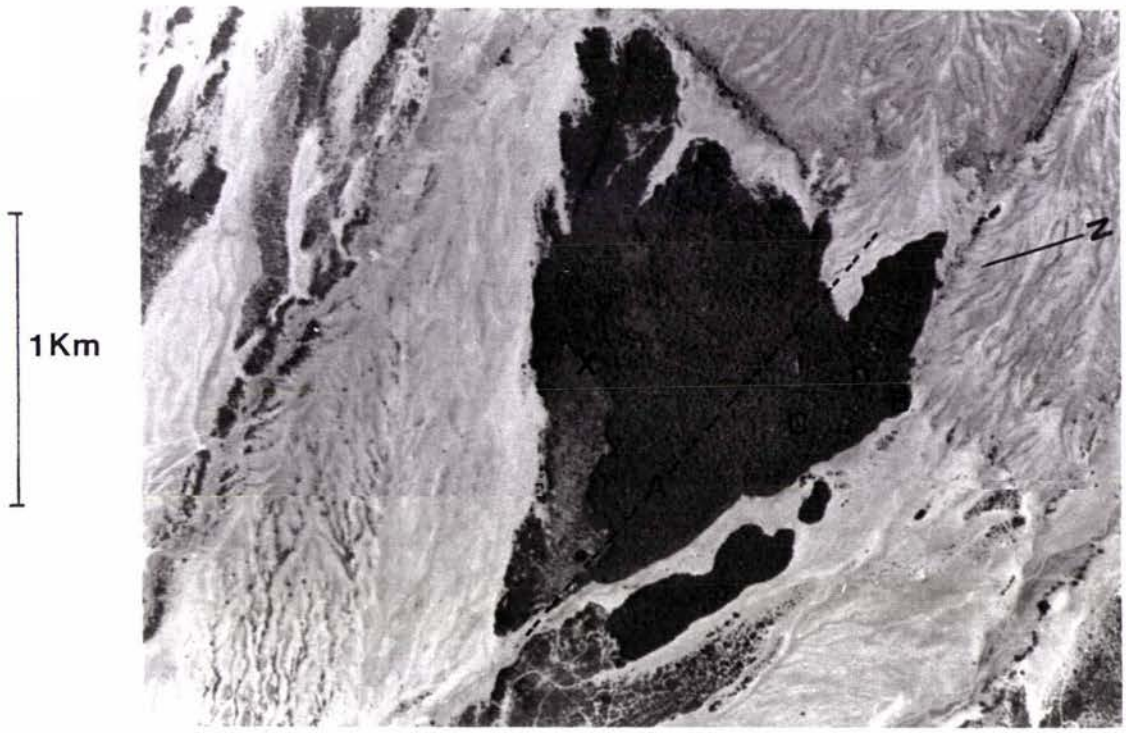

Plate 3.9 Aerial photograph taken in 1980 of Large *N. solandri* Enclave. The enclave also contains *Phyllocladus* forest and scrub which is the lighter vegetation with less texture. The black stippled line represents an estimated boundary between the coalesed dune sands on the right and the sheet sands on the left. Much of the south-western (left) margin of the enclave is also occupied by dune sands.

The black dot represents the location of section 21. The patch-work nature of the vegetation here represents a mosaic of low shrubs with emergent *Phyllocladus* which have re-colonised the area after a fire about 110 years ago. The margin between this area and the *N. solandri* trees represents a burn line. At locality X outlier *N. solandri* trees may represent an earlier burning episode between 250 and 350 years ago.

Letters represent the localities of *N. solandri* stands which were investigated (chapter 4). The dull lines are artifacts of the photograph.

The dune on which section 17 is located has received an unhindered supply of aeolian sand and, because of this, is now over 6 metres in height. It appears that the formation of forest, albeit a forest with many canopy gaps, has stabilised the accumulating sand. If vegetation cover diminishes on these high dunes, the exposed sands are quickly re-worked, and the dunes soon destabilise and begin to collapse.

The development of the dune sands at section 16 occurred when an excess of source material became available, probably from lahar deposit 6, and coalesced against the sheet sands at Large *N. solandri* Enclave. As the source material became depleted the accumulation rates (Fig. 3.12) decreased and soil formation correspondingly increased.

In summary, the dunes have been forming on all the surfaces of the study area. The presence of older dunes, providing shelter, has allowed plants to fix drifting sand and form younger dunes. Dune fields, therefore, are continuing to encroach on to the surfaces of the study area, and provided plant cover is maintained, this process seems likely to continue.

3.3.6 Comparison Of Estimated Accumulation Rates And post-Taupo Pumice Chronology

The development of a post-Taupo Pumice chronology for the interbedded Tufa Trig members has provided the time planes necessary to estimate the accumulation rates of the Makahikatoa Sands as shown in the previous sections. A converse approach may also be taken by checking the validity of the chronology, by comparing the accumulation rates with the rates of observed pedogenesis.

A major discrepancy is found between accumulation rates and observed pedogenesis when Tufa Trig member 15 is used in the accumulation rate profile calculations. In sections 1,7,13, and 16 a marked decrease in the the accumulation rate occurs between Tufa Trig member 7a and 15, and a marked increase occurs in the rate above member 15 (Figs. 3.4, 3.7, and 3.12) This is contrary to both field and laboratory evidence. Allophane (Figs. 3.2, 3.8, and 3.15) and carbon (Figs. 3.3, 3.9, 3.15) trends indicate little change between Tufa Trig member 7a and the surface. This suggests that the 'modern' (<200 years) radio-carbon age on the beech leaves in Tufa Trig member 15 is an incorrect date. Due to the small sample weight, this date was measured using an accelerator mass spectrometer, and as a result, possible contamination by fine roots may have led to a younger than true date.

Section 21, illustrated in Fig. 2.6, contains undated charcoal. In the locality of section 21, tree-ring dating of emergent *Phyllocladus* in seral shrubland indicates that burning occurred about 110 years ago. However, the presence of outlier *N. solandri* in the same locality suggests that burning also occurred well over 200 years ago. If this charcoal was deposited after the earlier burning episode then the stratigraphy would suggest that Tufa Trig member 15 was deposited between 300-400 yrs B.P. A date of this order would explain the discrepancy between calculated accumulation rates and observed pedogenesis.

A further refinement of the post-Taupo chronology would lead to more accurate estimates of accumulation rates. This would allow examination of the relationships between depositional rates, depositional environments and pedogenesis in more detail.

3.3.7 Implications For The Erosional History Of The Rangipo Desert

Introduction

The degree to which deforestation has triggered landform instability and erosion in New Zealand is currently controversial. Grant (1985) and McFadgen (1985) favour cycles of climatic change over the last 2,000 years as the primary cause of both inland and coastal erosion and instability. In essence, they claim, that certain periods are characterised by high frequencies of intense cyclonic rainstorms which induce slipping over very wide areas. However, McGlone (1989) argues that it is premature to claim that alluvial sedimentation periods (Grant, 1985) match the coastal depositional episodes (McFadgen, 1985) in New Zealand. He believes that Grant's 7 stable-forming episodes and McFadgen's 2 stable forming episodes are a fortuitous match given the uncertainty of radiocarbon dates in this time range. McGlone (1983, 1989) asserts that while climatic variation may have affected regional areas at different times, the widespread deforestation by Polynesians and Europeans caused massive destabilisation of weak soft substrates.

A peculiarity to the landscape of the Rangipo Desert has been its susceptibility to inundation of lahars. Crawford (1880) described how a lahar crossing the Rangipo Desert tore up bushes and scarred the surface in its way. Overseas workers have reported lahars that have destroyed forests (Loomis, 1926; Crandell, 1971) and severely eroded valley walls and floors (Waldron, 1967). Given this background, the possible causes which may have initiated the deflation at c. 800 yrs B.P. of the now widespread erosion are discussed.

Fire

McGlone (1989) has concluded from pollen spectra that rapid extensive deforestation from burning by Polynesians began at 750 yrs B.P. throughout the country. Only sporadic and limited burning occurred before this time. Polynesian conflagrations, however, did not occur around north-west Ruapehu until c. 600 yrs B.P. (Steel; 1989) and in the Moawhango head waters until c. 530 yrs B.P. (Rogers, 1987; see chapter 1). The charcoal found on the lower slopes of the study area (section 4, Plate 2.1), dated at 500 ± 70 yrs B.P. (WK 1487), would suggest that this fire correlates to the widespread conflagration at 530 yrs B.P., recorded by Rogers. This could represent the opening up of the provincial track between the Rangipo Desert and the Moawhango River, postulated by Lethbridge (1971). Rogers (1987) concludes that the fires were set deliberately at the high altitudes to clear forest or encourage open vegetation for ease of navigation and movement during travels. He found the major forest fires spatially correlated with interdistrict routes in the north.

Deforestation from natural fire has been recorded in the Moawhango Ecological District by Rogers (1987) who, from pollen evidence, found that natural fires depleted forest cover well before the Taupo Pumice ignimbrite. Support for this in the Rangipo Desert comes from localised charcoal found in the Mangatawai Tephra. It is probable that this localised burning was due to lightening strike. There are no distinguishable deposits around the charcoal which indicate burning due to the deposition of hot tephra. Although several of the Tufa Trig members erupted from Mount Ruapehu have stripped *N. solandri* and *Coprosma sp.* leaves from trees and shrubs, it is very unlikely they caused fire. This is in accordance with McGlone's (1981) conclusion that airfall tephra less than 600 mm thick will not lead to deforestation.

The present erosional surface observed in the study area began to deflate at c. 800 yrs B.P., and therefore, does not correlate to periods of regional Poynesian deforestation. Although charcoal is detected in one area adjacent to the deflating surface, its age is predicted to be either around 250 yrs B.P. or 90 yrs B.P. No charcoal was found in any localities near the 800 yrs B.P. stratigraphic time plane. Therefore, I believe that fire was unlikely to be responsible for the present erosion seen in the Rangipo Desert.

Had fire been an agent of vegetation destruction during this period it may have initiated erosion on the upper, steeper slopes of the deflating surfaces; however, the majority of the deflating area occurs on slopes of only 2° to 3°. Other areas of similar slopes burnt in more recent times (chapter 4), have recovered very quickly after burning, and little apparent erosion has occurred.

Climatic Instability

It is difficult to draw any direct correlations between climatic instability and the beginning of an erosion period at c. 800 yrs B.P. Hubbard and Neall (1980) recorded a period of aggradation in the Ruahine Range (Tamaki River catchment) at 770 ± 60 yrs B.P., which they attribute to storminess. However, Grant (1985) records 800 yrs B.P. as a period of relative stability in the ranges. This period falls within a coastal unstable phase, called the Tamatean chronozone by McFadgen (1985); however, the problem with the Tamatean chronozone is that it lasts from the time of the Taupo Pumice eruption (c. 1764 yrs B.P.) to about 600 yrs B.P. In the Rangipo Desert the landscape was relatively stable prior to c. 850 yrs B.P. as evidenced by the post-Taupo paleosol.

Lahars And Floods

There is a strong correlation between when the erosional surfaces began to develop and the increased periodicity of lahars that inundated the desert at this time. It is likely that lahar 6 engulfed the present erosional surfaces (chapter 2) at the same time as the surfaces began to deflate.

The effects of lahar 6 on vegetation was probably devastating, both directly, by knocking over trees and tearing up bushes in its path, and indirectly, by burying much of the vegetation in its path. A 40cm thick, fines depleted lahar deposit, typical of lahar deposit 6, was found preserved on a ridge on the higher slopes of the eroding surface (chapter 2). Given the locality of this deposit, it is likely that thicker deposits occur in lower areas, where the lahar would have spread out and decreased in velocity.

The coarse nature of these deposits is an extremely drought prone medium for plant growth that is also chemically infertile (section B, this chapter). This has resulted in an almost non-existent plant cover on the surfaces covered by these deposits. I envisage that re-colonisation of vegetation would have been inhibited after lahar burial. Subsequently, over time, the down cutting of channels by stream action, would have re-exposed the underlying tephra, and erosion by hoar frosts would have expanded these channel widths, until only remnant lahar deposits on scattered ridge tops were left.

This process is still in action today near Death Gully (fig 1.1) at the margin of the constructional surface. Here advanced deflation of the erosional surface could be due to a lahar deposit which, whilst significantly thick to inhibit rapid plant re-colonisation, was sufficiently thin to allow the underlying tephra to be re-exposed by fluvial and frost action.

This suggestion, however, does not accommodate the erosion observed on the eastern slopes of Mount Tongariro, described by Topping (1974). Further work is needed to assess when the erosion in those areas began.

In summary, there is no evidence that fire initiated the erosion found in the Rangipo Desert today; and I believe fire on its own would not have initiated the erosion. Subsequent fires, widespread in early European settlement may have accelerated the erosional processes, but it appears that the native plants cannot readily re-establish on the eroding surface, thus leaving the surface exposed to the elements. Although a series of floods could possibly destabilise the landscape, a lahar would seem a more plausible cause, because of the shear volume of flow associated with an event. It must be emphasised that the total volume of lahar 6 was estimated (chapter 2) to be between 1.8×10^8 m^3 and 2.4×10^8 m^3, which is 100 to 240 times the volume of the 1975 event; it was clearly a devastating event. Therefore, evidence from this study suggests that disruption to the landscape, caused by lahar 6 about 800 yrs B.P. is the most likely cause for the initiation of the present erosion witnessed in the study area.

SECTION B: Comparitive Soil Fertility Measurements in the Rangipo Desert

3.4 Introduction

The inability of native plants, except for a few scattered prostrate shrubs or clumps of *Rytidosperma setifolia* and *Raoulia albosericea,* to colonize the fluvial and laharic surface has resulted in a patchwork vegetation pattern. Cockayne (1908) believed the porus substratum, and the absence of humus or clay, the presence of wind, and particularly the absence of water were the main causes of the desert. In this study the drought potential and the chemical fertility of soils developed in the Makahikatoa Sands is compared to the incipient soils developed on fluvial and laharic surfaces.

3.5 Methods

3.5.1 Introduction

A soil-moisture balance combined with estimates of total available water holding capacities are a useful method of modelling potential drought conditions. A soil-moisture balance, based on Penman's formula (Cambell, 1977), is presented for the Rangipo Desert.

Selected measures on pH, total N, and total and available P are presented to provide an indication of the fertility status of the soils. Phosphate retention is also a useful measure of available P because of the potential of allophane to adsorb P (Parfitt, 1986,1989). Allophane as well as hydrous oxides of iron and aluminium (Theng, 1980; Parfitt, 1980) and organic matter (Tate and Theng; 1980) possess a high surface area whose net charge varies with pH. Both the pH of H_2O and KCl were measured in some samples to determine if the natural pH was above or below the point of zero charge (pzc).

3.5.2 Estimation Of Drought Potential

The two climatic inputs required for a soil moisture balance are rainfall and evaporation. The average monthly Waiouru rainfall data from 1941-1970 is normalised to the 2000mm total annual rainfall of the Rangipo Desert (chapter 1), thus producing an average monthly rainfall for the Rangipo Desert. In absence of real evaporation measuring equipment, monthly regional evaporation rates were derived using long-term average Penman data supplied by N.Z. Meteorological Service.

The equilibrium evaporation rate of Penman's equation: $\frac{s}{s + \gamma}$ (Cambell,1977)

is considered the dominant term in New Zealand conditions (McNaughton, 1979). Therefore, by employing a correction factor for the temperature, Manaia's (E94512) regional evaporation data is used as a first approximation for Waiouru (Fig. 3.19). This carries with it the assumption that net radiation is similar between Manaia and Waiouru, which is reasonable, given their same latitude.

Figure 3.16 Corrected Regional Evaporation Figures For Waiouru.

	Temperature (°C)	$\frac{s}{s+\gamma}$
Waiouru	9	.53
Manaia	13	.58

Correction factor for Waiouru = $E^r \times \frac{.53}{.58}$

	Jan	Feb	Mar	Apr	May	Jun	Jul	Aug	Sep	Oct	Nov	Dec
E^r Manaia	116	104	80	49	27	20	22	36	54	81	109	119
E^r Waiouru (corrected)	106	95	73	55	35	18	20	33	49	74	100	109

The correction factor could have been avoided if Thornthwaite's (1948) formula was used, but because it seriously underestimates regional evaporation in New Zealand conditions (Coulter, 1973), it was not considered.

Bulk Density

Bulk density of samples was measured using the procedure of Gradwell and Birrell (1979). Thin-walled metal cylinders, of internal dimensions 50mm long and 48mm in diameter, were used to collect intact cores from the field. The soil cores were dried for 24 hours at 105°C in a ventilated oven, before being weighed.

Total Available Water-Holding Capacity

In order to estimate the total available water-holding capacity (TAWC) of soils both field capacity (FC) measurements and 15-bar water retention or permanent wilting point (P.W.P) measurements are required, where

$$T.A.W.C.(vol./vol.\ \%) = (F.C. - P.W.P) \times \text{dry bulk density } (km.m^{-3})$$

Field Capacity

Samples for F.C. measurements were collected in October 1989, two days after rainfall. The soil-moisture indicates that soils are at field capacity during spring, and the preceeding months were no drier than usual (M. Edwards pers. comm.).

15-Bar Water Retention

A pressure Plate apparatus, as described by Gradwell (1971) was used to determine the water content of soil samples, equilibrated at a pressure of 15 bars, for one week. Soil samples, were lightly packed into plastic rings, 10mm long and 52mm wide, and placed on a ceramic Plate. These were wetted, and left over night to ensure that the soil was saturated before a pressure of 15 bars was applied. The 15-bar water retention is then calculated as the gravimetric water content of soils, which attained an equilibrium water content under a pressure of 15 bars, after one week.

$$\text{15 bar water retention} = \frac{\text{weight of water}}{\text{weight of dry soil}} \times \frac{100}{1}$$

(the soil is dried overnight, at a temperature of 105-110°C)

3.5.3 Estimation Of The Fertility Status

Soil pH (H_2O and KCl), Olsen P

Procedures for determining soil pH in H_2O and Kcl were used following Blakemore *et al.* (1987).

Total Nitrogen, Total Phosphorus,

The method used in this study follows that of Twine and Williams (1971).

3.6 Results and Discussion

3.6.1 Drought Potential

The soil-moisture balance for the Rangipo Desert shows (Fig. 3.17) that in a normal year there is no apparent monthly soil-water deficit. However 10th percentile rainfall figures indicate a potential summer soil-water deficit of up to 150mm can exist in one in 10 years.

Volumetric water content calculated for 2 sheet-sands deposits and 1 dune-sand deposit (Fig. 3.18) indicates that total available water holding capacities for these 3 deposits is approximately 200mm for every metre of soil. In these deposits very fine roots were found down to depths greater than 4 metres; however, in most cases, the majority of roots were located in the top metre. These results suggest that a soil-water deficit will not occur in these soils even in a one in ten year drought, given a rooting depth of 1m. Therefore, enough water is available for plant growth survival in most drought periods.

On the other hand, because the rooting depths of native plants is restricted to the top 15cm of the fluvial and laharic surface, only 16mm of total water is available to these plants (Fig. 3.18). Therefore, the wilting points would be surpassed for 3 consecutive months during a 1 in 10 year summer drought. However, it is likely that wilting point will be reached regularly in the soils on the laharic and fluvial deposits, because it would take only about a week of sunshine in January or February in any 1 year to create a moisture deficit greater than -1500 kPa (15-bars).

Figure 3.17
Soil-moisture balance for Rangipo Desert

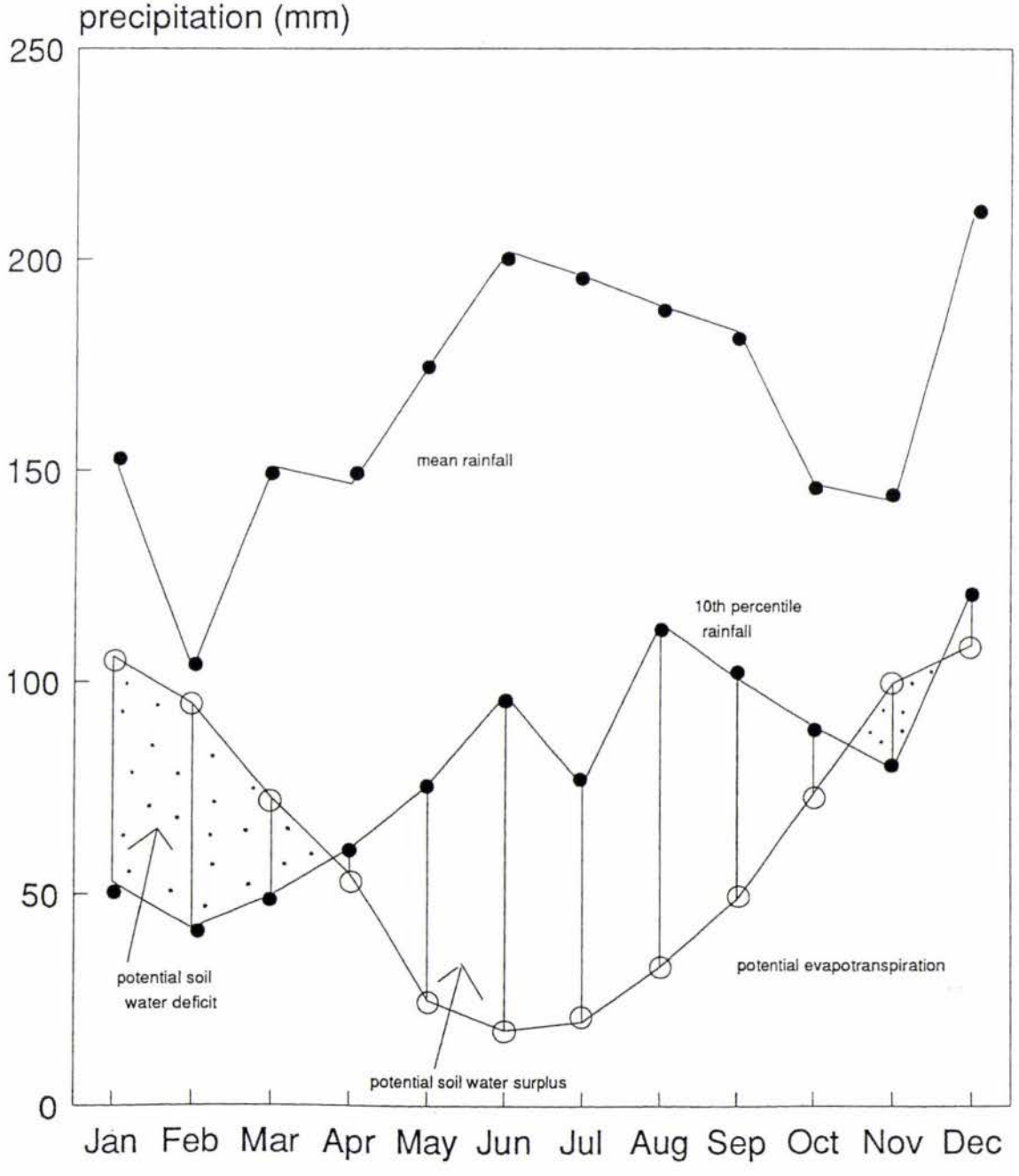

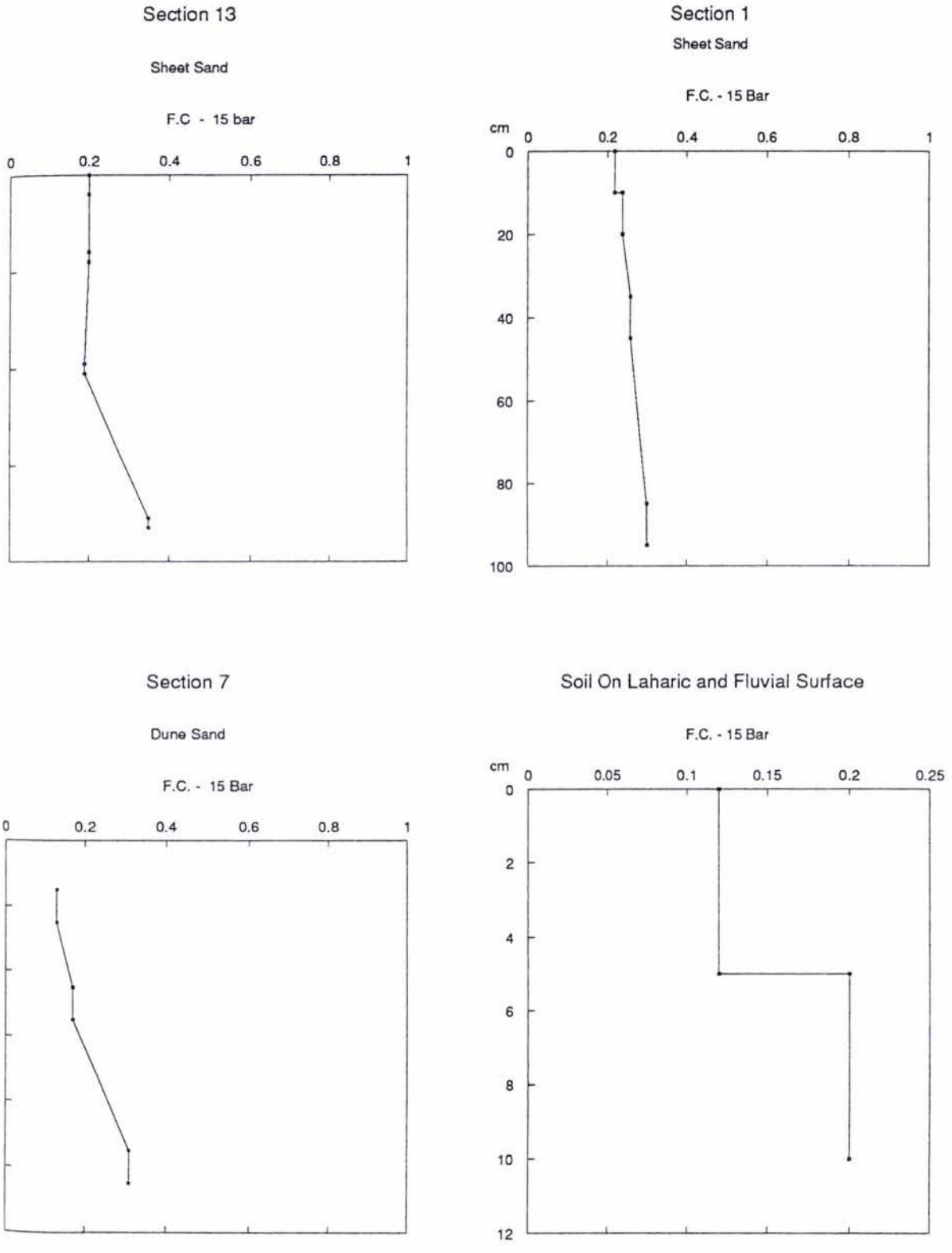

Figure 3.18 Total available water holding capacities

3.6.2 Fertility Status.

The soils saturated with KCl (Table 3.1) gave a lower pH reading than the soils saturated with H_2O. This indicates that the natural pH of the soils in the Rangipo Desert is greater than the point of zero charge for these soils. Therefore, it is expected that the base cations are more readily available in these soils because the cations are more readily adsorbed on the colloid surfaces (Parfitt, 1980). Allophane and ferrihydrite are not only the main contributors to the variable charge of volcanic soils but are also a major cause of P deficiency (Parfitt, 1980,1989). Olsen P values were low in all soils sampled (Figs. 3.19, 3.20), except in the topsoil of a profile under a mature stand of *N. solandri*. Here, the breakdown of litter and the mineralisation of the released P would be the principal cause of increased P availability (Table 3.1). However, the acidic pH in this topsoil could also, to a small degree, enhance dissolution of apatite (R. Tillman pers. comm.).

Total P measurements suggest that much of the inorganic P is being adsorbed by allophane and ferrihydrite and the organic P adsorbed by carbon. The increased amounts of allophane in the Makahikatoa Sands have been paralleled by increased phosphate retention values (appendix 3b) and very low available P values (Figs. 3.19, 3.20). Allophane percentages between one and two percent resulted in phosphate retention values of between 10 and 30 percent, whilst allophane percentages of 3 to 5 percent resulted in 60 to 70 percent retention values. In the pTPp allopane percentages were measured between 7 and 9 percent which resulted in retention values exceeding 80 percent. The total P measured in a Tufa Trig member (Table 3.1) is considerably lower than for the Makahikatoa Sands. This suggests that the levels of apatite are lower in the recently erupted tephras from Mount Ruapehu.

Total N results (Table 3.1) for the Makahikatoa Sands range from medium in the topsoil under mountain beech to very low in the poorly developed soils of the dune sands and primary tephra deposits. C/N ratios are very high in topsoils which are influenced by a *Phyllocladus* or *N. solandri* litter, but then drop lower in the profiles. These are typical ratios from litter of of low base status vegetation such as conifers or beech (Taylor and Pohlen, 1970). On the other hand C/N ratios are medium under the tussockland, indicating a mulloid organic profile.

Table 3.1 Additional Laboratory Analyses Not Graphed

Depth (cm)	pH		Total P	Total N	C/N	
	H^2O	KCl	µg/g	%		
Section 13						
130-140	6.3	5.5	230	.15	11	
202-210	6.2	5.4	70	.03	8	
377-399	6.2	5.7	280	.21	12	
Mangatawai Formation	6.2	5.6	320	.16	13	
Section 1						
1-6			220	.23	13	
37-50			190	.17	9	
Section 14						
1-10	6.0	5.0	260	.27	14	
10-20	6.3	5.4	260	.27	12	
32-49	6.5	5.7	150	.15	8	
Section 7						
3-8			190	.07	12	
8-11			160	.17	15	
80-115			180	.17	13	
Section 19						
0-20	5.9	5.4	140	.07	41	
25-50			120	.1	23	
Section 16						
3-20			120	.12	29	
28-42			270	.15	9	
75-85			110	.04	8	
						Olsen P
Sample from interior of beech forest at site 4 (see plate 4.1).						(µg/g)
8-17	4.8	4.4	310	.35	31	13
28-42	6.1	5.3	310	.25	13	2
42-57			290	.24	14	2
Soil on laharic and fluvial surface.						
Sample from barbed wire gully (see plate 2.2)						
0-5				0.09		1
5-10	5.7	5.7		0.02		Trace
10+	6.5	6.0		Trace		Trace

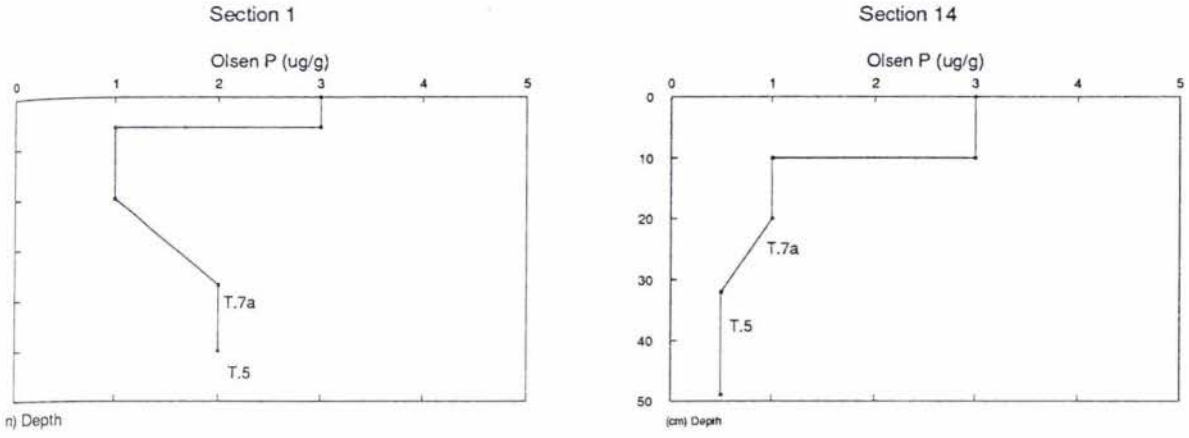

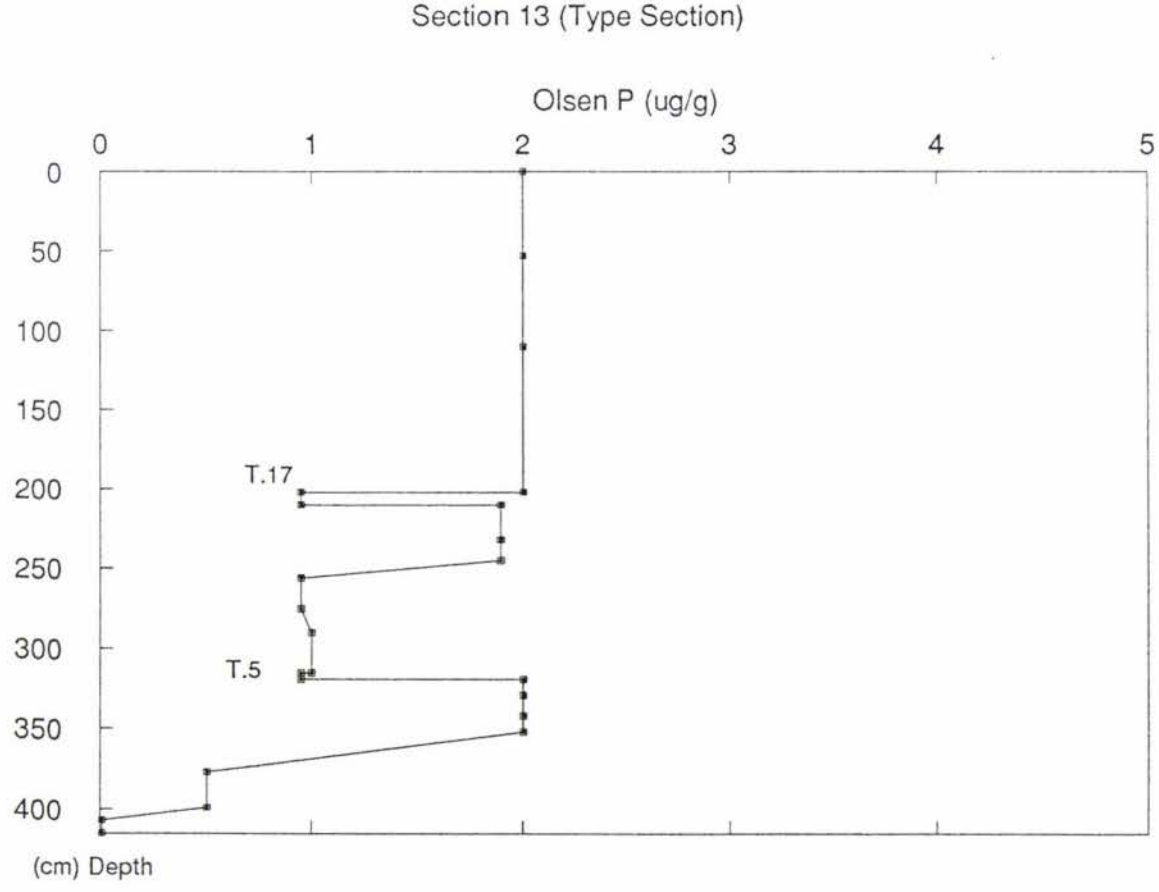

Figure 3.19 Olsen extractable P for sheet-sand deposits

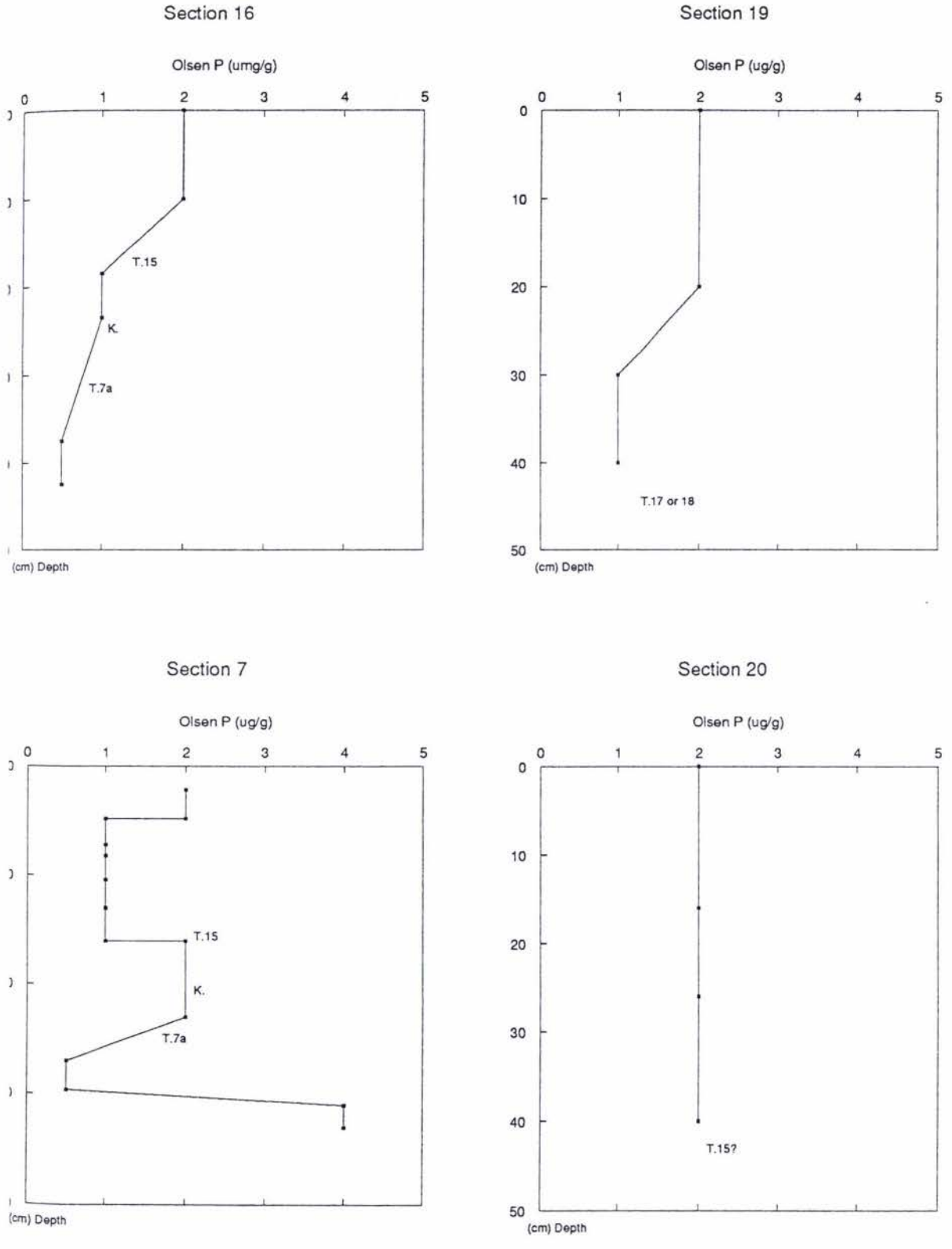

Figure 3.20 Olsen extractable P for dune-sand deposits

The soil on the laharic and fluvial surface contained only 1 µg/g of available P in the top 5cm (Table 3.1) and below 5cm none could be measured (trace). Similarly total nitrogen (Table 3.1) had only trace levels below 10cm. These soils, therefore, not only suffer from being drought prone but are also deficient in available P and N below a depth of 10cm. The lack of water and nutrients below a depth of 10cm explains the restricted rooting depth of the native plants found on these surfaces. The only shrubs to survive directly on these surfaces are prostrate shrubs such as *Raoulia albosericea* and *Cyathodes fraseri* that can extend roots laterally to extract water and nutrients from the surface horizons. It seems only *Pinus contorta* trees can tolerate these extreme conditions. Until recent eradication programmes, they were managing to colonise these exposed surfaces.

3.7 Concluding Remarks

The influx of sediment into the Rangipo Desert transported by lahars or floods, combined with erosion of adjacent tephric coverbeds, is providing a huge supply of sand and silt available for aeolian re-working. The aeolian deposits in the study area have been formally named the Makahikatoa Sands.

The Makahikatoa Sands are divided into 2 groups according to their geometrical forms. They are known as sheet sands or dune sands. The sheet sands have been deposited over an area at a similar accumulation rate, and therefore, are of similar thickness. As a consequence the landscape itends to be flat. The dune sands, on the other hand, form discrete dunes which take on a variety of shapes.

The oldest dunes began forming about 850 yrs B.P., when lahars 5-9 (chapter 2) transported at least 18.8 x 10^6 m^3 of debris into the study area. Since this time, the dunes have been forming extensively over the surfaces of the Rangipo Desert. The presence of the oldest dunes, providing shelter, has allowed nearby plants to fix drifting sand, and therefore facilitate the formation of younger dunes. Hence dune fields are continuing to encroach on to all surfaces, and provided plant cover is maintained and the environmental factors remain similar, it is believed this process will continue.

The sheet sands are found in areas where the coverbed stratigraphy indicates no erosion has occurred for at least 2,500 years. The depositional history of the sheet-sand deposits can be divided into 2 periods since the Taupo Pumice eruption. The first period, lasting for about 900 years to c. 850 yrs B.P., was one of slowly accumulating Makahikatoa Sands evidenced by a paleosol found overlying the Taupo Pumice ignimbrite. Since about 850 yrs B.P. accumulation rates have increased resulting in a decline in soil formation. However, the magnitude of the increased accumulation rates and the degree of pedogenesis varies between localities.

Accumulation rates for the sheet-sand deposits found in localities close to the fault escarpment have not increased dramatically since 850 yrs B.P., despite a marked decline in pedogenesis. The decline in pedogenesis is attributed to the increased input of unweathered aeolian sand, which is derived from the extensive post-Taupo Pumice lahar and fluvial deposits. On the hand, sheet-sand deposits that are located adjacent to the large erosional surfaces found in the western part of the study area have shown a dramatic increase in the accumulation of Makahikatoa Sands since 800 yrs B.P. The presence of re-worked Taupo Pumice, and comparatively high levels of allophane and carbon measured, is evidence that the source of these deposits is from pre-weathered tephra exposed on the adjacent eroding terrain.

The post-Taupo Pumice chronology developed in this study suggests that the influx of Makahikatoa Sands began c. 800 yrs B.P. Therefore, it is interpreted that eroding surfaces began to deflate at this time. Present evidence indicates lahar 6, the largest known lahar to inundate the Rangipo Desert, was responsible for the creation of the eroding surface. It is envisaged that a coarse deposit from lahar 6, now largely eroded away, was responsible for both killing and inhibiting re-colonisation of the now eroding surface. Similar coarse deposits found on the laharic and fluvial constructional surface are severely drought prone and nutrient deficient, and as a result, are only sparsely covered by a few hardy native plants.

In the last several hundred years the deposition rate of the Makahikatoa Sands has escalated on adjacent areas to the eroding surfaces. This suggests that an increased erosion rate or expansion of the eroding surface (or both) has occurred. This is probably due to gullies continuing to expand and undermine the remnant interfluves; acceleration of this process due to increased climatic instability may be possible. The erosion in the Rangipo Desert will continue until the exposed tephra coverbeds are stripped to the underlying laharic constructional surfaces. Thus continuing erosion of the tephra, and the huge reservoir of debris found on the laharic and fluvial surfaces, ensures continued deposition of Makahikatoa Sands, providing vegetation is there to entrap it.

CHAPTER 4

VEGETATION

Introduction

The Rangipo Desert's biotic landscape is made up of an intricate vegetation pattern, consisting of disjunct forest, scrub, tussock, sedge and rush communities. Yet 1800 years ago a simpler vegetation pattern, dominated by *Nothofagus* forest, is envisaged to exist. In this chapter the distribution and ecology of the plant communities are examined to explain why this intricate pattern has developed.

4.1 Vegetation Map

A physiognomic-floristic vegetation map is produced in this study (Fig. 4.1) to complement the map of Tongariro National Park (Atkinson 1981, 1985). A physionomic-floristic map contains two pieces of information. The first is the name of the species that are most important in the canopy (floristic); these are indicated with lettering on the map. The second is the growth form or structure of the vegetation (physionomic); this is indicated with colour and patterns. For example green cross hatching indicates forest, whereas dots indicate sparse vegetation on open ground.

Delineating the plant communities in the field was completed using aerial photographs taken in 1978 (at a scale of 1:28000) for the map base. The area was examined and mapping units delineated during the summer of 1988 and parts were re-surveyed in the summer and autumn of 1989. Once the mapping units were delineated, estimations of the percentage cover of growth forms in the canopy for each mapping unit were obtained from selected sampling sites (Plate 4.1).

Sampling methods to determine the species in a canopy varied depending on the vegetation type. In *N. solandri* forest point-quarters (Brower and Zar, 1984) were used. The point-quarters were performed on random compass bearings in selected sites and the canopy trees identified and their circumferences measured at each point. In *Phyllocladus* dominant forest

20 m^2 plots were used. All canopy trees identified and circumferences measured. In shrublands, tussocklands, and on lahar and fluvial surfaces, and on eroding surfaces, the step-point method (Atkinson, 1962) was used. A stick was placed on the ground after five paces and the plant touching the highest point on the stick was designated as the cover plant. At each site either 300 or 500 points were sampled within five parallel transects. To avoid bias when placing one's stick down, the eyes were focused on a distinct object while pacing out the steps. Dunes, covered with *Phyllocladus* scrub, were more difficult to assess because of the tree and shrub mixtures. To overcome this the cover of several representive dunes was estimated by eyeball estimation. To make this easier dunes were sub-divided into plots. Only the 'wetland' mapping units have not been classified, although a description is given in an area in the larger wetland. This was because the diverse vegetation assemblage that occurs there would require very detailed mapping.

One major problem to overcome was the effect of burning that has occurred this last summer (1988-89). The extent and sporadic nature of burning over the study area has made it impossible to re-map all the areas now burnt; however, major areas that have been burnt were recorded.

Description Of Mapping Units

The common canopy and understory plant species found within a mapping unit are described below. Full details of percentage cover of growth forms in the canopy from the sampled sites are given in appendix 3a. The Makahikatoa Sands form the parent material for the soils located under the majority of forests, scrub, shrublands, tussocklands, and wetlands. A thin soil formed on lahar and fluvial deposits (chapter 3) supports only scattered plants, while the areas of eroding tephra also support only scattered plants.

Figure 4.1 Vegetation Map Of The Rangipo Desert

-accompanying map (Map 2) is located in back pocket

Vegetation Symbols

A dash (-) joins names of species of simialar height
A forward slash (/) separates names of taller species, left of symbol, from shorter species, to the right of the symbol

ie. Chionochloa rubra is taller than Poa cita Cr/Pc

Pc	Cover of species underlined	>50%
Pc	Cover of species	20-49%
(Pc)	Cover of species so bracketed	10-19%
[Pc]	Cover of species so bracketed	1-9%

Vegetation Ledgend

Note: Lettering is only placed on the map when there is more than one community type with the same colour and hatching or when there is no colour.

Forest

N. solandri Forest Nc= 

Phyllocladus Forest Pa= 

Scrub

Phyllocladus Pa= 

Absence of a boundary line around the dashes indicate that the dunes of Phyllocladus scrub are more scattered.

Shrubland 

Ds-Cr Dracophyllum subulatum-Chionochloa rubra

[Cv/Csp.] Cassinia vauvilliersii/Coriaria sp.

Hb-Hv-(On) Halocarpus bidwillii-Hebe venustula-Olearia nummularifolia

[Hb-Hv] Halocarpus bidwilli - Hebe venustula

Tussockland

Cr/Pc Chionochloa rubra/Poa cita 

(Cr)/Pc " 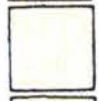

[Cr]/Pc " 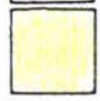

(Cr)/Pc/(Hp) Chionochloa rubra/Poa cita/Hieracium pilosella(adv)

(Pc-Ao)/(Hp)-Cf Poa Cita-Anthoxanthum odoratum/
Hieracium pilosella-Cyathodes fraseri

Scattered vegetation located on eroding tepra coverbeds 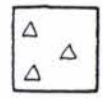

[On/Rs] Olearia nummularifolia/Rytidosperma setifolia

Scattered vegetation located on lahar and fluvial surfaces 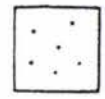

[Cf] Cyathodes fraseri

[Ra] Raoulia albosericea

Wetland 

Areas Burnt Since 1987/88 Summer

The red circle near the bottom of the map marks the reference locality Scorpion Gully (see Plate 4.1 and Fig. 1.2) while the two circles near the top of the map marks the reference localities Death Gully (left) and Barbed wire gully (right).

Plate 4.1 Localities of detailed sampling sites for vegetation map and vegetation studies.

Sites 1 to 3 are located in *Phyllocladus* dominant forest. Sites 4 to 6 are located in tussockland. Site 7 is located in seral shrubland. Site 8 is located on dunes colonised with *Phyllocladus* scrub. Site 9 is located on the lahar amd fluvial deposits. Site 10 occurs on an eroding surface.

The white arrow lower in the photograph points to reference locality Scorpion Gully (see Fig. 1.2). The white arrows higher in the photograph from left to right point to reference localities Death Valley, Barbed Wire Gully and The Chute respectively. The dark region at the top of the photograph is part of Large *N. solandri* Enclave.

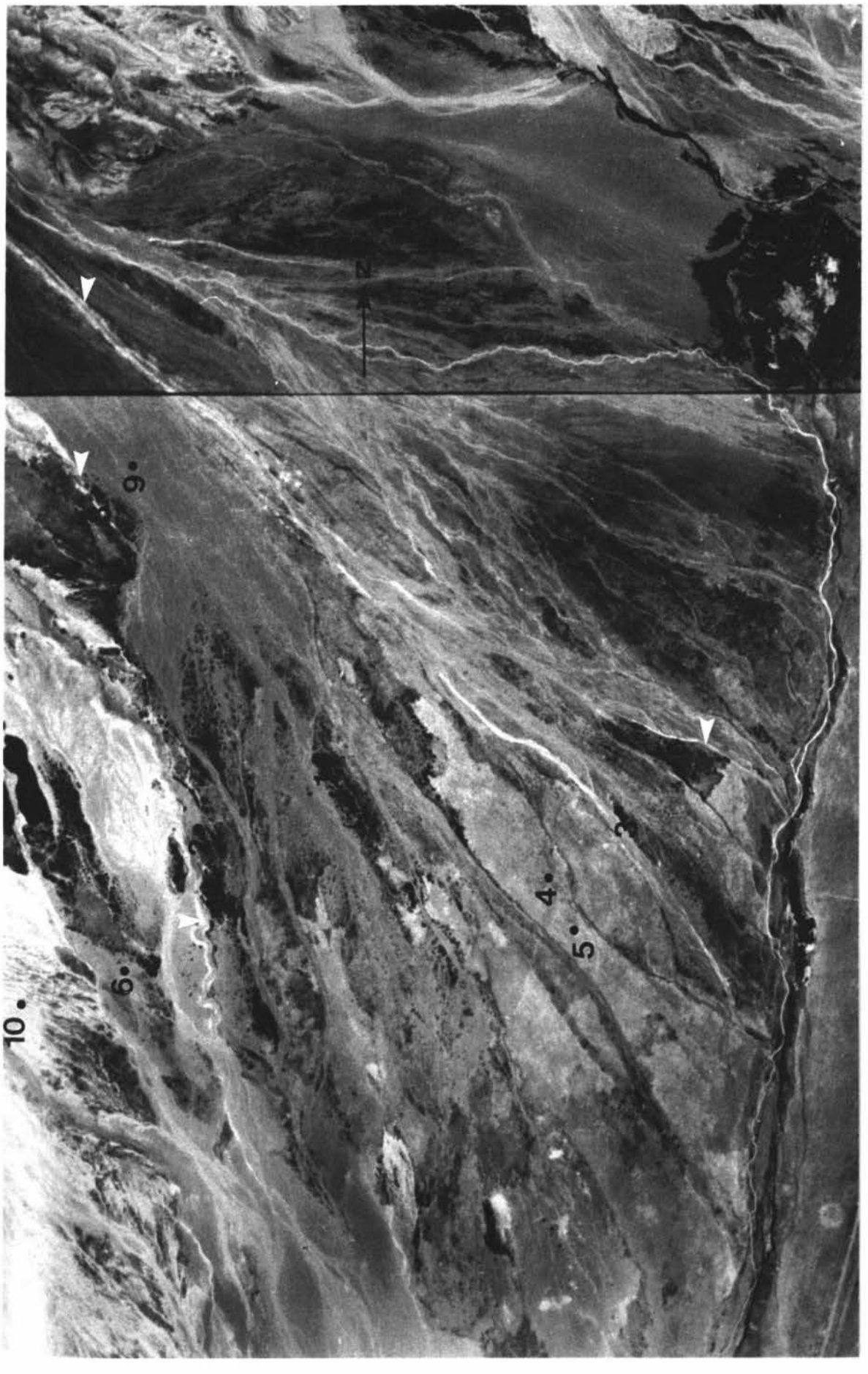
N
10.
6.
9.
5.
4.
3.
1 Km

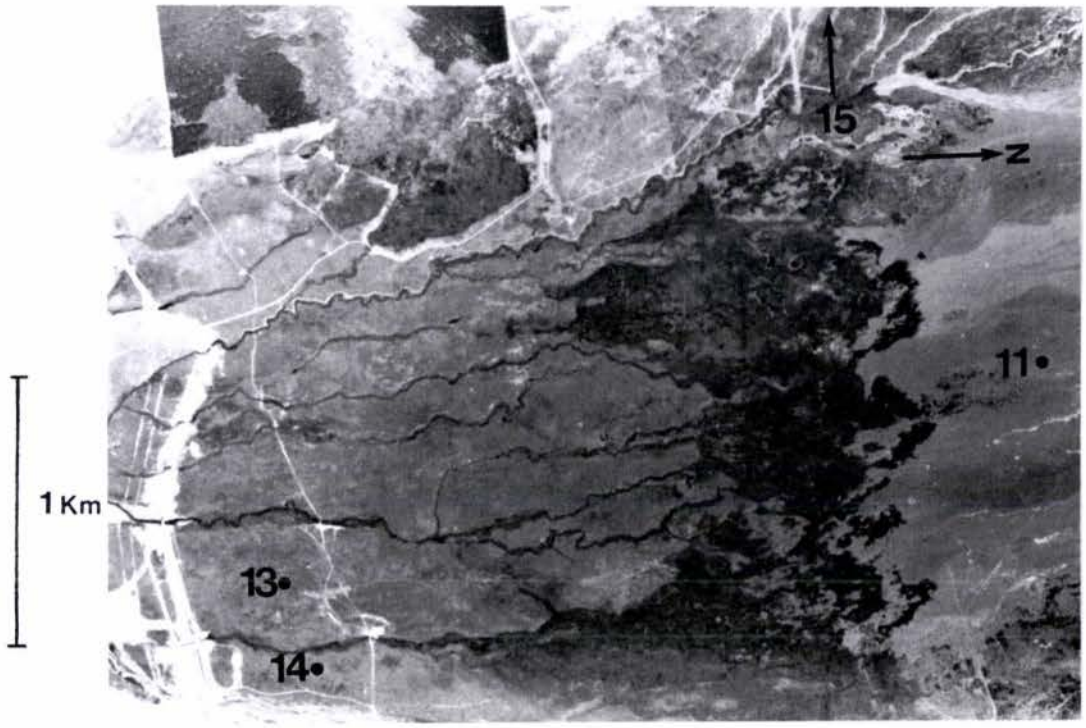

Plate 4.1 cont. Localities of detailed sampling sites used for the vegetation map and vegetation studies.

Site 11 located on fluvial and veneer lahar deposits. Site 12 located in wetlands. Site 13 and 14 located in sparse tussockland. Site 15 located on small dunes colonised with shrubs west of photograph at T20/405025.

Mountain Beech Forest, Nc

Canopy: canopy consists of *N. solandri* with *Phyllocladus, Griselinia littoralis, Podocarpus cunninghamii* and *Pseudopanax simplex* found in partial canopy gaps.

Common Understory Plants:

Tree Seedlings: *N. solandri* seedlings are ubiquitous and *Griselinia littoralis* and *Pseudopanax simplex* are relatively common but are small.

Shrubs: *Coprosma foetidissima, Coprosma pseudocuneata, Coprosma sp. "tx0"* hybrid (Eagle), *Coprosma sp.*"t" (Eagle) and *Muehlenbeckia axillaris* Herbs: *Laginefera strangulata.*

Ferns: *Blechnum penna-marina* and *Polystichum vestistum* and *Hymenophyllum multifidum.*

Mosses: *Dicranoloma billardieri, Hypnum cupressiforme, Bryum dichotomum,* and *Ptychomnion aciculare* common on the forest floor with *Leptostomum inclinans* common on bark of beech.

Sedge: *Uncinia clavata*

Phyllocladus Forest, Pa

Canopy: *Phyllocladus* forms about 70% of the canopy with *Halocarpus bidwillii, Griselinia littoralis, Pseudopanax simplex,* and *Podocarpus cunninghamii* forming the other 30%.

Common Understory Plants

Tree Seedlings: *Griselinia littoralis* and *Pseudopanax simplex* are common as small seedlings.

Shrubs: *Coprosma pseudocuneata* and *Coprosma* sp. "t" (Eagle) in sheltered forest with *Coprosma foetidissima* common in only one stand. *Gaultheria antipoda* and *Hebe venustula* are relatively common when canopy is more open. *Cyathodes sp.* (*C. jurniperina* agg.) is common to both situations.

Herbs: *Laginefera strangulata,Hypochaeris radicata*(adv), *Acaena anserinifolia,* and *Euphrasia cuneata*

Ferns: *Hymenophyllum multifidum* and *Blechnum penna-marina*

Mosses: *Dicranoloma billardieri, Hypnum cupressiforme* are common with *Leptostomum inclinans, Leptotheca gaudichaudii,* and *Dendroligotrichum dendroides* locally common.

Other Plants: *Lycopodium fastigiatum* is common.

Phyllocladus Scrub, Pa

Canopy Plants: *Phyllocladus* is often the only tree species forming 30-50% of the plant cover on dunes; however, on some dunes *Halocarpus bidwillii* may be the dominant tree. *Podocarpus cunninghamii* is sometimes present as young trees but is never dominant. Shrubs that commonly form the rest of the plant cover include *Dracophyllum subulatum, Hebe venustula, Olearia nummularifolia, Podocarpus nivalis, Coriaria sp., Cassinia vauvilliersii*, and *Epacris alpina* with *Pentachondra pumila* and *Cyathodes fraseri* found on dune edges.

Common Understory Plants

Shrubs: *Cyathodes sp. (C. jurniperina* agg.), *Gaultheria colensoi, Pentachondra pumila*, and *Lepidothamnos laxifolium* are found under *Phyllocladus* or nestled between the larger shrubs.

Herbs: *Euphrasia cuneata, Wahlenbergia albomarginata var. pygmaea, Celmisia gracilenta, Celmisia spectabilis, Geranium sp.*, and *Hypochaeris radicata*(adv).

Mosses: *Dicranoloma billardieri, Hypnum cupressiforme* and in sheltered areas with *Rhacomitrium langinusum, Polytrichum juniperinurn* and *Campylopus clavata* in exposed areas.

Grasses: *Poa ancepts* is reasonably common.

Other Plants: *Pterostylis pateans* is common in early summer.

Shrubland

Dracophyllum subulatum-Chionochloa rubra, Ds-Cr

Total Plant Cover: ≈ 100%

Common Canopy Plants: *Hebe venustula* is also common forming up to 20% of the cover in places. *Poa cita* fills much of the interstitial cover. Other common shrubs include *Dracophyllum recurvum, Halocarpus bidwillii, Gaultheria colensoi, Epacris alpina*, and *Cassinia vauvilliersii*. Emergent *Phyllocladus* are scattered throughout these areas.

Note: *Dracophyllum subulatum* includes hybrid *subulatum x recurvum*.

Common Understory Plants:

Shrubs: *Pentachondra pumila, Coriaria sp., Lepidothamnos laxifolium, Podocarpus nivalis, and Cyathodes sp. (C. jurniperina agg.).*

Herbs: *Anisotome aromatica, Celmisia gracilenta, Hypochaeris. radicata(adv), Wahlenbergia albomarginata var. pygmaea.*

Mosses: *Rhacomitrium langinusum, Polytrichum juniperinurn, Hypnum cupressiforme*, and *Campylopus clavata.*

Cassinia vauvilliersii-Coriaria sp. [Cv-Csp.]

Total Plant Cover: 66%

Common Understory Plants:

Shrubs: *Pentachondra pumila.*

Grasses: *Poa cita Holcus lanatus(adv).*

Herbs: *Hypochaeris radicata*(adv), *Senecio jacobaea* (adv).

Mosses: *Rhacomitrium langinusum, Polytrichum juniperinurn.*

Tussockland

Chionochloa rubra/ Poa cita, Cr/Poa cita

Total Plant Cover: ≈98

Common Understory Plants:

Shrubs: *Cyathodes fraseri, Pentachondra pumila, Cyathodes suaveolens, Coprosma cheesemanii,* and *Muehlenbeckia axillaris.*

Herbs: *Hieracium pilosella(adv), Wahlenbergia albomarginata var. pygmaea, Hypochaeris radicata(adv), Helichrysum bellidioides, Hydrocotyle* sp., *Celmisia gracilenta,* and *Epilobium alsinoides.*

Mosses: *Polytrichum juniperinurn.*

Lichens: *Cladia aggregatum.*

Poa cita [Cr]/PC and (Cr)/Pc

Total Plant Cover: ≈94%

Common Understory Plants:

Shrubs: *Cyathodes fraseri.*

Grasses: *Holcus lanatus(adv).*

Herbs: *Hypochaeris radicata(adv), Hieracium pilosella(adv), Helichrysum bellidioides,* and *Celmisia gracilenta.*

Mosses: *Polytrichum juniperinurn.*

Chionochloa rubra/ Poa cita /Hieracium pilosella(adv) (Cr)/Pc/(Hp)

Total Plant Cover: ≈97%.

Common Understory Plants:

Shrubs: *Cyathodes fraseri, Muehlenbeckia axillaris*

Grasses: *Anthoxanthum odoratum(adv), Deyeuxia avenoides*

Herbs: *Hieracium pilosella(adv), Linum catharticum* (adv), *Wahlenbergia albomarginata var. pygmaea*

Mosses: *Polytrichum juniperinurn*

Poa cita-Anthoxanthum odoratum/Hieracium pilosella-Cyathodes fraseri (Pc-Ao)/(Hp)-Cf

Plant cover ≈94% of total plant cover

Common Understory Plants:

Shrubs: *Cyathodes fraseri, Muehlenbeckia axillaris, Pentachondra pumila.*

Grasses:*Deyeuxia avenoides,Holcus lanatus(adv),Rytidosperma gracile*

Herbs: *Hieracium pilosella(adv), Wahlenbergia albomarginata var. pygmaea, Linum carthaticum (adv)*

Mosses: *Polytrichum juniperinurn*

Vegetation on the Eroding Surfaces

Olearia nummularifolia/Rytidosperma setifolia [On/Rs]

Total Plant Cover: 14%

Coriaria sp., Cyathodes fraseri,Dracophyllum subulatum, and *Epacris alpina* are relatively common.

Vegetation on the Gravelfields

Raoulia albosericea [Ra]

Total Plant Cover: 7%

Other species present: *Cyathodes fraseri, Rytidosperma setifolia, Pimelea microphylla*

Cyathodes fraseri [Cf]

Total Plant Cover: 13%

Other Species Present: *Rytidosperma setifolia, Pimelea microphylla, Gentiana bellidifolia, Raoulia albosericea*

Small dunes (less 1m²) dot these surfaces and consist of small shrubs, principally, *Cassinia vauvilliersii, Epacris alpina, Olearia nummularifolia,* and *G. depressa var. novae-zealandiae).* These dunes are also found between larger dunes colonised with *Phyllocladus* scrub.

Wetlands

The wetland area contains a multitude of plant species. The common species in sandy areas with surface water, or at least saturated, include:

Shrubs: *Leptospermum scoparium.*

Rushes: *Juncus novae-zelandiae, Juncus articulatas, Empodisma minus, Centrolepis ciliata.*

Sedges: *Carex coriacea, Calpha alpina, Shoenus concinnus,* and *Shoenus pauciflorus, Eleocharis gracilis* and *Isolepis subtilissima.*

Grasses:*Rytidosperma gracile, Holcus lanatus(adv).*

Ferns: *Gleichinia dicarpa, Blechnum penna-marina.*

Herbs: *Drosera binata, Lagenefera pumila, Gunnera prorepens, Myriophyllum pedunculatum, Selliera microphylla, Centaurium erythaea*(adv) *Nertera depressa,* and *Hypericum japonicum.*

Mosses: *Breutelia pendula, Bryum laevigatum, Bryum sp. and Hypnum cupressiforme.*

The common species in the saturated peat areas include:

Ferns: *Gleichenia dicarpa.*

Rushes: *Empodisma minus.*

Sedges: *Carpha alpina.*

Grasses:*Anthoxanthum odoratum* (adv)

Herbs: *Celmisia sp. "rhizomatus", Nertera ciliata, Pratia angulata, Euphrasia cuneata, Viola cunninghamii* and *Hydrocotyle microphylla.*

Lycopods: *Lycopodium fastigiatum*

Mosses: *Breutalia pendula, Bryum sp. and Hypnum cupressiforme.*

Shrubs: *Leptospermum scoparium*

The common species in the drier dune areas include:

Shrubs: *Cassinia vauvilliersii, Leptospermum scoparium, Dracophyllum subulatum, Cyathodes empetrifolia, Coriaria plumosa, Gaultheria sp., Pentachondra pumila* and *Olearia nummularifolia.*

Grasses:*Poa cita, Rytidosperma gracile, Holcus lanatus(adv), Cortaderia fulvida.*

Herbs: *Wahlenbergia albomarginata var. pygmaea, Euphrasia cuneata, Hypochaeris radicata(adv), Hieracium pilosella(adv), Hydrocotyle sulcata* and *Gunnera dentata.*

Mosses: *Polytrichum juniperinurn, Ditrichum cylindrocarpum, and Campylopus sp.*

4.2 N. solandri Forest

4.2.1 Influence Of Drought On Forest Structure

Introduction

Over the last two decades the study of the dynamics of forest communities, especially in the role of disturbance, has precipitated the development of a kinetic model to describe the ecology of New Zealand forests (Ogden, 1985). This model accepts disturbance as a selective force where different tree species have become differentially adapted, and that regeneration gaps, localised in space and time, are a natural demographic phenomena.

The role of disturbance of *N. solandri* forests has been studied in some detail in recent years. This topic has been reviewed in detail by Wardle (1984), although much of the data is presented from the South Island. On the Central Volcanic Plateau drought has been documented as a major cause for recent *N. solandri* dieback. Recent extensive mortality of *N. solandri* on the western slopes of Mount Ruapehu is thought to be due to a protracted drought in the 1960's (Skipworth, 1983; Steel, 1989). Hosking and Hutcheson (1988) also ascribe drought as a trigger for dieback of mature and over mature stands of *N. solandri* in the Kaweka Range during the 1860's and between 1910-1920. In the Ruahine Range dieback of *N. solandri* and *N. fusca* is also attributed to drought in 1914-15 (Grant, 1984). Whilst the *N. solandri* enclaves in the Rangipo Desert are presently in a healthy state exhibiting no dieback, a reconnaissance survey of the area indicated the size distribution of *N. solandri* stands were variable. In this study the size distribution of four *N. solandri* stands was examined. Two sites possessed even-aged regenerating trees that indicated past disturbance and subsequent dieback had occurred. Dendrochronological methods were used to determine if any correlation existed between these regenerating stands and recorded dry periods.

Introduction

Annual rings produced by xylem growth in a tree record not only the growth over the tree's lifespan, but also provide information on a trees physiological responses to its micro-environment. Trees may suffer physiological shock after extremely wet or dry conditions (Phipps, 1982) which can lead to poor growth and narrow annual ring widths. Variation of annual ring widths shared among trees, due to shared environmental influences, enables tree-ring widths between trees to be compared, and trees cross-dated. Therefore, a period of environmental stress in a given area, such as drought, can be detected in a related set of narrow ring-widths from a number of cross-dated trees.

Steel (1989) attributed the narrow rings observed in *N. solandri* at west Ruapehu, during the 1960's, to an exceptionally dry year in 1961, followed by two exceptionally wet years in 1962 and 1963. *N. solandri* stands in the Rangipo Desert, however, occur on sandy soils that are very free draining (Chapter 3). Therefore, wet conditions are unlikely to adversely affect the growth of trees in the Rangipo Desert, unless a corresponding drop in temperatures (Norton, 1983) occurs with the wet conditions. Steel (1989) suggests that the growth release of *N. solandri* between 1917 and 1937 may be the result of some limited dieback after the 1914-15 drought which was recognised throughout the North Island.

Scott (1972) found there was a significant correlation between the tree-ring chronologies of *N. solandri* and *Phyllocladus* sampled around Mount Ruapehu. The main factors in causing suppressed growth of *Phyllocladus* at Mount Ruapehu was high summer temperatures, and the lack of moisture availability for the previous autumn (Scott, 1972). High summer temperatures, however, did not correlate to that summer's moisture availability. Therefore, a tree-ring chronology for selected *N. solandri* and *Phyllocladus* trees in the Rangipo Desert was produced to see if suppression of growth occurred in these species after the recorded droughts in the region.

Methods

For dendrochronology, live boles of *N. solandri* were cut, while larger trees were cored using a 0.5m Swedish increment corer. Stems of *Phyllocladus* and *Halocarpus bidwilli* were also cut. It can be reasonably assumed from earlier work that ring formation occurred annually at this altitude for these species (Wardle, 1963b; Dunwiddie, 1979; Norton 1983). However, cross-dating was employed to check for missing or false annual rings. Techniques for the preparation and measuring of increment cores followed Stokes and Smiley (1968). Exceptions to these methods were that cores were mounted in corrugated cardboard mounts. Stem sections were prepared by a machine sander. Ring- widths were measured under a 30 x binocular microscope and indexed to a 10 year running mean following the method of Stokes and Smiley (1968).

The stems of six *Phyllocladus* trees were analysed, cross-dated to produce a master tree-ring chronology for that species. The stems of two *N. solandri* tree were analysed and cross-dated to produce a composite chronology.

Monthly rainfall figures were not available for Waiouru in this study, however, data from the meteorological station at Taihape (E 95683) was available. Taihape is located 30km south of Waiouru and has an altitude of 433 metres compared to an altitude of 823 metres for Waiouru. A correlation co-efficient between the two station's monthly mean rainfall (New Zealand Meteorological Service, 1982) yields: r=0.8 and r^2=.64 or 64% (p=.001). In other words, 64% of the mean monthly rainfall variability at Waiouru can be explained with the Taihape data.

An analysis of the Taihape monthly rainfall figures by Grant (1984) showed that 3 major droughts occurred at Taihape this century. These occurred in the summers of 1907-08, 1915-16, and 1945-46. The 1907-08 and 1945-46 dry periods were intense, and lasted for a duration of 3 to 4 months, while the 1914-15 drought was less intense but lasted for 12 months. These same dry periods were also recorded just east of the Ruahine Ranges at Gwavas (Grant, 1984).

Figure 4.2 A = Phyllocladus tree-ring chronology
B = N. solandri tree-ring chronology

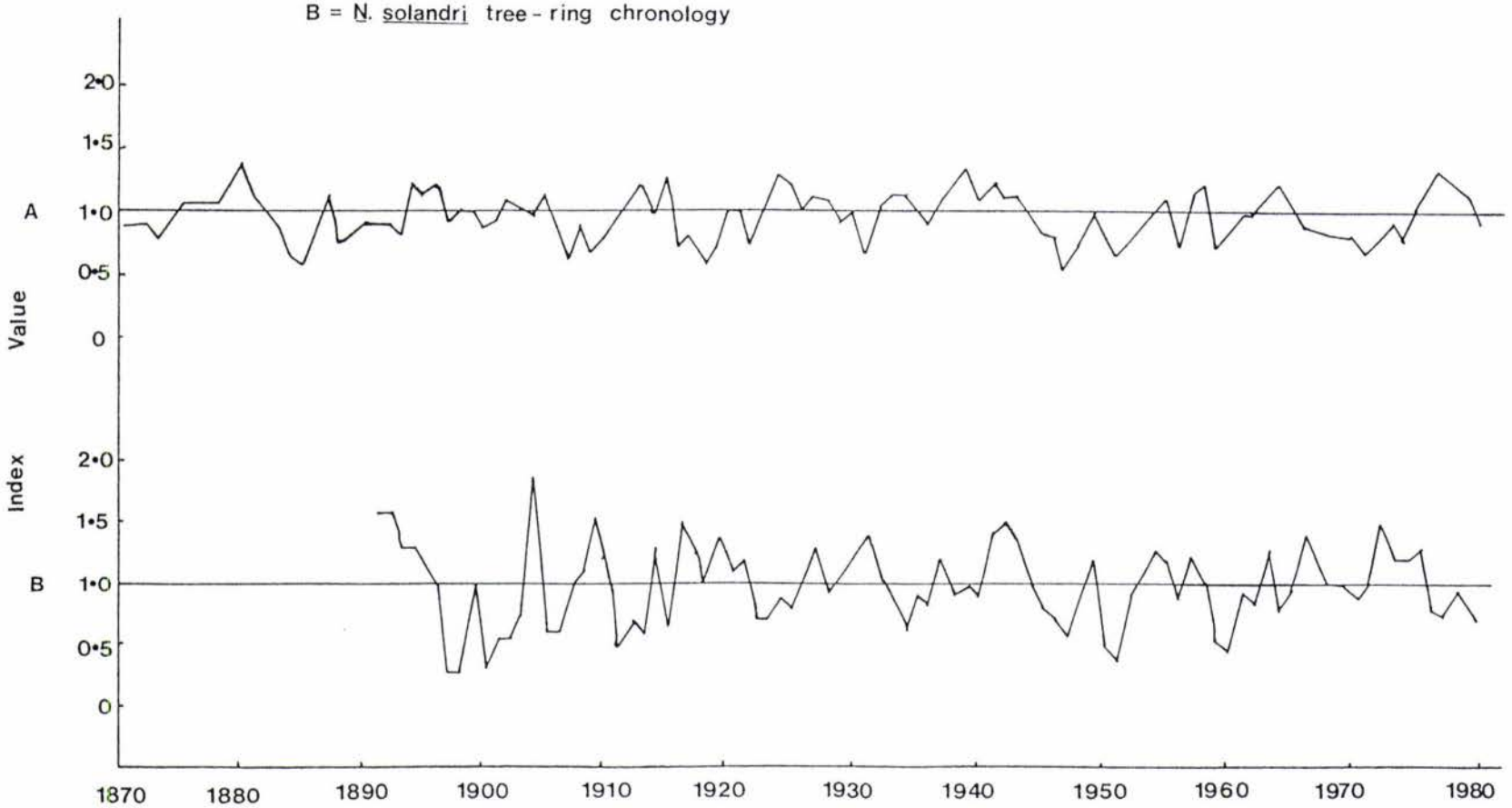

Results And Discussion

Growth suppression of *Phyllocladus* recorded in the study area (Fig. 4.2) correlated well to the dry periods documented for the Ruahine Ranges by Grant (1984). The chronology reveals a suppression of growth for 4 years after the 1907-1908 drought, for 5 years after the 1915-16 drought, and 8 years after the 1945-46 drought. An extended period of growth suppression for both *N. solandri* and *Phyllocladus* after the 1945-46 drought could well have been due to a further dry period recorded at Taihape between Nov-Feb 1947-48. Growth suppession was also severe for *Phyllocladus* in 1885.

Growth suppression in *N. solandri* correlated well to the 1945/46 drought but did not correlate well to the 1907-08 or 1915-16 droughts at Taihape. The reason for growth suppression occurring before the droughts maybe due to the presence of false rings. False rings were not apparent but the sample size is inadequate to exclude this possibility. This may also account for the lack of correlation between *N. solandri* and *Phyllocladus* ring-widths shown by Scott (1972). There is no evidence of major growth suppression through the 1960's documented by Steel (1989). Growth is suppressed, in common with Steel (1989) but growth then recovers subsequently.

Despite indexing the ring-widths to 10 year running means, the mean sensitivities of the *N. solandri* ring-widths are observed to increase before 1910. These increased mean sensitivities were due to the faster growth rates of the *N. solandri* trees which were only 25 and 30 years old respectively at 1910. Therefore, the increased growth fluctuations appear to be the result of the wider ring-widths, not related increased climatic fluctuations. The fitting of a standardized growth-curve (Norton and Ogden, 1988) for *N. solandri* may have removed this effect. On the other hand, the *Phyllocladus* mean sensitivities appeared constant. In this case the trees were at least 70 years old by 1910 and consequently their biological growth rates appeared relatively constant.

In summary, suppressed growth of *Phyllocladus* correlated well to the three major drought events recorded in Taihape since 1906. This infers that there is a negative growth response to drought of *Phyllocladus* trees located in the Rangipo Desert. The longevity of *Phyllocladus* and *Halocarpus bidwilli* and the clarity of their rings make them useful species to pursue dendrochronological studies. Growth is also suppressed after the 1945-46 drought in the *N. solandri*, but does not correlate well to the earlier drought episodes documented by Grant (1984). The 1945-46 drought was observed (Elder, 1962) to cause widespread death of *N. solandri* extending from the Kaweka Range westwards across the southern Kaimanawa Range.

4.2.1.2 Stand Structures

N. solandri trees from 4 sites (Plate 3.9) were sampled to encompass the different size distributions recognised after a reconnaissance survey. Point-quarters (Brower and Zar, 1984) were performed following the method described in section 4.1, except the circumferences of both canopy and understory *N. solandri* trees were measured and converted to diameters.

Size distributions of *N. solandri* stands in sites A and B (Fig. 4.3) are positively skewed because a large population of young, even-aged stems dominated these sites. However, in site C regenerating boles occurred only in localized canopy gaps dispersed between mature trees. As a result site D is positively skewed to a lesser degree. Site D is also positively skewed because large, semi-dormant, seedlings and saplings were included in the sample. If these seedlings and saplings were excluded from the histogram, the size distribution for this site would be near a normal population distribution, which is typical for an older mixed-aged stand (Wardle, 1984).

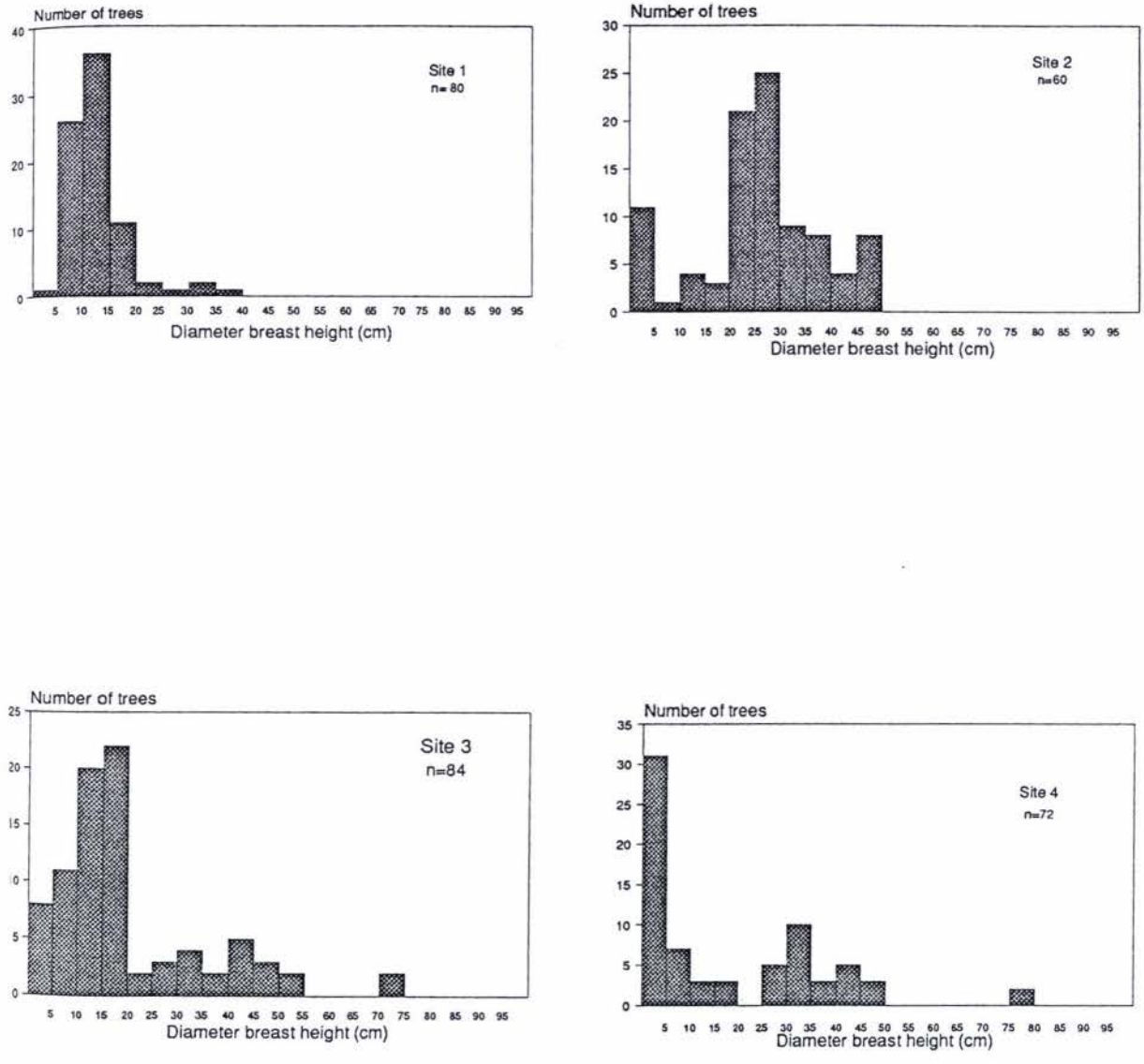

Figure 4.3 Histogram showing size class distributions of N. solandri at each of 4 sites

The ages of some trees were determined at three sites using the dendrochronological methods described earlier. The diameter and age for selected trees from the sites A,B and D follow:

Site	Diameter (cm)	Age (years)
A	16	47
	19	46
	11	39
B		
	15	78
	17	104
	28.5	105
D		
	75	≈235*
	79	≈253*

* increment cored; extrapolated to the centre

Discussion

The even-aged stands at sites A and B reveal that dieback, and the subsequent recruitment of a young cohort has occurred. The cut stems from site A indicate that dieback was contemporaneous throughout this site and occurred around 40 years ago. The tree-ring widths of the two larger stems indicate growth release (distinct increase in ring width) began when they were 7 or 8 years old, whilst the smaller stem was released immediately after germination. This suggests that release for these trees began 39 years ago or 1950; and therefore, dieback occurred during this period. Dieback during this period correlates to the 1945-46 dry period recorded by Grant (1984) for the Ruahine Range; and also the 8 year period of growth suppression recorded for *N. solandri* and *Phyllocladus* recorded in this study. Elder (1962) noted that regeneration of *N. solandri* had become typical in the Kaweka and southern Kaimanawa ranges during 1947 and some, though not all, of this regeneration dated from the 1946 drought. The same drought is suspected to have also caused a partial dieback in site C; however, no ages were obtained from cut stems to confirm this.

Ages of three cut stems in site B suggest the regeneration is also the result of dieback due to drought which must have occurred around 1884. The tree-ring chronology for *Phyllocladus* (Fig. 4.2) shows that 1885 was the only other time that growth was suppressed to levels found for 1906-07, 1914-15, and 1945-46, which were the driest periods recorded this century from Taihape (Grant,1984).

Site D appears to be an multi-aged stand. The ages of the largest trees are an estimate and must be treated with caution (see Norton et. al., 1987), because the increment corer could not penetrate to the tree centre. Nevertheless, an age of well in excess of 200 years is highly probable. Further work is needed to determine whether a specific cohort age exists for these larger trees. They may, for example, represent the 1740 yrs B.P. cohort that suffered extensive mortality in the late 1960's and early 1970's in the west Ruapehu *N. solandri* forest (Steel, 1989).

Recent results, including this study, indicate that mortality caused by drought is a relatively common phenomenon in the North Island's *Nothofagus* forests. Listed below are the dates of droughts that have been predicted as a trigger for dieback:

1) Drought in 1862; mortality of *N. solandri,* Kaweka Ranges, (Hosking and Hutcheson, 1988),
2) Drought in 1885?, mortality *N. solandri*, Rangipo Desert, this study,
3) Drought sometime around 1910-20, mortality of *N. solandri*, Kaweka Range (Hosking and Hutcheson, 1988),
4) Drought in 1907/08, limited mortality? of *N. solandri*, west Ruapehu (Steel, 1989),
4) Drought in 1914/15, extensive mortality of *N. solandri* and *N. fusca*, Ruahine Range (Grant, 1984),
5) Drought in 1945/46 mortality of *N. solandri*, Rangipo Desert, this study,
6) Drought in 1945/46, extensive mortality of *N. solandri*, Kaweka and southern Kaimanawa Ranges (Elder, 1962) and probably areas of Ruahine Ranges (Grant, 1984),
7)Drought in 1945/46, mortality of *N. menziesii,* Kaimai Ranges (Jane and Green, 1982),
8) Drought followed by excessively wet seasons 1961-1963, extensive mortality of *N. solandri*, west Ruapehu, (Steel, 1989).
9) Drought in 1972/73, mortality of *N. truncata*, Mamaku Plateau, (Hosking and Hutcheson, 1986).

It would appear that drought can trigger dieback to a greater or lesser extent over different areas, at different times. Hosking and Hutcheson (1988) suggest that *N. solandri* forest becomes susceptible to dieback when it is 100 to 150 years old; whereas, Steel (1989) suggests that the recent dieback in west Ruapehu is of a cohort aged about 250 years. In this study it appears that many of the mature trees found in site D escaped the dieback recorded in site A. Further detailed studies are needed to determine why this is the case particularly since their micro-environments appear very similar.

4.2.2 Distribution Of N. solandri

Effect Of The Taupo Pumice Eruption

Prior to the Taupo Pumice eruption evidence suggests that much of the Rangipo Desert was clothed in *N. solandri* forest. Landscapes immediately east of the Rangipo Desert (Rogers (1987) were clothed in *N. solandri* and numerous fossilized beech leaves are found in the Mangatawai Tephra which occurs throughout the Rangipo Desert (see chapter 1). However, in c. 186 A.D. Taupo Pumice pyroclastic flows destroyed vast areas of forest on the volcanic Plateau (Elder, 1962, McKelvey, 1963, 1973). In Tongariro National Park beech and podocarp forests on the western slopes of Hauhungatahi and Ruapehu survived the eruption because these massifs were a barrier to the pyroclastic flow (Atkinson, 1983a). However, in the northern and eastern sectors of Tongariro National Park, and in the Rangipo Desert, beech is missing or present as only 'enclaves' as a result of the destruction of the Taupo Pumice pyroclastic flows (Atkinson, 1983a; Wardle, J. 1984).

The orientations of the charred logs in the Taupo Pumice ignimbrite (Fig. 4.4), on the western margin of the large *N. solandri* enclave found in the Rangipo Desert (Fig. 1.1) confirms that the ignimbrite did flow in a south south-west direction through the area now occupied by *N. solandri* trees. However, indications are that some trees survived the eruption because some of the logs found in the Taupo Pumice ignimbrite were only slightly charred. The bark still preserved on the partially charred logs was that of *N. solandri* which further confirms the presence of this species at the time of the eruption.

Figure 4.4 Orientation of charred logs found in Taupo Pumice ignimbrite

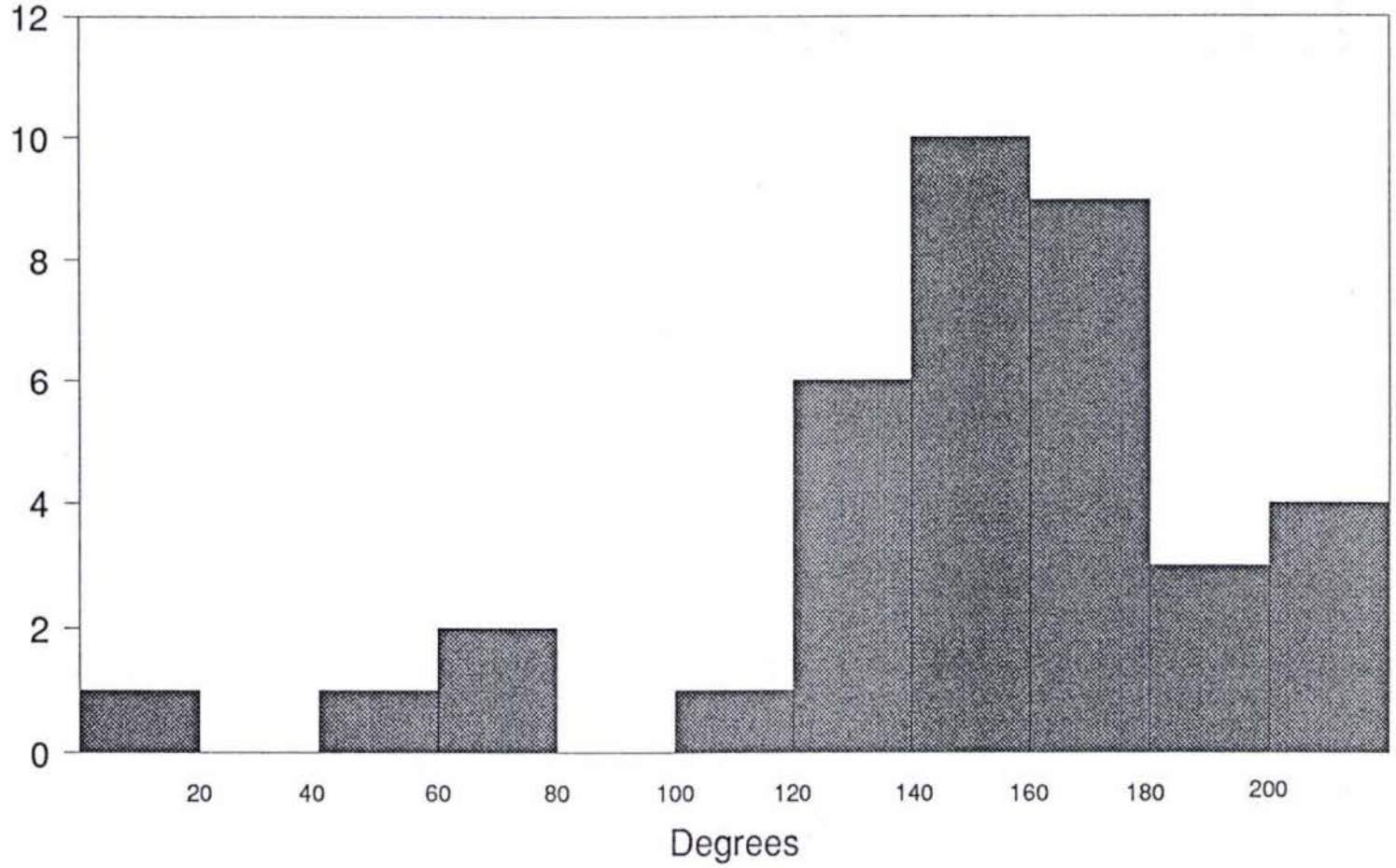

Post-Taupo Pumice Expansion of N. solandri

Atkinson (1983a) believes that complete re-invasion of beech over eastern and northern Tongariro National Park did not occur because 1) beech has limited power of dispersal and production of viable seed (see Wardle, 1984), 2) beech shows poor germination in tussockland or in open communities and, 3) a possible lack of mycorrhizal fungi. He suggests if the tussock-shrubland were removed, exposing andesitic ash, then re-invasion would be facilitated. However, he also mentions that the present distribution is probably smaller now since the arrival of man and the advent of fire. Pollen evidence in the Moawhango headwaters shows a permanent reduction in *Nothofagus* forest after the Taupo Pumice eruption, with *Phyllocladus* and *Halocarpus* spreading into sites vacated by *Nothofagus* (Rogers,1987). The pumice infilled basins of the Moawhango headwaters were also rendered inimical to forest because of edaphic dryness. On the other hand, pollen evidence by Steel (1989) indicates *N. solandri* rapidly recovered on the western slopes of Mount Ruapehu, but did not migrate back on to the ring plain.

The presence of preserved *N. solandri* leaves within Tufa Trig member 4, a coarse tephra deposited c. 850 yrs B.P., provides a clue to the post-Taupo pumice expansion of *N. solandri* in the Rangipo Desert. Tufa Trig member 4 is found in post-Taupo stratigraphic sequences both under the present *N. solandri* enclaves in the western part of the study area, and also in the eastern areas, located near the fault escarpment. However, the preserved *N. solandri* leaves were found in the tephra only in the western areas under the *N. solandri* enclaves, and not in the tephra to the east. This indicates that *N. solandri* forest had re-established itself by c. 850 yrs B.P. in at least the areas which are presently located under *N. solandri* forest but had not re-established itself in the eastern areas. It is envisaged that the *N. solandri* forest had actually expanded across much of the western areas by 850 yrs B.P. with both marginal expansion from the parent enclaves and the establishment of outlier stands. However, its distribution then contracted again in c. 800 yrs B.P. due to widespread destruction from the lahar 6 (chapter 3), the largest recorded post-Taupo Pumice lahar.

A major hinderance for the establishment of *N. solandri* across the desert (eastern areas) after the Taupo Pumice eruption would have been the presence of the laharic and fluvial deposits. Although these deposits may not have been as extensive in earlier post-Taupo Pumice times, the harsh edaphic properties of these substrates (chapter 3) must have limited both marginal expansion and establishment of outlier *N. solandri* stands. Three small outlier stands of *N. solandri* are present today about 1km east of Large *N. solandri* Enclave. However, these stands have established within the last 800 years on aeolian sands previously fixed by other plants. It is therefore likely that the *Phyllocladus* dominant forest, not *N. solandri* forest, existed in the eastern parts of the study area (ie. closer to the fault escarpment.) between the Taupo Pumice eruption to the present day.

Today, *N. solandri* enclaves are expanding marginally in some areas but are static in many others. A major problem for *N. solandri* expansion is its ability to establish on the surrounding, actively eroding, tephric substrate. It is possible that the eroding tephra lacks ectomycorrhizae, which are suggested as necessary for establishment of *Nothofagus* seedlings (Baylis, 1980; Wardle, 1984). Only where slopes are minimal and eroded tephra accumulates in association with the N fixing *Coriaria plumosa*, has *N. solandri* became established.

4.2.3 Recent Fire In N. solandri Forest

Fire has at least once, quite possibly twice, encroached on parts of the southern margin of Large *N. solandri* Enclave (Plate 3.9). Tree-ring dating of one larger emergent *Phyllocladus* tree indicates burning occurred at least 110 years ago. However, the presence of two outlier *N. solandri* stands surrounded by mature *Phyllocladus* trees (Plate 4.2), at the western margin of this locality, suggests an even earlier fire episode may have occurred. These stands radiate out from mature *N. solandri* trees which possess between 70 and 82cm wide basal diameters.

Plate 4.2 Arrows in the background point to 2 small outlier stands of *N. solandri* which are surrounded by mature *Phyllocladus* forest. The oldest trees of these stands may have become established after a fire between 250 to 350 years ago. The arrow in the foreground shows a seral shrub mosaic with emergent *Phyllocladus* which has recolonised the area after a burning episode about 110 years ago.

Plate 4.3 Arrow shows the expansion of *N. solandri* forest back into *Hebe venustula* and *Chionochloa rubra* tussock shrubland after fire. The original burning episode probably occurred at the same time as the one described in the above photograph ie. about 110 years ago.

Map 2. Vegetation of the study area

1Km

N

[On/Rs]

Hb–Hv–(On)

Ds–Cr

[Cf]

Nc

[Cv/Csp.]

Nc

Hb–Hv–(On)

[Ra]

(Cr)/Pc/(Hp)

[Hb–Hv]

[Cf]

(Pc–Ao/Hp)–Cf

Whangaehu River

Whangaehu River

Map 1. Distribution of the informal members of the Whangaehu Formation